UNIVERSIDADE TECNOLÓGICA FEDERAL DO PARANÁ

ALVARO TORRES AMAYA

EVALUATION OF VANET PROTOCOLS FOR DRIVING ASSISTANCE OF CONNECTED VEHICLES: A STRATEGY BASED ON A MULTI-ANTICIPATIVE CAR-FOLLOWING MODEL

DOCTORAL THESIS

CURITIBA

2022

ALVARO TORRES AMAYA

EVALUATION OF VANET PROTOCOLS FOR DRIVING ASSISTANCE OF CONNECTED VEHICLES: A STRATEGY BASED ON A MULTI-ANTICIPATIVE CAR-FOLLOWING MODEL

Avaliação de protocolos VANET para direção assistida em veículos conectados: uma estratégia baseada em modelo multi-antecipativo de seguimento de veículos

Doctoral thesis submitted to the Graduate Program in Electrical and Computer Engineering of the Universidade Tecnológica Federal do Paraná as partial requirement for the Doctor of Science (D.Sc.) degree.

Advisor: Prof. Dr. Alexandre de Almeida Prado Pohl

Co-advisor: Prof. Dr. Ricardo Lüders

CURITIBA

2022

Ministério da Educação
Universidade Tecnológica Federal do Paraná
Campus Curitiba

ALVARO TORRES AMAYA

EVALUATION OF VANET PROTOCOLS FOR DRIVING ASSISTANCE OF CONNECTED VEHICLES: A STRATEGY BASED ON A MULTI-ANTICIPATIVE CAR-FOLLOWING MODEL

Trabalho de pesquisa de doutorado apresentado como requisito para obtenção do título de Doutor Em Ciências da Universidade Tecnológica Federal do Paraná (UTFPR). Área de concentração: Engenharia De Automação E Sistemas .

Data de aprovação: 26 de Setembro de 2022

Dr. Erik Anders Jenelius, Doutorado - Kth, Royal Institute Of Technology

Dra. Keiko Veronica Ono Fonseca, Doutorado - Universidade Tecnológica Federal do Paraná

Dr. Mauro Sergio Pereira Fonseca, Doutorado - Universidade Tecnológica Federal do Paraná

Dr. Miguel Elias Mitre Campista, Doutorado - Universidade Federal do Rio de Janeiro (Ufrj)

Dr. Ricardo Luders, Doutorado - Universidade Tecnológica Federal do Paraná

Documento gerado pelo Sistema Acadêmico da UTFPR a partir dos dados da Ata de Defesa em 27/09/2022.

I dedicate this work to my family, especially my father, who understood my absence and now supports me from heaven.

ACKNOWLEDGEMENTS

This work could not have been finished without the help of several people and institutions to which I pay my tribute. Perhaps these paragraphs will not serve all the people who were part of this important phase of my life. Therefore, I apologize to those not present in these words; they can be sure they are part of my thoughts and gratitude.

To my family for their love, encouragement, and total support throughout my life.

To my advisors, Professors Alexandre Pohl and Ricardo Lüders, who showed me the paths to be followed and for their trust.

To all the professors and colleagues of the department who helped directly and indirectly in completing this work.

To the COIMBRA group of Brazilian Universities and the PAEC OAS-GCUB program for granting the scholarship. Likewise, the Smart City Concepts in Curitiba Project for providing additional insights.

Finally, thanks to all who contributed in some way to the completion of this work.

This study was financed in part by the Coordenação de Aperfeiçoamento de Pessoal de Nível Superior - Brasil (CAPES) - Finance Code 001.

My brain is only a receiver, in the Universe there is a core from which we obtain knowledge, strength and inspiration. I have not penetrated into the secrets of this core, but I know that it exists (Nikola Tesla).

RESUMO

AMAYA, Alvaro Torres. **Avaliação de protocolos VANET para direção assistida em veículos conectados: uma estratégia baseada em modelo multi-antecipativo de seguimento de veículos**. 2022. 90 p. Tese de Doutorado - Programa de Pós-Graduação em Engenharia Elétrica e Informática Industrial, Universidade Tecnológica Federal do Paraná. Curitiba, 2022.

As redes de comunicação veiculares "ad-hoc" (VANETs) tem se tornado uma área de pesquisa com amplo destaque en anos recentes devido ao seu potencial de aumentar a conectividade das pessoas e providenciar um canal alternativo às redes de comunicação tradicionais. A ideia principal de uma VANET é aproveitar a distribuicão espacial dos veículos e os recursos avançados de tecnologia de comunicação no intuito de estabelecer um canal autogerenciado e confiável destinado à comunicação entre veículos e qualquer dispositivo com capacidade de acessar a rede. Devido à sua natureza independente, as VANETs têm sido consideradas também para aplicações de mobilidade veicular, especificamente nos sistemas cooperativos avançados de assistência à condução CADAS ("Cooperative Advanced Driver Assistance Systems"). Nesse tipo de sistema, cada veículo coleta as informações cinemáticas dos vizinhos mais próximos por meio de mensagens curtas e periódicas conhecidas como "beacons", cujo conteúdo pode contribuir não apenas na tomada de decisões de mobilidade, mas também para melhorar a estabilidade da própria rede de comunicação veicular. As abordagens de pesquisa tradicionais abordam tanto a comunicação com VANETs quanto os sistemas de assistência à mobilidade de forma independente. Portanto, pouca atenção tem sido dada ao estudo da coexistência de CADAS e comunicação do usuário final. Esta tese apresenta um estudo abrangente sobre os impactos práticos que o controle da mobilidade de um veículo conectado por meio de mensagens periódicas em VANETs tem no desempenho da rede. Além disso, é proposta uma estratégia baseada em rede e ciente do tráfego veicular para assistência à condução de um veículo elétrico e conectado por meio de um modelo de seguimento de carro. Os resultados mostram que um protocolo tradicional com "beacons", como o "Greedy Perimeter Stateless Routing" (GPSR), pode ter um melhor desempenho do que um conjunto de abordagens que utilizam o protocolo "Delay Tolerant Network" (DTN). Entretanto, uma estratégia de "beacon" com conhecimento do tráfego é necessária para reduzir o impacto negativo que um intervalo de tempo curto de "beacon" tem na rede.

Palavras-chave: vanet; protocolo de roteamento; modelo de seguimento de veículo; veículo conectado; baliza.

ABSTRACT

AMAYA, Alvaro Torres. **Evaluation of VANET protocols for driving assistance of connected vehicles: a strategy based on a multi-anticipative car-following model**. 2022. 90 p. Doctoral thesis - Graduate Program in Electrical and Computer Engineering, Universidade Tecnológica Federal do Paraná. Curitiba, 2022.

In recent years, Vehicular Ad-hoc Networks (VANETs) have become a remarkable research area due to their potential to improve communication among people and to become an alternative offload channel for traditional networks. The main idea behind a VANET is to harness the spatial distribution of vehicles and advanced technical resources in communication networks to establish a self-managed and reliable channel to communicate with vehicles and any device able to access the network. Due to their independent nature, VANETs have also been envisioned for vehicular mobility solutions, more precisely with the so-called Cooperative Advanced Driver Assistance Systems (CADAS). In such systems, each vehicle is expected to gather its closest neighbor's kinematic information by transmitting short and periodic messages, known as beacons, whose content may contribute not only to decision-making on mobility but also to improving the own vehicular network's stability. Traditional research approaches address communication with VANETs and mobility assistance systems independently, so little attention has been given to studying the coexistence of CADAS and end-user communication. This thesis presents a comprehensive study on the practical impacts that controlling the mobility of a connected vehicle through periodic messages in VANETs has on the network performance. In addition, a network-based and traffic-aware strategy for driving assistance of electric and connected vehicles through a car-following model is proposed. The results show that a traditional protocol featuring beacons, like the Greedy Perimeter Stateless Routing (GPSR), can perform better than a set of approaches using the Delay Tolerant Network (DTN) protocol. However, a traffic-aware beacon strategy is necessary to reduce the negative impact a short time interval of beacons has on the network.

Keywords: vanet; routing protocol; car-following model; connected vehicle; beacon.

LIST OF FIGURES

Figure 1 – Dynamics of vehicle braking. **30**

Figure 2 – DSRC channels distribution. **33**

Figure 3 – A taxonomy of routing protocols for VANET. **34**

Figure 4 – Greedy forwarding strategy in Greedy Perimeter Stateless Routing (GPSR). **36**

Figure 5 – Perimeter forwarding strategy in GPSR. **36**

Figure 6 – Format of *Hello* message broadcasted by every node. **36**

Figure 7 – Topology for cluster-based V2V networks. **37**

Figure 8 – A taxonomy of DTN routing protocols. **38**

Figure 9 – NS-2 standard VANET simulation scheme. **46**

Figure 10 – Scheme for the adapted simulator. **47**

Figure 11 – Two-road crossing scenario. **49**

Figure 12 – highway scenario. **49**

Figure 13 – Comparison of the adapted simulator and the results of SUMO: (a) Speed with adapted ns-2, (b) Speed with SUMO, (c) Position with adapted ns-2, (d) Position with SUMO, (e) Acceleration with adapted ns-2, (f) Acceleration with SUMO, (g) State of charge with adapted ns-2, (h) State of charge with SUMO. **51**

Figure 14 – Results in the urban scenario: (a) Speed with Krauss model, (b) Speed with MA model, (c) Position with Krauss model, (d) Position with MA model, (e) Acceleration with Krauss model, (f) Acceleration with MA model, (g) State of charge with Krauss model, (h) State of charge with MA model. **52**

Figure 15 – Results in the highway scenario: (a) Speed with Krauss model, (b) Speed with MA model, (c) Position with Krauss model, (d) Position with MA model, (e) Acceleration with Krauss model, (f) Acceleration with MA model, (g) State of charge with Krauss model, (h) State of charge with MA model. **55**

Figure 16 – Communication among four vehicles of the traffic flow: (a) Four vehicles communicate at the intersection, (b) Communication links once the traffic light opens. **58**
Figure 17 – Results of Delivery rate with: (a) TR=100 m, (b) TR=500 m. **61**
Figure 18 – Results of Average End-to-End Delay with: (a) TR=100 m, (b) TR=500 m. **62**
Figure 19 – Results of Overhead with: (a) Transmission Range (TR)=100 m, (b) TR=500 m. **63**
Figure 20 – Average number of hops with: (a) TR=100 m, (b) TR=500 m. **64**
Figure 21 – Impacts of the Beacon interval time: (a) Packet delivery ratio, (b) Average End-To-End Delay. **65**
Figure 22 – Angle between two neighbors of vehicle i. **68**
Figure 23 – Space of solutions for all feasible combinations of K_1, K_2 and K_3. . . . **69**
Figure 24 – Evolution of the beacon interval using the proposed strategy. **70**
Figure 25 – Average Delay of beacon schemes: (a) Processing Delay, (b) Transmission Delay. **71**
Figure 26 – Communication Metrics using the MA model in the urban scenario: (a) PDR, (b) E2E Delay, (c) Overhead, (d) Jitter. **73**
Figure 27 – Communication Metrics using the MA model over the highway scenario: (a) PDR, (b) E2E Delay, (c) Overhead, (d) Jitter. **75**
Figure 28 – Mobility metrics using MA CFM over an urban scenario with high density: (a), (b) and (c) Speed, (d), (e) and (f) Position, (g), (h) and (i) Acceleration, and (j), (k), (l) State of charge. **77**
Figure 29 – Mobility metrics using MA CFM over a highway scenario with high density: (a), (b) and (c) Speed, (d), (e) and (f) Position, (g), (h) and (i) Acceleration, and (j), (k), (l) State of charge. **78**

LIST OF TABLES

Table 1 – ISO protocol layer for V2X communications. **33**
Table 2 – Comparison among mobility simulators. **41**
Table 3 – Comparison of network simulators. **43**
Table 4 – Comparison of VANET simulators. **44**
Table 5 – Energy model parameters. **50**
Table 6 – Simulation parameters. **59**

LIST OF BOARDS

Frame 1 – Main contributions. **21**

Frame 2 – Average local densities. **72**

LIST OF ABBREVIATIONS AND ACRONYMS

Pseudo-Acronyms

AODV	Ad-hoc On-demand Distance Vector
BIT	Beacon Interval Time
BS&W	Binary Spray And Wait
CACC	Cooperative Adaptive Cruise Control
CADAS	Cooperative Advanced Driver Assistance Systems
CFM	Car-Following Model
CSMA/CA	Contention-Based Carrier Sense Multiple Access with Collision Avoidance
CV	Connected Vehicle
DD	Direct Delivery
DR	Delivery Rate
DSDV	Destination-Sequenced Distance Vector
DSRC	Dedicated Short Range Communications
DTN	Delay Tolerant Networks
E2E	End-To-End
ETSI	European Telecommunications Standards Institute
EV	Electric Vehicle
FCC	Federal Communication Commission
FE-RBS	Fully Regenerative Systems
FVD	Full Velocity Difference
GPS	Global Positioning System
GPSR	Greedy Perimeter Stateless Routing
HBS	Hybrid Braking Systems

IDM	Intelligent Driver Model
IEEE	Institute of Electric and Electronic Engineers
ISO	International Organization for Standardization
LCM	Lane-Changing Model
MA	Multi-Anticipative
MANET	Mobile Ad-hoc Networks
OFDM	Orthogonal Frequency Division Multiplexing
OVM	Optimal Velocity Model
PBR	Position-Based Protocols
PDR	Packet Delivery Ratio
PLCP	Physical Layer Convergence Procedure
PMD	Physical Medium Dependent
PRoPHET	Probabilistic Routing Protocol using History of Encounters and Transitivity
RBS	Regenerative Braking Systems
SoC	State of Charge
TABI-GPSR	Traffic Aware Beacon Interval for GPSR
TBR	Topology-Based Protocols
TCP	Transmission Control Protocol
TR	Transmission Range
UDP	User Datagram Protocol
V2I	Vehicle To Infrastructure
V2P	Vehicle To Person
V2V	Vehicle To Vehicle
V2X	Vehicle To Everything
VANET	Vehicular Ad-Hoc Networks

LIST OF SYMBOLS

Latin Letters

a	Acceleration	$[\mathrm{m/s^2}]$
A_d	Acceleration Deviation	$[\mathrm{m/s^2}]$
A_f	Frontal area of the vehicle	$[\mathrm{m^2}]$
b	Braking deceleration	$[\mathrm{m/s^2}]$
b_m	Maximum deceleration of a vehicle in Krauss model	$[\mathrm{m/s^2}]$
B	required distance for braking	$[\mathrm{m}]$
d	Distance between vehicles in Krauss model	$[\mathrm{m}]$
D	Effective length of current vehicle	$[\mathrm{m}]$
F	Required tractive force	$[\mathrm{N}]$
F_d	Tire–road friction force	$[\mathrm{N}]$
g	Gravity acceleration	$[\mathrm{m/s^2}]$
I	Electric current	$[\mathrm{A}]$
J	Wheel inertia	$[\mathrm{Kg \cdot m^2}]$
m	Mass of the vehicle	$[\mathrm{Kg}]$
M_b	Braking force generated by the motor functioning as generator	$[\mathrm{N}]$
N	Total Number of time steps	$[\mathrm{No\ unit}]$
p	Mechanical power	$[\mathrm{Kg \cdot m^2/s^3}]$
P	Electrical power	$[\mathrm{W}]$
P_m	Motor's electric losses	$[\mathrm{W}]$
r	Conductor resistance	$[\Omega]$
Q	Traffic flow	$[\mathrm{Vehicle/km/h}]$
R	Tire radius	$[\mathrm{m}]$
R_a	Aerodynamic resistance	$[\mathrm{N}]$

R_g	Grade resistance	[N]
R_{rl}	Rolling resistance	[N]
s_n	Distance between vehicle n and $(n-1)$	[m]
s_0	Minimum headway between the current and immediate vehicle in front	[m]
T	Time headway to safely follow immediate leader vehicle	[s]
t_r	Driver's reaction time in Krauss model	[s]
v	speed	[m/s]
V	Average speed	[m/s]
v_{max}	Maximum speed	[m/s]
v_o	Desired speed of current vehicle	[m/s]
v_{safe}	Safe velocity in Krauss model	[m/s]
x	Position of a vehicle	[m]

Greek Letters

α	Control factor for BIT in TABI-GPSR	[No units]
δ	Exponent for vehicle's acceleration	[No units]
η	Efficiency factor	[No units]
ϕ_d	Magnetic flux	[Wb]
ρ	Local vehicular density	[vehicle/km/lane]
ρ_a	Air density	[kg/m^3]
τ	Torque	[N $\cdot$ m]
τ_r	speed relaxation time	[s]
θ	Roadway grade	[Rad]
ω	Wheel rotational speed	[Rad/s]
σV	Change in speed	[m/s]

Subscripts

f	Follower vehicle in Krauss model

l	Preceding vehicle in Krauss model
op	Optimum
n	Current vehicle
$n-1$	Preceding vehicle
rl	Rolling resistance
D	Drag
i	vehicle i

Notations

$\dot{x}_n$	First derivative of position (Speed)
$\ddot{x}_n$	Second derivative of position (Acceleration)
s^*	Desired minimum distance between vehicles
$\dot{x}_o$	Desired speed when driving on a road

CONTENTS

1 INTRODUCTION 18
1.1 Motivation 19
1.2 Objectives 20
1.3 Methodology 20
1.4 Contributions 21
1.5 Thesis structure 22
2 CAR-FOLLOWING AND ENERGY CONSUMPTION MODELS 23
2.1 Car-following models 23
2.1.1 Optimal Velocity Model OVM 24
2.1.2 Intelligent driver model IDM 25
2.1.3 Krauss model 26
2.1.4 Multi-Anticipative model (MA) 27
2.2 Energy consumption model for electric vehicles 27
2.2.1 Regenerative braking 29
2.3 Chapter summary 30
3 VEHICULAR AD-HOC NETWORKS 32
3.1 Standards in VANETs 32
3.2 Traditional Routing Protocols 34
3.3 Delay Tolerant Network Protocols 37
3.3.1 Direct Delivery 38
3.3.2 Epidemic 38
3.3.3 Binary Spray and Wait 39
3.3.4 PRoPHET 39
3.4 Simulation tools 40
3.4.1 Mobility simulators 40
3.4.2 Network simulators 41
3.4.3 Vanet simulators 42
3.4.4 Selected Tools 44
3.5 Chapter Summary 45
4 A NS-2-BASED PLATFORM FOR SIMULATION OF VANETS 46

4.1 A standard Simulation of VANET using ns-2 . . . 46
4.2 Improvement of the NS2 simulator to study a VANET-based CFM . . . 47
4.3 Mobility scenarios . . . 48
4.3.1 Urban Scenario . . . 48
4.3.2 The Highway Scenario . . . 49
4.4 Validation of the adapted ns-2 . . . 49
4.5 Evaluation of the Multi-anticipative CFM (MA Model) . . . 50
4.6 Chapter Summary . . . 54
5 ASSESSMENT OF ROUTING PROTOCOLS IN VANET . . . 57
5.1 Description of the experiment . . . 57
5.2 Performance Metrics . . . 59
5.3 The Impact of Vehicular Density . . . 60
5.3.1 Delivery Rate (DR) . . . 61
5.3.2 Average End-To-End Delay . . . 61
5.3.3 Overhead . . . 62
5.3.4 Average number of hops . . . 63
5.4 The impact of beacon interval time . . . 64
5.5 Chapter Summary . . . 65
6 AN ADAPTIVE BEACON STRATEGY FOR A VANET-BASED CFM . . . 67
6.1 Evaluation through a standard VANET simulation . . . 69
6.2 Evaluation of network and mobility performance . . . 71
6.2.1 Network performance . . . 71
6.2.2 Mobility performance . . . 76
6.3 Chapter Summary . . . 79
7 CONCLUSION . . . 81
7.1 Future work . . . 82
BIBLIOGRAPHY . . . 84

1 INTRODUCTION

Vehicular Ad-hoc Networks (VANETs) are a subcategory of the Mobile Ad-hoc Networks (MANET) with particular features, such as high mobility and dynamic topology (RAMAMOORTHY; THANGAVELU, 2021). VANETs aim to operate as a self-managed network backbone or as an offloading channel for other networks, such as 4G and 5G. For studying the numerous challenges of VANETs, extensive work on routing protocols has been carried out in recent years, including adaptations of MANET protocols and specific VANET-oriented approaches.

Routing protocols in VANETs can be classified as topology-based, position-based, broadcast, and cluster-based (ABDALLA; SALAMAH, 2022). Among them, the position-based ones have proven to be the more promissory choice (ALZAMZAMI; MAHGOUB, 2021). These protocols employ a kind of periodic and small-size messages, the so-called beacons or *Hello* messages. Such messages contain, among other information, an identifier number, the position and speed of a node, and a timestamp that helps establish the age of the information (BAO *et al.*, 2020). The content of a beacon is helpful to keep the nodes updated with the current localization of neighbors, and therefore better routing decision-making can be performed by the protocol (LI; WANG; WANG, 2016).

VANETs have also been proposed to support various services on Intelligent Transportation Systems (ITS) (HAMZA-CHERIF *et al.*, 2018). An example of ITS is the so-called Cooperative Advanced Driver Assistance Systems (CADAS). In CADAS, vehicles are expected to exchange traffic information to help other vehicles avoid high-congested areas, prevent accidents, improve energy efficiency, or even perform autonomous driving. Such information is also transmitted through beacons. In this case, two transmission modes are available, periodic or event-triggered. The use of a beacon transmission mode depends on the specific updating-rate requirements.

Most works in the literature have addressed both the communication and the CADAS performance over VANETs independently, for instance Houssaini *et al.* (2018), Bengag, Bengag e Elboukhari (2020), Bala e Krishna (2015) for evaluation of routing protocols or Forster *et al.* (2014), Rabsatt e Gerla (2017), Won, Park e Son (2017) for CADAS over VANETs. However, in a real deployment of VANETs both applications are expected to perform simultaneously. Such a coexistence may cause an overload of the network, as multiple beacons eventually containing the same information are simultaneously broadcasted. In addition, many proposals for CADAS are time-consuming and high computational efforts are required (REGHELIN; ARRUDA, 2016).

This thesis proposes studying the use of routing protocols of VANETs in different traffic density conditions for exchanging information among connected vehicles. Such information is expected to be transmitted through a controlled stream of periodic messages or beacons, which can provide the necessary surrounding kinematic data for the decision-making of a connected vehicle through a car-following model.

Other works have previously studied the control of beacons in routing protocols for VANETs, including Naderi, Zargari e Ghanbari (2019), Zidani, Semchedine e Ayaida (2018), Silva *et al.* (2019), Aznar-Poveda *et al.* (2022), Alsaqour *et al.* (2015). However, most of them require a high computational effort whereas others have proposed traffic-aware approaches with low computational requirements but limited effectiveness (LI; WANG; WANG, 2016). In this work, a novel and more effective traffic-aware approach is proposed.

The results of this work show that the optimal beacon interval time for both networking and driver assistance systems is quite different. Hence, operating with the most suitable interval for one of the two applications implies sacrificing the performance of the other one. However, both applications can simultaneously operate using the same routing protocol's information only if a traffic-aware beacon strategy, like the one proposed in this work, is employed.

1.1 Motivation

Routing protocols and cooperative driving systems are usually addressed individually as the final purposes can be slightly different in each case (HOUSSAINI *et al.*, 2018; FORSTER *et al.*, 2014; RABSATT; GERLA, 2017). However, in real deployments, both applications are expected to perform simultaneously. This work aims to study the advantages and drawbacks of the mobility and network performance in a unified manner. Likewise, this work proposes a feasible way to harness the kinematic information transmitted through the network.

Most works in the literature have studied VANETs from the point of view of connectivity among nodes. Therefore, extensive research efforts are devoted to keeping a stable communication path or rapidly finding an alternative one once a communication link has broken (HU; DING; SHI, 2012). This work seeks to study cooperative approaches in highly variable environments where sudden traffic density changes may occur, for instance, a typical urban traffic intersection or a sudden event over a highway.

On the other hand, many approaches for deployment of CADAS in automated driving (FORSTER *et al.*, 2014; RABSATT; GERLA, 2017; WON; PARK; SON, 2017) are described in the literature, including Maximum Power Point Tracking (MPPT) over platoons, linear and quadratic programming, and heuristic solutions, among others. However, most works conclude about the computational limitations due to the high complexity of the algorithms. This work seeks to demonstrate the potential of a VANET-based car-following model (CFM) in controlling a connected vehicle using a reduced computational effort and a controlled stream of data.

1.2 Objectives

The general objective is the evaluation of using vehicular ad-hoc network protocols for driving assistance of connected vehicles and propose a traffic-aware strategy for changing the behavior of vehicles as a beacon-based car-following model applied to electric vehicles.

The specific objectives are:

1. Identify and review the elements related to vehicular networks, mobility models and electric vehicles.
2. Evaluate routing protocols in VANETs for many vehicular density conditions.
3. Evaluate conditions for integration and simulation of car-following models in vehicular network communication scenarios.
4. Propose a traffic-aware strategy for the use of routing protocols in driving assistance of an electric vehicle through a car-following model.

1.3 Methodology

This work is developed through the integration of mathematical models and simulation tools. The main applications of mathematical models are: car-following, energy consumption, and beacon interval models. As for the simulation tools, the SUMO simulator generates mobility traces using traditional car-following models, like the Optimal Velocity Model (OVM), Intelligent Driver Model (IDM), and modified Krauss model. Because of the need to validate the results using a well-established platform, the network simulator (NS-2) is employed to perform simulations of wireless networks. The VANET simulation is performed in association with the SUMO (Simulator of Mobility) tool.

The NS-2 is also chosen due to the possibility of enhancing the software by linking new libraries and modifying the source code, which is built in C++, a well-known programming language. The adaptation of the network simulator is necessary to embed the mobility model (usually implemented by a traffic simulator as SUMO) into the network simulator (usually carried out by NS-2). This approach allows for controlling the movement of vehicles according to the information exchanged among them.

Initially, a standard simulation of VANETs using NS-2 and SUMO over a typical traffic intersection with a traffic light is carried out. Such a test aims to evaluate the performance of a set of publicly available routing protocols when employed for transmitting periodic messages (like beacons) in a large variety of traffic densities and transmission ranges. In such evaluation, particular focus is given to assessing the latency and reliability of the protocols, as they are essential for a successful exchange of traffic information.

Once the evaluation is performed, a routing protocol is chosen, and an adaptive strategy for integrating networking and driver assistance systems (represented by a car-following model) is developed. Such integration is performed using a tailored version of the software and two mobility scenarios: urban and highway. In this case, the main focus is given to keeping a low latency, as accurate decision-making depends on using updated information. Likewise, the frequent transmission of messages contributes to tolerating data loss over short periods.

1.4 Contributions

Many contributions can be drawn from this thesis. They are found in this document as well as some of them in the papers published. The reader can find contributions about exploring little-studied conditions for the operation of VANETs and the application of car-following models in VANET environments. Such contributions and their relationship with the specific objectives are summarized in Frame 1.

Frame 1 – Main contributions.

Contribution	**Objective**			
	1	**2**	**3**	**4**
Characterization of the main impacts that a high traffic density has on the network performance for small-scale scenarios	✓	✓		
Demonstration of the better performance of traditional Vehicular Ad-Hoc Networks (VANET) routing approaches, like GPSR and AODV in high traffic-density scenarios, if compared with Delay Tolerant Networks (DTN) approaches.	✓	✓		
Evaluation of a Multi-Anticipative VANET-Based car-following model in a network simulation environment	✓		✓	
Adaptation of a novel VANET simulation platform to evaluate car-following models	✓		✓	
Evaluation of energy savings of the Multi-Anticipative model if compared to a typical CFM for electric vehicles	✓		✓	
Characterization of the impacts that the beacon interval time yields in position-based protocols for different traffic densities	✓		✓	
Proposition of a novel adaptive traffic-aware and unified beacon strategy for both operation of a CFM and employment in networking purposes	✓			✓
Demonstration of how both networking routines and cooperative advanced driver assistance systems can simultaneously operate using a routing protocol if an adaptive beacon strategy is employed	✓			✓

Source: Own authorship (2022).

The following papers are results of this thesis (AMAYA; POHL; LÜDERS, 2021), (AMAYA *et al.*, 2022a), and (AMAYA *et al.*, 2022b):

AMAYA, Alvaro Torres; FONSECA, Mauro Sergio; POHL, Alexandre; LÜDERS, Ricardo. Performance assessment of DTN and VANET protocols for transmitting periodic warning messages in high vehicular density networks. Journal of Communication and Information Systems, v. 37, n. 1, p. 91–103, 2022. Available at: https://doi.org/10.14209/jcis.2022.10.

AMAYA, Álvaro T; POHL, AA; LÜDERS, Ricardo. Performance evaluation of gpsr and aodv routing protocols for high vehicular density vanets. In: SBRT. SBrT 2021, XXXIX Simposio Brasileiro de Telecomunicaçoes e Processamento de Sinais. DOI: 10.14209/sbrt.2021.1570724253. Fortaleza, CE., Brazil, 2021.

AMAYA, Alvaro T.; FONSECA, Mauro Sergio; POHL, Alexandre; LÜDERS, Ricardo. Traffic-aware beacon interval for position-based protocols in VANETs. 2022 IEEE Latin-American Conference on Communications (LATINCOM). Rio de Janeiro, Brazil, 2022 (to be published).

The papers contain most of the results of this work, including the evaluation of routing protocols in high traffic density environments, the comparison of DTN and traditional routing protocols for transmission of traffic information among neighbors, and the proposal for controlling the beacon time interval.

1.5 Thesis structure

The second chapter presents an overview of the mathematical models for: i) mobility of vehicles, with a special focus on microscopic models and car-following models; ii) and the energy consumption model. In Chapter 3, vehicular ad-hoc networks are introduced. This chapter includes the main structure of a VANET, the international standards, and protocols. In addition, a section with the main simulation tools is also presented. The adapted platform for simulation of VANETs is described in Chapter 4. Besides the enhanced software, the traditional method for the simulation of VANETs is also described. Two car-following models are simulated and compared for evaluation purposes. Chapter 5 presents an evaluation of a set of publicly available routing protocols for operation in a wide range of vehicular densities. This chapter allows the selection of the most suitable protocol for implementing the proposed scheme. The beacon scheme is presented in Chapter 6 with extensive simulations whose results are characterized by mobility and communication metrics. Conclusions and future work are presented in Chapter 7.

2 CAR-FOLLOWING AND ENERGY CONSUMPTION MODELS

This chapter presents a set of mathematical models that represent the typical behavior of a human-driven vehicle and an electric vehicle's energy consumption. The first part presents the most well-known car-following models (CFM), including a recently proposed VANET-based CFM. These models are expected to be ruled by traffic information transmitted through VANET. On the other hand, the energy model encompasses all the vehicle's physical dynamics responsible for energy consumption. It will be helpful for the evaluation of the energy efficiency of each CFM model.

Many traffic rules govern traffic flow for the safety of vehicles on the road. Researchers have introduced traffic flow models for analyzing road conditions and drivers' behavior. Traffic models usually employ microscopic and macroscopic parameters such as speed, flow, density, and inter-vehicle distance, as well as mathematical models and physicist theories. For instance, the fluid dynamics theory is employed to study the traffic flow from a macroscopic approach, and the kinetic theory is used to represent and establish a relationship between two different flow regimes (UMER *et al.*, 2010).

2.1 Car-following models

Vehicular traffic flow models can be classified into three categories: the level of aggregation (i.e. how reality is presented), the mathematical structure, and the conceptual aspects. Likewise, when considering the level of aggregation, there are three forms of mathematical modeling for real traffic events: macroscopic, microscopic, and mesoscopic (hybrid micro and macro) (JORDANOSKA; GJURKOV; DANEV, 2018).

- Macroscopic models: This kind of model describes the traffic flow as a fluid flow. Dynamic variables are quantities added locally, such as vehicular density $\rho(x,t)$, traffic flow $Q(x,t)$, average speed $V(x,t)$ or change in speed $\sigma V(x,t)$. Macroscopic models describe collective phenomena such as the evolution of congestion regions or the propagation speed of traffic waves. Likewise, they give an overview of the general traffic situation without distinction between single vehicles (FORSTER *et al.*, 2014). The observable values for this class of models are the vehicular density, the traffic flow, and the average velocity observed within a given road segment. The base equation for those models is the flow equation:

$$Q(x,t) = \rho(x,t) \cdot V(x,t) \tag{1}$$

  Typically, these parameters can be measured with loop detectors, the less common radar detectors, or visual detectors (FORSTER *et al.*, 2014).

- Microscopic models: These models describe the behavior of each driver (headway distance, acceleration, braking, changing lines) stemming from traffic around them (HARRI; FILALI; BONNET, 2009). This category includes the so-called Car-Following Model (CFM) and the overtaking model or lane change model Lane-Changing Model (LCM).

- Mesoscopic models: They are hybrid models built as a combination of macroscopic and microscopic models. In local models, the parameters of the microscopic model may depend on macroscopic quantities such as traffic density or local speed and changes in speed (JORDANOSKA; GJURKOV; DANEV, 2018).

Microscopic models can be helpful for energy efficiency strategies, this thesis focuses specifically on the CFM, as they encompass braking procedures, which are a possible source of energy recovery in Electric Vehicle (EV). Hence, in the following, three of the most popular CFMs are broadly described: The Optimal Velocity Model (OVM), the Intelligent Driver Model (IDM), and the modified Krauss (LAQUAI *et al.*, 2013). A recently proposed Multi-Anticipative (MA) model is also described.

2.1.1 Optimal Velocity Model OVM

The OVM is a simple and realistic traffic flow model that considers traffic congestion dynamics. The OVM was first proposed by Bando in 1995 (JIA; NGODUY; VU, 2018) and seeks to define the next acceleration step depending on the previous speed, the motorist's reaction time and a special function named the optimal velocity, which mainly depends on the inter-vehicular distance. The general formulation, as stated in (RAHMAN *et al.*, 2017) is as follows:

$$\ddot{x}_n(t) = \frac{1}{\tau_r}[V_{op}(\Delta x_n(t)) - \dot{x}_n(t)] \tag{2}$$

$$\Delta x_n(t) = x_{n-1}(t) - x_n(t) \tag{3}$$

with:
n - current vehicle,
$(n-1)$ - immediate leader vehicle,
$x_n(t)$ - position of vehicle n at time t,
$\dot{x}_n(t)$ - Speed of vehicle n at time t,
$\ddot{x}_n(t)$ - Acceleration of vehicle n at time t,
$\Delta x_n(t)$ - headway between the current and immediate vehicle at time t,
$x_{n-1}(t)$ - position of vehicle $(n-1)$ at time t,
τ_r - speed relaxation time, and
$V_{op}(\Delta x_n(t))$ - optimum velocity function of vehicle n at time t.

Later, in 1998 a delay parameter (t_d) was introduced to consider the reaction time of a driver (RAHMAN *et al.*, 2017) and equation (2) was revised as follows:

$$\tau\ddot{x}_n(t) + \dot{x}_n(t) = V_{op}(\Delta x_n(t - t_d)) \tag{4}$$

The optimum velocity (V_{op}) is the function of space headway, which is the distance from the subject vehicle's bumper to the preceding vehicle's bumper. Various versions of optimum velocity have been put forward. For instance, in (RAHMAN *et al.*, 2017) authors use the equation (5).

$$V_{op}(\Delta x_n(t - t_d)) = v_o \left[\tanh\left(\frac{\Delta x_n(t - t_d) - D}{B} - C_1\right) + C_2\right] \tag{5}$$

with:

v_o - desired speed of current vehicle,

D - effective length of current vehicle,

B - required distance for braking,

C_1 - length constant, and

C_2 - dimensionless constant

2.1.2 Intelligent driver model IDM

This model was proposed by Helbing in 2006 (JIA; NGODUY; VU, 2018). Similar to the OVM, the IDM is aimed to represent the next acceleration step depending on current speed and inter-vehicle distance. However, the IDM employs additional parameters, like the desired speed and distance. The formulation can be more complex than in OVM, as shown in (6).

$$\ddot{x}_n = a\left[1 - \left(\frac{\dot{x}_n}{\dot{x}_0}\right)^{\delta} - \left(\frac{s^*(\dot{x}_n,\Delta\dot{x}_n)}{s_n}\right)^2\right] \tag{6}$$

with:

a - acceleration,

$\dot{x}_0$ - desired speed when driving on a road,

$s^*(\dot{x}_n,\Delta\dot{x}_n)$ - desired minimum distance between vehicle n and $(n-1)$,

s_n - distance between vehicle n and $(n-1)$, and

δ - exponent for vehicle's acceleration

$$\Delta\dot{x}_n = \dot{x}_n - \dot{x}_{n-1} \tag{7}$$

The desired gap s^* is defined as follows:

$$s^*(\dot{x}_n,\Delta\dot{x}_n) = s_0 + \max\left\{0, \left(\dot{x}_n T + \frac{\dot{x}_n \Delta\dot{x}_n}{2\sqrt{ab}}\right)\right\} \tag{8}$$

with:
T - time headway to safely follow immediate leader vehicle,
b - braking deceleration, and
s_0 - minimum headway between the current and immediate vehicle in front.

2.1.3 Krauss model

This model was introduced by Stefan Krauss in 1998 and is one of the most employed. Particularly, the SUMO mobility simulation software (LOPEZ *et al.*, 2018a) utilizes this model in default configuration (MINTSIS; MITSAKIS, 2018). Like previous models, the Krauss employs current speed and distance values from the preceding and the driven vehicle. However, unlike other models, the Krauss computes the next speed step and employs a more straightforward formulation. According to Krauss model (ASAITHAMBI *et al.*, 2018), the safe speed v_{safe} at time t can be computed as:

$$v_{safe} = v_l(t) + \frac{d(t) - v_l(t)t_r}{\frac{v_l(t)+v_f(t)}{2b_m} + t_r} \tag{9}$$

such that $v_l(t)$ is the speed of the preceding vehicle, $v_f(t)$ is the speed of the follower vehicle, $d(t)$ is the distance between vehicles, t_r is the driver's reaction time (around one second), and parameter b_m is the maximum deceleration of a vehicle.

Due to the dynamic constraints of a vehicle, given by its maximum speed v_{max} and acceleration a, the new vehicle speed is calculated, within a given sample time t, according to:

$$v_{des} = \min\{V_{max}, v + a\cdot t, v_{safe}\} \tag{10}$$

With the rising of vehicular communication technologies and connected vehicles, the more recent approaches have focused on enhancing the CFM capabilities by harnessing vehicular kinematic information (i.e. position and speed). Such information can be transmitted across ad-hoc networks and introduced for computation in the above described mathematical models or even for connected vehicles control formulations. One of the most recent approaches is the Multi-Anticipative model described in the following.

2.1.4 Multi-Anticipative model (MA)

Proposed in 2019 by (KUANG *et al.*, 2019), the Multi-Anticipative model MA corresponds to an adaptation of the Full Velocity Difference (FVD) model (JIANG; WU; ZHU, 2001), which in turn is an enhancement of the OVM. The anticipative model extends the optimal and average speed concepts to all preceding vehicles in the transmission range. The general formulation is as follows:

$$\frac{dv_n(t)}{dt} = a[(1-p)V(\Delta x_n(t)) + pV_{mf}(\Delta x_n(t)) - v_n(t)] + \lambda[\overline{v}_n(t) - v_n(t)] \tag{11}$$

Where $V(\Delta x_n(t))$ corresponds to the optimal speed used in OVM, and can be computed according to (5). The factor $V_{mf}(\Delta x_n(t)) = \frac{1}{r}\sum_{l=1}^{r}(\Delta x_{n+l}(t))$ is called the mean expected speed, and reflects the optimal average speed of all the r preceding vehicles. The $\overline{v}_n(t)$ element represents the current average speed of preceding neighbors, and p corresponds to the weight of the current optimal speed regarding the $V_{mf}(\Delta x_n(t))$ factor. The driver sensitivity to headway a and the relative speed sensitive coefficient λ are consistent with the formulations of the OVM and FVD, respectively.

Many other VANET-based CFM approaches are available in literature, for instance (CAO; WANG; CHEN, 2020; LI *et al.*, 2020; JIAO *et al.*, 2020; RAHMAN *et al.*, 2017; BAKIBILLAH *et al.*, 2019), most of them considering a restricted group of neighbors. However, the hypothesis guiding this work is that the more information a vehicle has, the more energy savings it achieves. Hence, the MA model is chosen.

2.2 Energy consumption model for electric vehicles

As stated previously, this work aims to propose novel strategies for sharing information among vehicles to enhance energy efficiency. Different from gasoline vehicles, the electric motor of an EV is more efficient at lower torques and can perform more complex speed profiles for energy saving (VAHIDI; SCIARRETTA, 2018). Therefore, the energy consumption model described in the following is developed explicitly for this kind of vehicle.

According to the fundamental theory of vehicle dynamics, the instant power of an electric vehicle is given by the vehicle speed and acceleration besides the road slope (WU *et al.*, 2015). According to physics laws, the required tractive force acting upon a vehicle can be described as

$$F = m\,a + R_a + R_{rl} + R_g \tag{12}$$

where F is the required tractive force, m is the mass of the vehicle, a is the acceleration, and R_a, R_{rl} and R_g are aerodynamic, rolling, and grade resistance, respectively, given in SI units. In this work, the force F, from (12) is required to be computed in a discrete form at each

mobility update interval. The resistance factors are expressed as follows:

$$R_a = k\,v^2 = \frac{\rho_a}{2} C_D A_f\,v^2 \tag{13}$$

$$R_{rl} = f_{rl}\,m\,g \tag{14}$$

$$R_g = m\,g\,sin(\theta) \tag{15}$$

where v corresponds to the vehicle speed, and k is a constant that depends on the air density ρ_a, the frontal area of the vehicle A_f, and the drag coefficient C_D. In the other factors, f_{rl} means the rolling resistance constant, g is the gravity acceleration, and θ the roadway grade. For simplicity in the initial approach, the roadway grade is assumed as zero, so the R_g factor is dismissed.

The mechanical power p required for a vehicle to move at speed v can be calculated with:

$$p = Fv = (m\,a + k\,v^2 + f_{rl}\,m\,g)v \tag{16}$$

The mechanical power corresponds to the output power of the electric motor shaft, while the electrical power P, which is consumed by the motor, is related to the output power through the efficiency factor η as

$$p = \eta P \tag{17}$$

If accessories for entertainment or temperature control are disregarded, the major sources of electrical losses correspond to those related to the motor windings (in the case of a DC motor) or losses in the iron (for an AC motor). In general, electric power losses can be represented as the product of the square of the electric current I and the conductor resistance r (TANAKA; ASHIDA; MINAMI, 2008; WU *et al.*, 2015). As a result, efficiency can be calculated by

$$\eta = \frac{(P - I^2 r)}{P} \tag{18}$$

with I given in Ampere and r in Ohms. From (18), (16) and (17) we obtain

$$P = I^2 r + F\,v \tag{19}$$

where F is the motor induced force, which can be represented as the ratio of the torque τ and the tire radius R. The torque, in turn, can be expressed as the product of the armature constant K_a, the magnetic flux ϕ_d, and the electric current I.

$$F = \frac{\tau}{R} = \frac{K_a\,\phi_d\,I}{R} \tag{20}$$

The magnetic flow ϕ_d corresponds, in the case of the DC motor to the flux in the direct axis by pole, and for the case of AC motors to the rms value. If the flow is regarded as a constant, then

$$K = K_a \phi_d \tag{21}$$

Then, equation (20) becomes:

$$F = \frac{KI}{R} \tag{22}$$

Using F as stated in (16) and solving (22) for I, the motor's electric losses Pm, represented by the I^2r factor in (19) can be expressed as:

$$Pm = \frac{R^2}{K^2}(m\,a + k\,v^2 + f_{rl}\,m\,g)^2 \cdot r \tag{23}$$

The remaining (Fv) factor in (19) can be expressed from (16) as the sum of energy losses due to resistance to movement (P_t) as stated in (24), and the possible energy gains as a result of accelerating or decelerating (P_g) as in (25).

$$P_t = v\,(k\,v^2 + f_{rl}\,m\,g) \tag{24}$$

$$P_g = m\,a\,v \tag{25}$$

Finally, the total motor input power can be obtained as

$$P = Pm + P_t + P_g \tag{26}$$

As stated before, the computation of force and, hence, power is to be made into a mobility update interval, which we can define as Δt. So, the flux of energy, from or towards the battery, for a given time interval can be computed as

$$E = P\Delta t \tag{27}$$

2.2.1 Regenerative braking

Regenerative Braking Systems (RBS) have been widely addressed, and some publications outline the overall process and the mathematical modeling based on the vehicle's physical characteristics (mass, inertia, distance, speed, etc.). In (XU *et al.*, 2016) the authors describe the kinetic energy dissipated in the mechanical braking process states, which is equivalent to an average of 50% of the energy required for the normal traction process. Other studies point out an increase between 8 % and 25 % in the realizable distance using regenerative braking and a favored condition for applying this technology in scenarios with frequent speed fluctuations.

According to (CODY *et al.*, 2009), besides the conditions mentioned above, the regenerative braking process depends on the battery State of Charge (SoC); the lower the SoC, the highest the effectiveness of the brakes. If SoC is too high, energy must be dissipated over a resistance. The braking process still corresponds to Hybrid Braking Systems (HBS) (regenerative and mechanical), mainly due to safety reasons and the low effectiveness of regenerative braking at low speeds. However, authors such as (XU *et al.*, 2016) propose a fully regenerative system called Fully Regenerative Systems (FE-RBS).

There are mainly two kinds of forces during vehicle braking, as shown in Figure 1. One is the wheel braking force that the braking actuators directly apply on wheels to make them step down. Another is the vehicle braking force generated by the tire-road contact to decelerate the vehicle. From the wheel dynamics point of view, the vehicle braking force makes the wheel accelerate around the axle. Assuming that the forces on the left and right tires are the same, the dynamic equations of the wheel and the vehicle take the forms:

Figure 1 – Dynamics of vehicle braking.

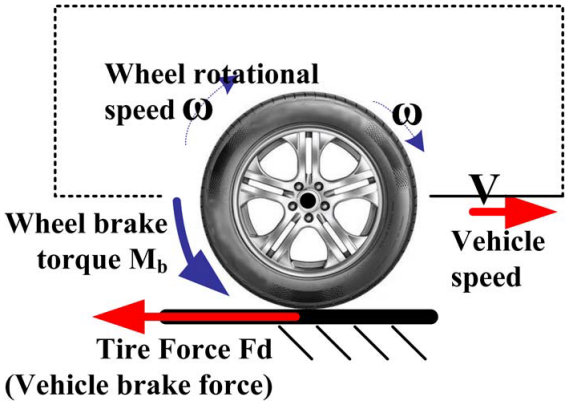

Source: Adapted from Xu *et al.* (2016).

$$-M_b + RF_d = J\dot{\omega} \tag{28}$$

$$-F_d = m\dot{V} \tag{29}$$

Where M_b is the braking force generated by the motor that functions as a generator; F_d, J, and ω are the tire–road friction force, the wheel inertia, and the wheel rotational speed, respectively; m is the vehicle mass, and V is the vehicle longitudinal speed.

2.3 Chapter summary

This chapter addresses theoretical concepts and related works, encompassing general traffic modeling concepts, such as flow, global and local density. Specifically, the OVM, IDM, Krauss, and Multi-Anticipative car-following models have been described. The last one has been chosen to implement the energy-efficient and traffic-aware proposal that guides this work.

This chapter also describes the energy consumption model for evaluating energy efficiency, including regenerative braking concepts. These concepts are addressed as they are necessary to understand the energy consumption profiles in microscopic modeling.

3 VEHICULAR AD-HOC NETWORKS

Vehicular Ad-Hoc networks VANETs are considered the basis of Cooperative Advanced Driver Assistance Systems (CADAS) (JIMÉNEZ *et al.*, 2016). They have become an active area of research in recent years due mainly to the great benefits their implementation can bring to the so-called “Smart Cities". This chapter presents a general review of standards, routing protocols, and simulation tools. Special focus is given to publicly available resources.

The VANETs can be regarded as a subcategory of the Ad-hoc mobile networks (MANETs) with specific and challenging characteristics, mainly due to the high mobility of nodes and frequent breaking of communication links. A VANET can help in preventing accidents, reducing traffic congestion, avoiding obstacles, preventing speed limit violations, internet access, weather information, and multimedia services, among others (QURESHI; ABDULLAH; LLORET, 2016).

A VANET can provide communication Vehicle To Vehicle (V2V), Vehicle To Infrastructure (V2I), Vehicle To Person (V2P), or hybrids Vehicle To Everything (V2X) (ALLOUCHE; SEGAL, 2015). Despite the flexibility and stability that hybrid networks can entail (JUSSIANI *et al.*, 2019), this work focus specifically on V2V networks as major attention is given to studying the high-density traffic impact on VANETs. In such conditions, multiple routing paths are simultaneously available, so no need for additional network resources exists.

An example of exclusive V2V approach can be found in (WON; PARK; SON, 2017), where authors propose a phantom jam’s control scheme using V2V topology and consider road segments, including a fuzzy inference system with a congestion detection algorithm. Another example can be found in (LI *et al.*, 2020), where authors assess the impact of V2V messages on traffic dynamics by performing a test using a set of vehicles.

Also in V2V focused to provide information for a CFM, authors in (CAO; WANG; CHEN, 2020) present a traffic-density awareness approach. A similar approach can be found in (RAHMAN *et al.*, 2017), where the beacon transmission delay is taken into account. The proposal in (JIA; NGODUY; VU, 2018) is a platoon approach wherein leader vehicle information is transmitted to followers with a certain probabilistic delay over V2V links.

3.1 Standards in VANETs

The objective to be achieved with a V2X network is that each vehicle, infrastructure item, and road-user equipment use a module for vehicular communications specifically enabled for Dedicated Short Range Communications (DSRC). The DSRC is a set of protocols grouped in an International Organization for Standardization (ISO) tower, as shown in Table 1. These protocols include, for example, the well-known Internet protocols for the Network and Transport layers, i.e., Internet Protocol version 6 (IPv6), User Datagram Protocol (UDP) and Transmission Control Protocol (TCP) (KENNEY, 2011).

Table 1 – ISO protocol layer for V2X communications.

ISO Layer	Protocol
Application	Application Message Set
TCP and Basic Transport Sublayer	ETSI EN 302 636-5-1
GeoNetworking Layer	ETSI EN 302 636-4-1
Logical Link Layer	IEEE 802.2
MAC Layer	IEEE 802.11
Physical Layer	IEEE 802.11p

Source: Own elaboration (2022).

As for the physical layer, the DSRC PHY protocol is defined in Institute of Electric and Electronic Engineers (IEEE) 802.11, as amended by IEEE 802.11p. It is divided into two sublayers: the Physical Medium Dependent (PMD) sublayer and the Physical Layer Convergence Procedure (PLCP) sublayer. As its name suggests, the PMD interfaces directly with the wireless medium. It utilizes the Orthogonal Frequency Division Multiplexing (OFDM) technique, originally added to 802.11 in the 802.11a amendment. The PLCP defines the mapping between the MAC frame and the basic PHY layer data unit (KENNEY, 2011).

The IEEE 802.11p supports data transmission at the physical layer in a range of up to 1000 meters (HUANG; SHERE; AHN, 2010). As above-mentioned, this protocol is an extension of WiFi wireless data transmission, adapted to transport. Both the link and MAC layers use standard protocols inherited from classical wired communications (JIMÉNEZ *et al.*, 2016). IEEE 802.11p supports data exchange between high-speed vehicles and between the vehicles, and the roadside infrastructure (JIA; NGODUY, 2016). Additionally, IEEE Wireless Access in Vehicular Environment (WAVE) suite is the defacto vehicular networking standard adopted as the V2X communication protocol. According to the standard of IEEE 1609.4, all traffic information is broadcasted in the control channel via Contention-Based Carrier Sense Multiple Access with Collision Avoidance (CSMA/CA) mechanism (JIA; NGODUY, 2016).

As for the DSRC spectrum, the Federal Communication Commission (FCC) has allocated the spectrum from 5.850 GHz to 5.925 GHz, i.e. the B5.9 GHz band, for DSRC operation in the United States (KENNEY, 2011). This spectrum is divided into seven 10 MHz channels; four are for service purposes, one for beaconing, and the other for future use, as shown in Figure 2.

Figure 2 – DSRC channels distribution.

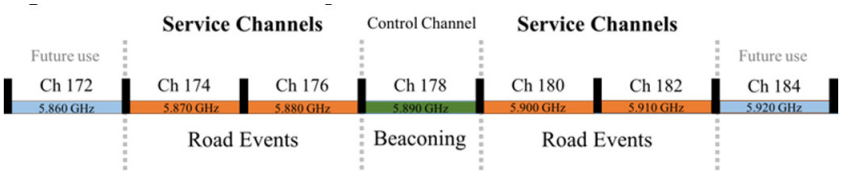

Source: Adapted from Rezgui, Dally-Bélanger e Rivest (2018).

In the control channel (Beaconing), there are two types of information; one of them is the notification of events, also known as Event-Driven (dangerous situations warning), which are quick messages that do not represent a significant burden on the network. The other one is the

dissemination of periodic warning messages, the so-called Beacons, where each vehicle reports its current state (position, speed, and direction), and even a unique vehicle identifier and a time stamp (KNORR *et al.*, 2012). Furthermore, in (QURESHI; BASHIR; ABDULLAH, 2017) authors point out that acceleration may also be embedded in beacons.

Security applications relying on beacon information are also known as cooperative warning applications, which usually need real-time characteristics (Vehicle Collision Warning and Cooperative Awareness Applications). Nevertheless, despite not having strict time requirements, beacons can cause a more significant load on the channel (ALLOUCHE; SEGAL, 2015).

The IEEE 802.11p standard uses CSMA/CA as the MAC method, which has already reported a vast number of limitations specially on high vehicle congestion scenarios (ALLOUCHE; SEGAL, 2015),(GUNTER; WIEGEL; GROSSMANN, 2007),(LU; POELLABAUER, 2010),(BILSTRUP *et al.*, 2008). Some scholars report situations with eight vehicles per kilometer density where only ten percent of the data is transmitted without collisions. Other sources report up to 80 % of packet losses, demonstrating that the 802.11p protocol could not be an option viable for real-time information transmission in security applications.

3.2 Traditional Routing Protocols

Because of the high mobility of nodes in VANETs, the projection of routing protocols has become a challenging and active research issue. So far, several routing protocols have been proposed. Some have been created, adapted, or enhanced from existing Mobile Ad-hoc Networks (MANET) protocols (YU; YOO; AHN, 2013). Four major categories of routing protocols can be found in VANET: Topology-based, Broadcast, Cluster-based, and Position-based protocols. The Figure 3 presents a general view of the taxonomy of routing protocols in VANET, along with examples of each category.

Figure 3 – A taxonomy of routing protocols for VANET.

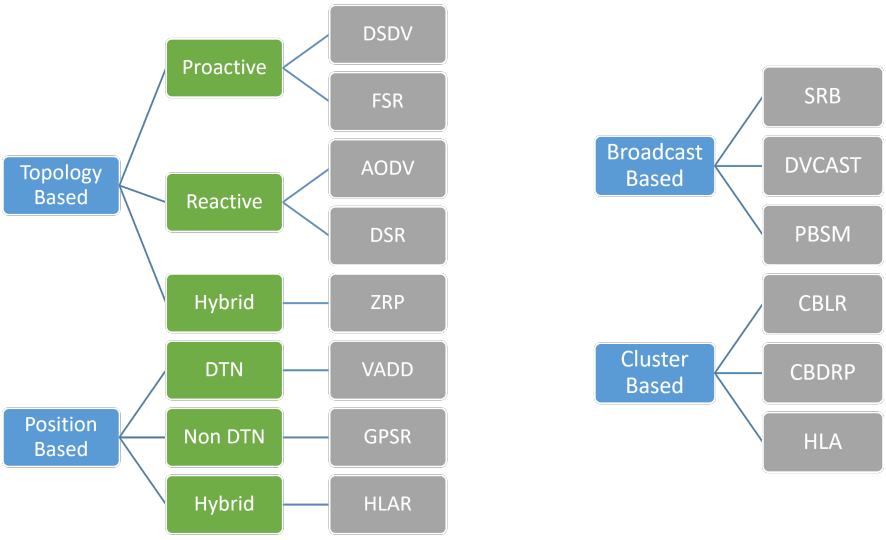

Source: Own authorship (2022).

The Topology-Based Protocols (TBR) can be either proactive or reactive, depending on whether the routing path is previously or dynamically created. A typical example of a proactive protocol is the Destination-Sequenced Distance Vector (DSDV) protocol (MOHAPATRA; KANUNGO, 2012), in which a routing table containing information about each node is continuously updated. A typical reactive protocol is the Ad-hoc On-demand Distance Vector (AODV) (RAJPUT *et al.*, 2010), which creates the routes depending on whether they are necessary or not.

The AODV is one of the most common routing protocols for mobile ad-hoc networks (WANG; CUI, 2008). AODV combines the destination sequence number and the on-demand route technique. This technique can cause low overhead as nodes do not need to maintain unnecessary route information. To handle route information, AODV utilizes three different kinds of route messages: Route Request (RREQ), Route Reply (RREP), and Route Error (RERR). The route discovery consists of two phases: i) sending RREQ through the network; ii) looking for a destination and waiting for RREP (WANG; CUI, 2008). Besides using RREQ, RREP, and RERR, AODV employs locally periodic broadcast messages, the so-called beacons or *Hello* packets.

Such packets can periodically exchange a wide variety of information, such as position, velocity, density, and direction of the vehicles (SILVA *et al.*, 2019). The *Hello* messages are employed to keep a node aware of the localization of other nodes into the transmission range and to detect the loss of connectivity with a specific neighbor.

As its name suggests, the Position-Based Protocols (PBR) depend on the nodes' localization to deliver a message. Among the PBR options, we find the Delay Tolerant Networks (DTN), the Vehicle-Assisted Data Delivery (VADD) (ZHAO; CAO, 2008); the Non-DTN protocol, such as the Greedy Perimeter Stateless Routing GPSR (KARP; KUNG, 2000), and the Hybrid protocols, such as the Hybrid Location-Based (HLAR) (AL-RABAYAH; MALANEY, 2010).

The localization information that PBR protocols need can be obtained via Global Position Systems Global Positioning System (GPS) or short-range localization devices. The GPSR is a PBR protocol that selects the next hop for transmission in a greedy manner (ALZAMZAMI; MAHGOUB, 2021). That means the next forward node is that with the minimum remaining euclidean distance to the destination. For instance, in Figure 4 the source node (S) chooses the forwarder (x) as it is the closest node to the destination (D) among the neighbors of (S). The same criteria are therefore used by the node (x) to choose the node (y), which finally delivers the packet to (D).

However, in certain situations, the greedy forwarding routing scheme reaches a local maximum. It occurs when the chosen forwarder node can not find a closer node to the destination than itself, as in the case of node (x) in Figure 5. In such a situation, node (x) must switch to the so-called perimeter mode (SILVA *et al.*, 2019), and the next forward node is selected using the right-hand rule (RAHIMI; JAMALI, 2019). This rule states that once the packet arrives at node (x), the next traversed path is the one that is sequentially counterclockwise around (x) from the

Figure 4 – Greedy forwarding strategy in GPSR.

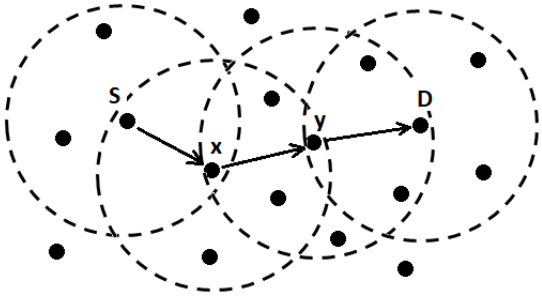

Source: Own authorship (2022).

incoming path (ALSAQOUR *et al.*, 2015). Hence in Figure 5 node (x) delivers the packet to node (y), and node (y) to node (z), who finds the destination (D).

Figure 5 – Perimeter forwarding strategy in GPSR.

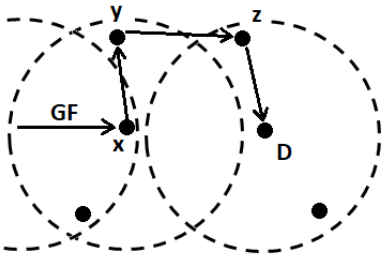

Source: Own authorship (2022)..

Each node in GPRS is expected to periodically exchange its kinematic information with its one-hop neighbor using beacon messages (*Hello* packets) in a broadcast fashion. Beacons are periodically transmitted by each vehicle and can include a wide variety of information, such as position, velocity, density, and direction of the vehicles (SILVA *et al.*, 2019). The format of a *Hello* message is shown in Figure 6.

Figure 6 – Format of *Hello* message broadcasted by every node.

Preamble	Broadcast time	Node ID	Node position	Node velocity	Check code

Source: Own authorship (2022).

Based on the information of *Hello* packets, the source node chooses the node closer to the destination. However, if the source does not receive any response from a neighbor within a time-out interval, it considers the communication link broken.

Other categories, such as the Broadcast Routing Protocols, seek to send traffic, weather, emergency, and road information to all neighbors without concern for entries on routing tables or specific paths. Most known broadcast routing protocols are Secure Ring Broadcasting (SRB) (TONGUZ *et al.*, 2007), Distributed Vehicular broadcast (DVCAST) (Tonguz; Wisitpong-

phan; Bai, 2010), and Parameterless Broadcast in Static to highly Mobile (PBSM) (TASSOULT *et al.*, 2019).

Finally, the Cluster-based Routing Protocols are useful in overcoming the instability of nodes in VANETs, stemming from the frequent mobility of vehicles. In a cluster, vehicles are self-organized in a structure with a leader (cluster head) and relay nodes for communication with other clusters (cluster gateways), as depicted in Figure 7. Most known clustered-based routing protocols are: Cluster-Based Location Protocol (CBLR) (KAKARLA *et al.*, 2011), and Cluster-Based Directional Routing Protocol (CBDRP) (ABUASHOUR; KADOCH, 2018).

Figure 7 – Topology for cluster-based V2V networks.

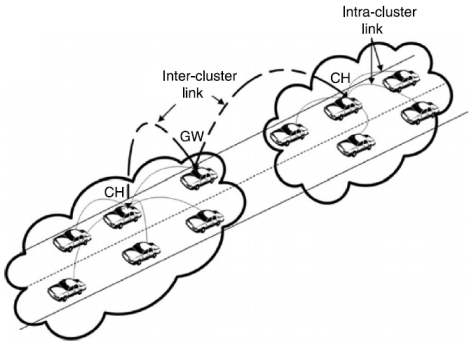

Source: Adapted from Maslekar *et al.* (2013).

3.3 Delay Tolerant Network Protocols

Delay tolerant networks (DTN) were first proposed for enabling communication between satellites, surface rovers, and other appliances in the interplanetary network (IPN) (HAMZA-CHERIF *et al.*, 2018). This network paradigm operates under the concept of Store, Carry, and Forward (SCF); and was envisioned to perform in harsh environments, such as space exploration. However, due to the remarkable advantages of DTN, they became to be applied to other kinds of networks, such as the Wireless sensor (WSN), MANETs, and VANETs.

Unlike traditional VANET, a DTN does not require a stable connection between sender and recipient to transmit a message (HAMZA-CHERIF *et al.*, 2018). In DTN, a forwarder vehicle stores a message and waits for a suitable hop. Therefore, these kinds of networks are well-adapted to network disconnections and disruptions. It makes the DTN the most suitable option for traditional routing protocols in VANETs (Gonçalves Filho *et al.*, 2016).

The DTN can be classified using a large variety of criteria. However, in this work, we categorize them according to the dependence upon knowledge. Hence, we can find both the knowledge-based and the zero knowledge-based, as depicted in Figure 8. The former, in turn, can also be classified in Contact & social, geographic, Road Map, and Online. The Figure 8 provides the classification and a representative example of each category.

Figure 8 – A taxonomy of DTN routing protocols.

Source: Own authorship (2022).

3.3.1 Direct Delivery

The Direct Delivery is the most straightforward DTN protocol and was presented by Spyropoulos, Psounis, and Raghavendra (SPYROPOULOS; PSOUNIS; RAGHAVENDRA, 2004) in 2004. In this zero-prior knowledge protocol, a node A, which intends to communicate with a node B, hosts and carries the message until it attains direct contact with node B, and finally delivers the data (Gonçalves Filho *et al.*, 2016). The direct delivery makes no intermediate forward, so the major drawback is the possibility of the sender not finding the recipient. Therefore, the Direct Delivery is likely to feature the lowest delivery ratio and the highest delay among all approaches, as stated by the same authors (HAMZA-CHERIF *et al.*, 2018).

3.3.2 Epidemic

Proposed by Vahdat et al. in (VAHDAT; BECKER *et al.*, 2000), the epidemic is a multi-copy protocol that implements flooding in a DTN and does not need prior knowledge of the network (BENAMAR *et al.*, 2014). Each bundle is exchanged with every node at a contact opportunity. Hence, thanks to the multiple-path options, each bundle is expected to fast arrive at its final destination. However, the epidemic protocol needs to compare which bundles are not in common with other nodes, which can lead to an increase in delay and generate more overhead than the non-DTNs (TORNELL *et al.*, 2015).

The flooding nature of the epidemic protocol could permit a high delivery rate. However, when the buffer achieves the maximum capacity, the arrival of a new message can lead to the drop of the older ones. This fact, in turn, reduces the delivery rate. To overcome this burden and

other issues, the Epidemic needs higher storage capacity and bandwidth than other protocols. Moreover, the Epidemic protocol could be the optimal solution in an environment with no buffer space/bandwidth limits (BENAMAR *et al.*, 2014).

3.3.3 Binary Spray and Wait

The Spray&Wait protocol (SNW) (SPYROPOULOS; PSOUNIS; RAGHAVENDRA, 2005) is also a zero-knowledge protocol, which combines features of both Epidemic and Direct Delivery approaches. However, unlike Epidemic, the Sprat&Wait limits the number of copies created per bundle to N. As its name suggests, Spray&Wait encompasses two phases. In the spray phase, a node disseminates a certain number of copies of a message, and in the Wait phase, when only one copy remains, the node hopes to find a suitable node to deliver the last copy of the message (Gonçalves Filho *et al.*, 2016).

The SNW can operate in two different Spray modes (SPYROPOULOS; PSOUNIS; RAGHAVENDRA, 2005). The normal Spray, where the source node forwards one of the copies to each neighbor node, and the Binary spray mode (BS&W), where the source node forwards (N/2) copies to the neighbor node and keeps (N/2) for itself. If only one copy remains, the Binary Spray And Wait (BS&W) switches to direct transmission and enters the Wait phase as before mentioned (TORNELL *et al.*, 2015).

3.3.4 PRoPHET

The Probabilistic Routing Protocol using History of Encounters and Transitivity (PRoPHET) (LINDGREN; DORIA; SCHELÉN, 2003) is an information-based forwarding protocol and was the first contact history-based protocol (HAMZA-CHERIF *et al.*, 2018). In Probabilistic Routing Protocol using History of Encounters and Transitivity (PRoPHET), the transmission of a message to a forwarded node depends on the probability of that node contacting the destination node. This protocol uses a metric called delivery predictability, which defines the probability of a node a to meet a node b ($P(a,b)$) and, consequently, the chance to deliver a message successfully. Hence, a suitable forwarder node is the one that has a high probability of meeting the recipient one.

The predictably enhances as long as the nodes meet each other more times. Hence, the more frequent the encounter of the two nodes, the higher the probability of delivering a message, and the more suitable the node a becomes to be a forwarder. On the other hand, if the nodes a and b lose contact, the value of $P(a,b)$ must age and will be reduced since the probability of meeting each other becomes lower (Gonçalves Filho *et al.*, 2016).

As stated in its name, the PRoPHET also employs the so-called transitivity metric. This property extends the concept of predictability to involve a third node. The transitivity represents

the potential of a node *a* to meet a node *c* given that *a* meets a node *b* and *b* meets the node *c*. As in the previous case, the higher the transitivity, the more suitable the node *a* becomes to be a forwarder.

Despite the large variety of approaches, evaluating routing protocols in real scenarios is still challenging, mainly because of the high cost of realistic deployment of VANET technology and the lack of conclusive evidence about the network's reliability. Hence, an affordable way is employing simulation tools, which can be used to evaluate the effectiveness of an approach and compare it with other proposals. In the following section, the most employed simulation tools will be described in order to find the most suitable choice for developing this work.

3.4 Simulation tools

The deployment of VANETs can be a very challenging and expensive mission, particularly if not enough attention is given to studying potential mobility issues and other technical constraints. Hence, simulation tools have been extensively employed to reduce costs and anticipate potential limitations. Typically, a VANET simulator features two parts: mobility and network simulators. These parts can also operate both separately or on a monolithic platform. In the following, both of them are described.

3.4.1 Mobility simulators

Mobility simulators are commonly used to generate mobility traces as input to a network simulator. These traces include the location of each vehicle at every time instant of the simulation, and their mobility profiles. In the following, some of those tools are briefly presented.

VanetMobiSim: This is an extension of the CANU Mobility Simulation Environment (CanuMobiSim), which focuses on vehicular mobility. This tool can be used for both macroscopic (a large number of cars) and microscopic (individual and detailed car behavior) simulations. For microscopic simulation, this software features mobility models such as Intelligent Driving Model with Intersection Management (IDM/IM), Intelligent Driving Model with Lane Changing (IDM/LC), and an overtaking model (MOBIL). VanetMobiSim is based on JAVA and can generate movement traces in different formats, supporting different simulation tools for mobile networks, including ns-2, GloMoSim, and QualNet (MARTINEZ *et al.*, 2009).

SUMO (Simulation of Urban Mobility): It is an open-source and free-of-charge traffic simulator. It can perform microscopic simulations with many roads (up to 10000 streets). This tool includes multi-lane streets, lane changing, collision-free vehicle movement, different types of vehicles, and even a graphical user interface (GUI). Likewise, SUMO can be combined with the OpenStreetMap platform to perform traffic simulation in different locations of the globe (LOPEZ

et al., 2018b). Despite SUMO being a pure traffic generator, its generated trace files can be directly used by the ns-2 network simulator.

MOVE (Mobility model generator for Vehicular networks): This is a traffic simulation tool built on top of SUMO. It also can generate trace files for VANET simulation, but these can be immediately used by popular network simulation tools such as ns-2 or GloMoSim. An important feature is a GUI that enables the user to generate simulations without concern for complex scripts or the internal functioning of the software (LAN, 2010).

CityMob v.2: This mobility traffic generator is ns-2 compatible. It includes various mobility models, which depend on the level of realism and complexity. The most known models are the Manhattan Model (MM) and the realistic Downtown Model (DM). CityMobDM also allows the user to use multiple lanes in both directions, vehicle queues due to traffic jams, and even the possibility of having more than a downtown (PEREZ, 2011).

Other traffic simulation platforms focus directly on driver assistance systems. For instance, the CARLA simulator, an open-source autonomous driving simulator primarily envisioned to support the development, training, and validation of autonomous driving systems (CARLA, 2022). Despite the realistic environment and the large variety of traffic simulation options, such a platform does not permit integration with a network simulator to evaluate VANETs.

A brief comparison of mobility simulators according to the most relevant features is presented in Table 2.

Table 2 – Comparison among mobility simulators.

	VanetMobiSim	**SUMO**	**MOVE**	**CityMob**	**CARLA**
Microscopic model	✓	✓	✓	✓	✓
Multilane	✓	✓	✓	✓	✓
ns-2 trace support	✓	✓	✓	✓	x
ns-3 trace support	x	✓	x	x	x
GloMoSim trace support	✓	x	✓	x	x
QualNet trace support	✓	x	✓	x	x
JiST/SWANS trace support	x	x	x	x	x
Continuous development	x	✓	x	x	✓
Opensource	✓	✓	✓	✓	✓

Source: Adapted from (MARTINEZ *et al.*, 2009).

3.4.2 Network simulators

Network simulators are used to reproduce communication schemes. They feature a set of resources, such as nodes, link protocols, channel models, etc. A network simulator helps study network behavior before the final deployment. Users can customize them for specific needs, for example, by defining nodes, links, traffic, or selecting routing protocols as necessary for VANET simulation. In the following, some network simulators are described.

ns-2: is a discrete event simulator developed at the University of California at Berkeley and later improved by the Monarch research group at Carnegie Mellon University. It is a widely known open-source tool for network simulation that features, among others, a realistic physical layer with a radio propagation model, radio network interfaces, and the IEEE 802.11 Medium Access Control (MAC) (MARTINEZ *et al.*, 2009).

ns-3: is another discrete-event network simulator targeted primarily for research and educational use. As with ns-2, it is a free of charge and open source tool, licensed under the GNU GPLv2 license, and is publicly available for research, development, and use. It has a slightly different structure from ns-2, so it is not considered a new release of ns-2 but a brand new software. Some remarkable features include models for Wi-Fi, WiMAX, or LTE, as well as a variety of static or dynamic routing protocols, such as OLSR and AODV for IP-based applications. However, ns-3 is often criticized for its lack of support for some protocols, which were supported in ns-2 (PROFENTZAS, 2012).

GloMoSim: is a discrete-event network simulator for wireless and wired networks, built using layers, each hosting different APIs. The widely used QualNet simulator is a commercial version of GloMoSim (CHITRA; SIVASATHYA; MUTHAMIZH, 2014).

JiST/SWANS: is a combination of two platforms, JiST and SWANS. The first is a Java-based discrete event simulation engine, which runs as a simulator into a virtual machine. This tool outperforms existing highly optimized simulation engines in time and memory consumption. On the other hand, SWANS is a scalable wireless network simulator built over the JiST platform. Its capabilities are similar to ns-2 and GloMoSim, but SWANS is able to simulate much larger networks, using the same amount of time and memory and with the same level of detail (MARTINEZ *et al.*, 2009).

OMNeT++ is an extensible, modular, component-based C++ simulation library and framework primarily for building network simulators. So, although it is not a network simulator itself, it has gained widespread popularity as a network simulation platform. OMNeT++ provides a component architecture for models. Components (modules) are programmed in C++, then assembled into larger components and models using a high-level language (NED) (OMNET++, 2022).

Table 3 summarizes and compares the most important features of the network simulators described above.

3.4.3 Vanet simulators

The VANET simulators can be regarded as platforms for integrating mobility and network simulators. These platforms can change vehicles' behavior depending on a given context. In the following, some of these tools are shortly described.

TraNS (Traffic and Network Simulation Environment): This open-source simulation platform project combines a mobility generator and a network simulator. It allows vehicles to change

Table 3 – Comparison of network simulators.

	ns-2	ns-3	GloMoSim	JiST/SWANS	OMNeT++
IEEE802.11p support	✓	✓	x	x	✓
Easy to setup	Easy	Easy	Moderate	Hard	Moderate
Easy to use	Hard	Hard	Hard	Hard	Moderate
Traffic road model	x	x	x	x	x
Support for learning	High	Poor	Poor	Poor	Poor
Support for Protocols	High	Poor	Poor	Moderate	Moderate
Continuous development	✓	✓	x	✓	✓

Source: Adapted from (MARTINEZ *et al.*, 2009).

their velocity behavior due to a broadcast transmission. TraNS is written in Java and C++ and works under Linux and Windows (trace-generation mode). The current implementation of TraNS uses the SUMO traffic simulator and the ns-2 network simulator. Some remarkable features of TraNS v1.2 include: support for realistic 802.11p, mobility trace generation for ns-2, the coupling of SUMO and ns-2 through the TraCI interface, the possibility to simulate road traffic events (e.g. accidents), and even allows for Google Earth visualization of simulations (PIORKOWSKI *et al.*, 2008).

GrooveNet: this platform was meant to communicate simulated and real vehicles. It incorporates mobility, trip, and message broadcast models over a variety of link and physical layer communication models. It even provides multiple network interfaces and allows simulations of GPS and event-triggered (from the vehicles' onboard computer). GrooveNet allows both V2V and V2I communication and supports multiple message types such as GPS messages, which are broadcasted periodically to inform neighbors about the vehicle's current position, and for transmitting vehicle emergency and warning event messages with priorities, (MARTINEZ *et al.*, 2009).

NCTUns (National Chiao Tung University Network Simulator): it is a high-fidelity and extensible network simulator and emulator for wired and wireless IP networks. Supported networks on NCTUns include wireless vehicular networks for Intelligent Transportation Systems (including V2V and V2I), multi-interface mobile nodes for heterogeneous wireless networks, IEEE 802.16e mobile WiMAX networks, IEEE 802.11p/1609 WAVE wireless vehicular networks, etc. The main drawback is its dependence on Fedora 9 Linux distribution to be installed, which limits its usage for most scholars (PEREZ, 2011).

Veins: it is an open-source framework for running vehicular network simulations. It integrates OMNeT++ and SUMO simulators and allows Online re-configuration and re-routing of cars in reaction to the network simulator. Likewise, it features fully-detailed models of IEEE802.11p and IEEE1609.4 DSRC/WAVE. Although such a framework enables vehicles to react to communication content, the coupling of SUMO and OMNeT++ is performed via TCP socket, which entails an additional delay to the simulation. For instance, the OMNeT++ spends more than 30 hours in real time for a 360 seconds simulation of a large-scale scenario (NOORI; OLYAEI, 2013).

Table 4 summarizes and compares the most important features of the VANET simulators before considered.

Table 4 – Comparison of VANET simulators.

	TraNS	GrooveNet	NCTUns	Veins
IEEE802.11p support	✓	✓	✓	✓
V2V and V2I support	✓	✓	✓	✓
Open Source	✓	✓	✓	✓
Support for learning	Poor	Poor	Poor	Poor
Operating System Options	Wide	Wide	Limited	Wide
Continuous development	x	x	x	✓

Source: Own authorship (2022).

3.4.4 Selected Tools

The description of freeware and open-source tools have revealed significant differences between each software option. Regarding mobility simulation, Table 2 shows support for microscopic and multi-lane simulation for all tools. Likewise, most of them produce trace support files for ns-2, except the Carla software, which does not produce a mobility trace file. On the other hand, VanetMobiSim and MOVE are the only options supporting files for GloMoSim and QualNet. In addition, CityMob software appears to have little support for network simulators, while the SUMO simulator is the only one with continuous development.

As for network simulators, JiST/SWANS appear to have a disadvantage because of a lack of integration with the most popular mobility simulators and the absence of a VANET physical layer model. Table 3 shows that ns-2, ns-3, and OMNeT++ are better candidates as they are the only options featuring the IEEE 802.11p standard and are more popular among researching community due to the availability of learning resources and code extensions developed by the enthusiast.

Although OMNeT++ has attracted much attention in recent years, this software is not a simulator of VANETs itself. It must be used in Veins's framework, which follows a predefined way of sharing information among mobility and communication environments. Unlike the OMNeT++, both the ns2 and ns3 can be customized independently from a global simulation frame, simplifying a possible software adaptation.

Regarding the software for VANET simulation, the Veins simulator seems to offer the best features, as the other options do not have a continuous development (BABU; P, 2022). However, Veins needs both SUMO and OMNeT++ to run, so any bug in one of those can cause Veins to give unreliable results (WEBER; NEVES; FERRETO, 2021). Because this work aims to employ a car-like monolithic unit for communication and movement control without including any inter-software coupling tool, we have then chosen a single software approach.

Among single software options, network simulators undertake most of the simulation routines as more complex algorithms are involved in communication duties than in traffic models as networking and routing strategies, for instance. Hence, we have chosen a network simulator as the base platform enhanced with mobility features. Given such a premise, both the ns-2 and ns-3 offer a suitable environment for extending the software's capabilities by adding new code as open-source platforms. However, ns-2 holds a more significant amount of publicly available resources, including code extensions, learning tutorials, and higher support by the research community.

3.5 Chapter Summary

In this chapter, the Vehicular Ad-hoc Networks (VANETs) were addressed. General features, such as applications, layers, standards, and routing protocols, were detailed in this chapter. Likewise, some simulation tools were described, aiming to choose a reliable option for evaluating microscopic traffic models and vehicular networks. The SUMO traffic simulator and ns-2 network simulator have been chosen because of their proven stability, learning resources, widespread adoption in scientific publications, and because they are open source and free of charge options.

4 A NS-2-BASED PLATFORM FOR SIMULATION OF VANETS

The ns-2 is one of the most popular network simulators, widely employed for academic research on MANETs and VANETs. In the case of VANETs, the ns-2 can be a flexible tool, as it enables the user to link external libraries and code new functionalities. Nonetheless, once linked to the external file, mobility patterns can not be changed anymore. Hence, studying improvements in mobility is not a feasible task when using the default version of ns-2. This chapter presents a general landscape of the standard simulation method and a detailed description of an improvement of ns-2 to increase its mobility features. The last one constitutes an additional contribution resultant of this work.

4.1 A standard Simulation of VANET using ns-2

In a standard simulation of VANETs, the ns-2 requires an external mobility file, which contains the mobility pattern and defines the exact movements of every vehicle at each time step. Such a file can be generated by the SUMO simulator and invoked by the ns-2 as depicted in Figure 9.

Figure 9 – NS-2 standard VANET simulation scheme.

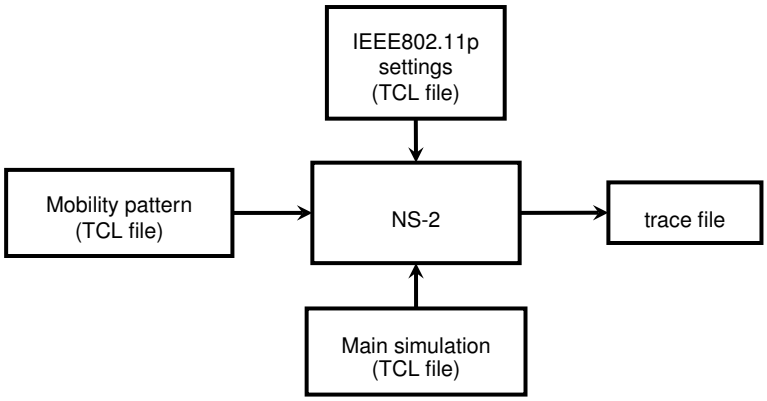

Source: Own authorship (2022).

Another essential input file is the IEEE802.11p settings, which contains definitions for parameters of the physical layer. The simulator's output is a trace file containing information labeled at each time step. Such information includes, for instance, the flags of sending and receiving a message, the size of the delivered package, the kind of traffic a node has conveyed, or the number of hops a packet has passed through, among other information.

Despite the high versatility of both ns-2 and SUMO for the simulation of VANETs, none of them has the capabilities to implement a VANET-based CFM. In the case of SUMO, mobility patterns can not be online modified, as they are generated according to specific rules previously defined by the user. In the case of ns-2, the software only deals with the communication process, and there is no control of the node's movements. A traffic generator, for instance, SUMO, prede-

fines such mobility patterns, which are then included in the ns-2 environment. Hence, performing a mobility pattern different from the input file is impossible with the default version of ns-2.

Therefore, a specific adaptation of the simulator becomes necessary to enable the ns-2 to perform VANET-based decision-making. Such adaptation will permit a realistic implementation of a typical CFM and the evaluation of the most recent VANET-based CFMs.

4.2 Improvement of the NS2 simulator to study a VANET-based CFM

For simulation of mobile networks, the ns-2 employs two specific modules: i) The mobility function and ii) The network protocol function. The mobility function deals with the mobility of nodes, updating position and speed according to the user-defined mobility pattern. The network protocol function contains the strategy for transmission of packets, including the beacons for position-based protocols, as depicted in Figure 10.

Figure 10 – Scheme for the adapted simulator.

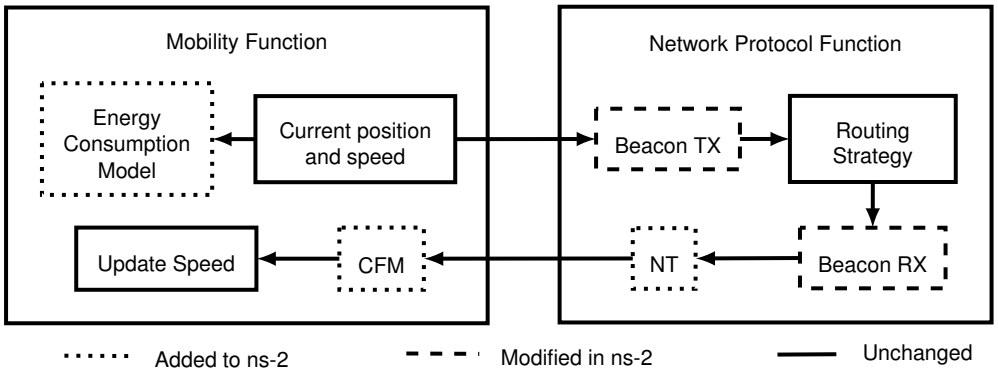

Source: Own authorship (2022).

The nodes using position-based protocols can exchange the beacon messages (*hello* messages), which permits a more accurate localization of the destination. A *beacon* is a small data packet containing kinematic information, for instance, position, speed, and direction of the vehicle (SILVA *et al.*, 2019). The position, for instance, can be obtained via GPS or short-range localization. Other measures can be gathered directly from additional technological resources, such as sensors, cameras, or radar.

The beacons are periodically transmitted into the one-hop neighborhood and support the routing strategy for better decision-making about the following message destination. In this work, beacons are expected to contribute to a better performance of the network protocols and to provide the necessary information that a CFM-ruled Connected Vehicle (CV) needs for safe and efficient driving.

The network simulator is then enhanced with new features, including an energy consumption computation module and a car-following model (CFM) module as part of the Mobility function and a neighbor table (NT) in the network protocol function. Other modules of the net-

work simulator are only modified, as in the case of the reception and transmission of beacon functions.

The energy consumption model receives kinematic information about the current position and speed. At the same time, the CFM module computes the next step speed depending on the information of the neighbor table. Such a table contains the latest position and speed reported by surrounding vehicles. Upon receiving a *Hello* message, the information is stored in the Neighbor Table (NT) and processed further in the CFM function, which models a typical driver's behavior.

The beacon transmission and reception modules (Beacon TX and RX) have been adapted to permit the transmission of speed and to control the beacon interval time, which is a core part of meeting the purpose of this work. Such adaptation also permits the transmission of other variables, including acceleration, density, and direction.

The above-described modifications enable the ns-2 to perform independently from the external mobility file described in Figure 9. It means the adapted ns-2 no longer needs the SUMO simulator to decide about the vehicle's movements, as vehicles using the adapted ns-2 can decide about future movements from the information received through the VANET.

4.3 Mobility scenarios

A large variety of mobility scenarios can be generated using the SUMO simulator. Depending on the target area, they can be classified into Urban or Highway scenarios. Urban scenarios are characterized by frequent stops and low velocities, whereas vehicles in highway scenarios can reach higher speeds and maintain a constant speed for extended periods. In this work, both types of scenarios have been studied: a two-road crossing scenario for the case of urban mobility and a two-kilometer long straight road for the case of the highway. In the following, we describe the features of each scenario.

4.3.1 Urban Scenario

The urban scenario is characterized by a four-legged crossing with a traffic light, as shown in Figure 11. Each leg has a two-way road with two lanes each and a length of 300 m, encompassing a total area of 0.36 km^2. Vehicles traveling with a maximum speed of 22.0 m/s or 80 km/h, over the highest typical limits for urban scenarios, can enter the scenario from the left and right sides and are expected to stop as long as the traffic light closes. Once the traffic light opens, vehicles can turn right or continue straight ahead with probability 0.5. The time interval of 20 seconds for the red light and the mobility patterns are generated by SUMO simulator (LOPEZ *et al.*, 2018b).

Figure 11 – Two-road crossing scenario.

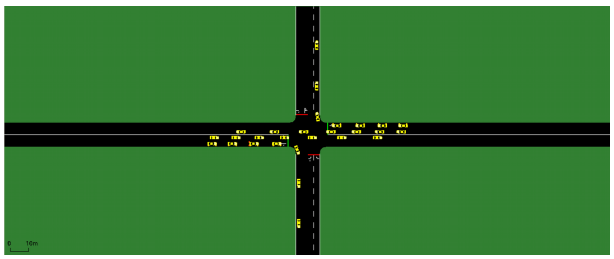

Source: Own authorship (2022).

4.3.2 The Highway Scenario

In the highway scenario, a two-kilometer long straight road with three lanes and a single way is employed. A speed bump at the middle way is added in order to reproduce the occurrence of a traffic event. Figure 12 illustrates the first part of the road, including the speed bump at the end of the way.

Figure 12 – highway scenario.

Source: Own authorship (2022).

Two groups of vehicles are configured to be part of the traffic stream. Both start at different times, as depicted in Figure 12. This kind of scenario is suitable for studying how vehicles at high speed can react to sudden occurrences on the road without complete stopping and how vehicles can harness the information about previous experiences of neighbors ahead.

4.4 Validation of the adapted ns-2

The improved ns-2, modified for reproducing a CFM as described in section 4.2, is evaluated in this part. In order to verify the correctness of the enhanced platform, a simple experiment is performed. It employs the two-road crossing scenario using a road length of 100 m and four vehicles. The vehicles depart from an intersection simultaneously and are forced to stop at the next traffic intersection. Once the traffic light opens, every vehicle resumes its trip according to the maximum acceleration rate.

For this comparison, two simulations are performed. In the first case, the SUMO simulator configured for electric vehicles using the Krauss CFM is evaluated. In the second one, the adapted version of ns-2, implementing the same CFM and the energy consumption model described in chapter 2, with the parameters listed in Table 5, is employed.

The results of speed, position, acceleration, and state of charge for both configuration are shown in Figure 13. Figures Figure 13a to Figure 13d show that the adapted ns-2 perfectly

Table 5 – Energy model parameters.

Parameter	Value
Vehicle mass (m)	2000 kg
Air density (ρ)	1.225 kg/m^3
Road friction coefficient (C_D)	0.9
Vehicle front area (A_f)	5 m^2
Road resistance f_{rl}	0.01 no unit
Slope angle (θ)	0
Tire radius (R)	0.152 m
Armature resistance (r)	0.1 Ω
Effective magnetic flux constant (K)	25 no unit

Source: Own authorship (2022).

matches the results of SUMO simulator for position and speed profiles in the evaluated scenario.

Other results, like the acceleration, show little variations, with peak values occurring at acceleration and deceleration phases, as shown in Figure 13e. It is the result of using the random updating interval employed by ns-2 for the mobility function on Figure 10, which implies that a very short updating interval may occasionally cause a high acceleration or deceleration step.

It is worth noting that oscillations on acceleration profile are present even in the SUMO simulator results, as depicted in Figure 13f. That means the oscillations result from the CFM itself and not from the adaptation of the software. Despite the higher amplitude of oscillations in adapted ns-2, little variations can be observed in the final SoC results, as shown in Figure 13g and Figure 13h.

4.5 Evaluation of the Multi-anticipative CFM (MA Model)

After verifying the correctness of the adapted version of ns-2, a large variety of CFM formulations can be studied. In this thesis, particular attention is given to the Multi-Anticipative (MA) model, as proposed by Kuang *et al.* (2019). For comparison purposes, we compare the (MA) model versus the Krauss model through the urban and highway scenarios using a Beacon Interval Time (BIT) of 100 ms and the GPSR protocol. Such a BIT is the recommended one for a good performance of CADAS (ETSI, 2011).

Figure 14 compares the Krauss and the MA models using the urban scenario. In order to facilitate the graphical comparison, just the first four vehicles from a total stream of 30, which belongs to the inner lane of one of the roads, are evaluated and their profiles depicted.

Figures 14a and 14b show the speed profiles of four vehicles. Though the maximum available speed is the same for both cases, vehicles featuring the MA model do not meet such a speed. That implies that vehicles spend more time reaching the intersection position, as depicted in Figure 14d.

Figure 13 – Comparison of the adapted simulator and the results of SUMO: (a) Speed with adapted ns-2, (b) Speed with SUMO, (c) Position with adapted ns-2, (d) Position with SUMO, (e) Acceleration with adapted ns-2, (f) Acceleration with SUMO, (g) State of charge with adapted ns-2, (h) State of charge with SUMO.

(a) Speed with adapted ns-2

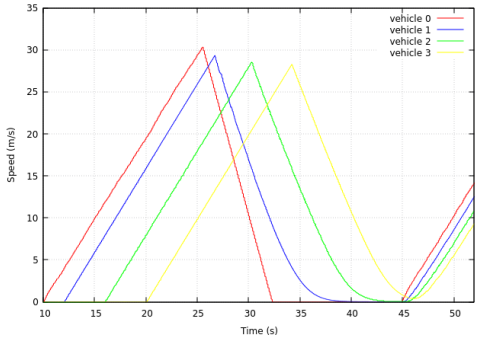

(b) Speed with SUMO

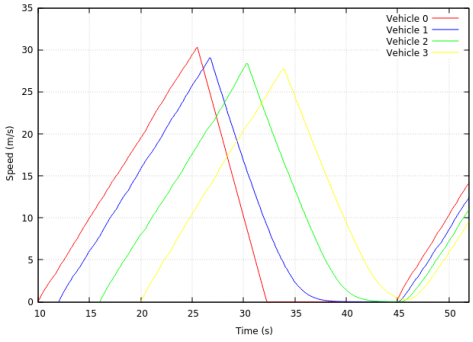

(c) Position with adapted ns-2

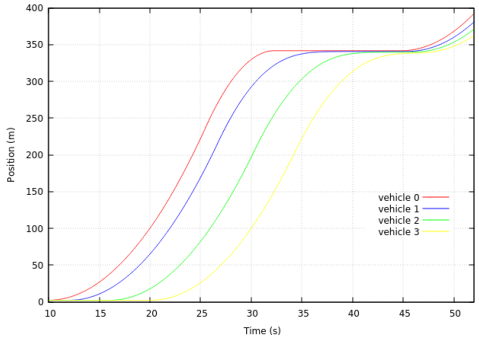

(d) Position with SUMO

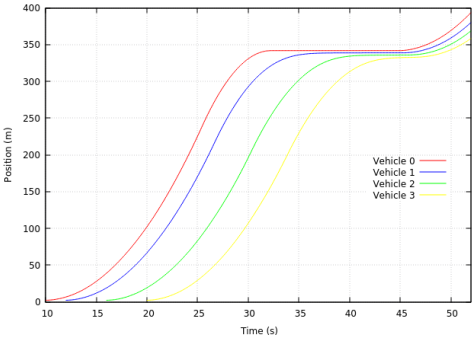

(e) Acceleration with adapted ns2

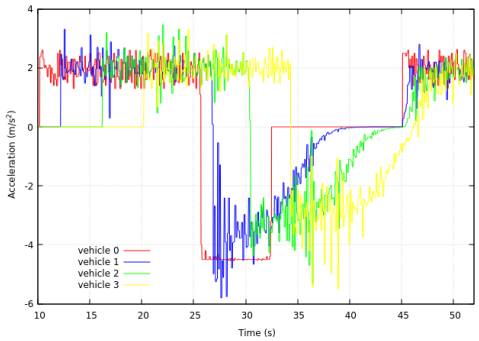

(f) Acceleration with SUMO

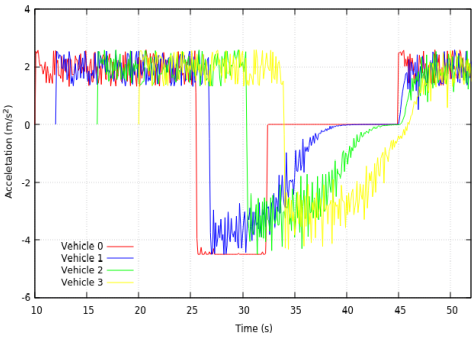

(g) State of charge with adapted ns-2

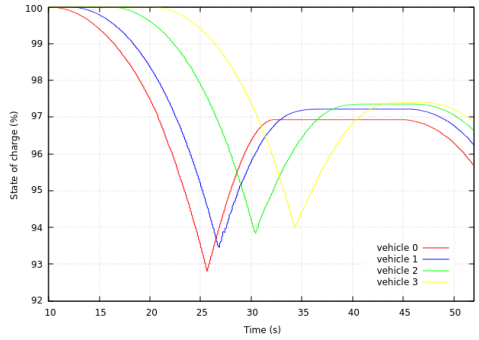

(h) State of charge with SUMO

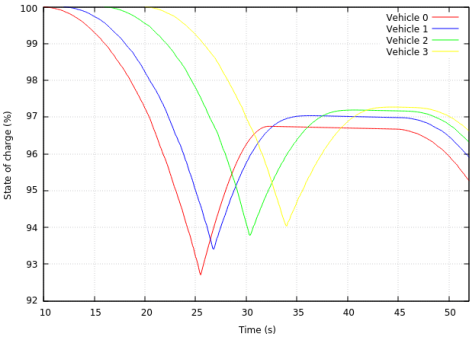

Source: Own authorship (2022).

Figure 14 – Results in the urban scenario: (a) Speed with Krauss model, (b) Speed with MA model, (c) Position with Krauss model, (d) Position with MA model, (e) Acceleration with Krauss model, (f) Acceleration with MA model, (g) State of charge with Krauss model, (h) State of charge with MA model.

(a) Speed with Krauss model

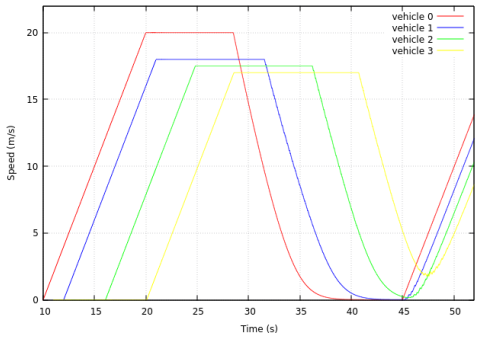

(b) Speed with MA model

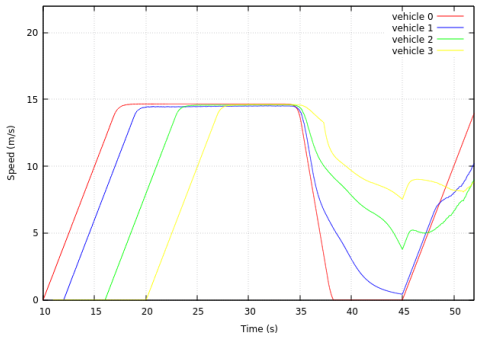

(c) Position with Krauss model

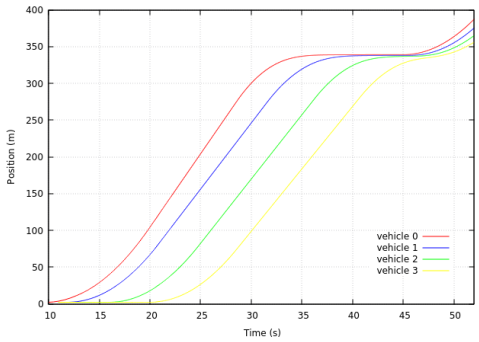

(d) Position with MA model

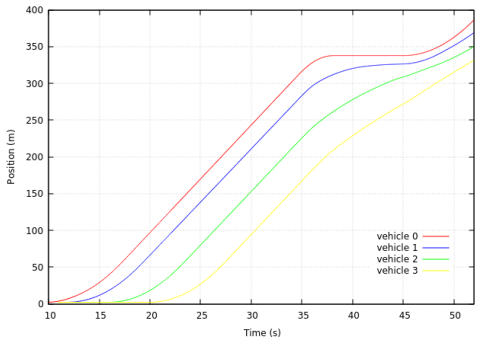

(e) Acceleration with Krauss model

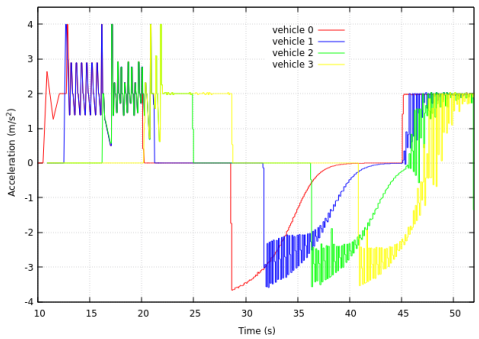

(f) Acceleration with MA model

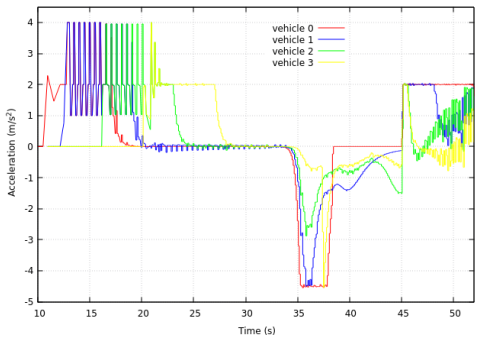

(g) State of charge with Krauss model

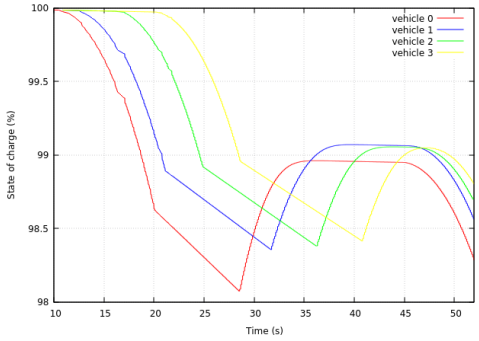

(h) State of charge with MA model

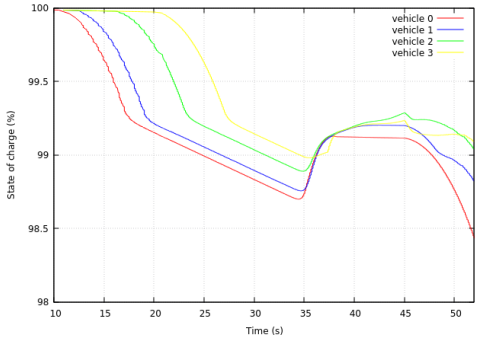

Source: Own authorship (2022).

Another remarkable difference is the time when vehicles start braking. In the case of the Krauss model, the braking phase starts at different times for each vehicle, whereas the vehicles start to brake approximately at the same time when featuring the MA model. Such a difference occurs because the MA model uses the information from all preceding vehicles; therefore, any movement variation of a vehicle ahead will influence the decision-making of its followers.

The crossing scenario also unveils a remarkable advantage of using the MA model. As the vehicles avoid rushing to meet the intersection, the waiting time at the traffic light is vastly reduced. Such effect mainly benefits the vehicles with many preceding neighbors, as in the case of the last vehicle (vehicle 3) in 14d, which unlike the Krauss results in 14c, it does not need to completely stop at the intersection while performing a linear-like position profile.

Figures 14e and 14f reveal that the acceleration profile in both CFM is highly sensitive to variations in speed and inter-vehicular distance. The proximity of vehicles at the beginning, for instance, rapidly forces the vehicles to stop speeding, so an oscillatory pattern appears. Such a phenomenon is worse in the case of MA, as vehicles trying to resign speeding are also encouraged to speed up because of the information from more ahead neighbors.

On the other hand, the braking phase shows a better performance in the case of the MA model, which can be explained by observing the speed differences. Once vehicles using the Krauss model start braking, the speed difference regarding the preceding vehicle is higher than in the MA model. Such a difference occurs because, in MA, the braking phase starts at the same time. Hence, vehicles using the MA model perform a smoothness deceleration than vehicles using the Krauss model.

The differences mentioned above in speed and acceleration profiles directly impact energy consumption. The more prolonged acceleration ramp of the Krauss model leads to an increase in energy use. Likewise, achieving a higher speed entails using more energy, as evidenced in Figure 14g. The MA model, on the contrary, avoids using unnecessary energy by performing a more conservative speed profile.

The comparison of Figures 14g, and 14h also shows that the Krauss model performs a high recuperation of energy. Such energy savings are resultant of a fast deceleration of each vehicle. On the other hand, vehicles featuring the MA model, which have not achieved a maximum speed as high as in the Krauss model, cannot recuperate as much energy as with such a model.

Despite the higher recuperation of energy the Krauss model can achieve, the final state of charge of vehicles using the MA model is higher than in the case of Krauss. For example, vehicles 0 and 3 using the MA model reach 98.4% and 99.08%, respectively, whereas they reach 98.3% and 98.8% when using the Krauss model.

In the case of the highway scenario, Figures 15a and 15b show the velocity profile using the Krauss and MA models, respectively. Four follower vehicles from a total stream of 30 were studied in this case. These vehicles are part of the inner lane's traffic and have been chosen for better evaluation of the anticipatory features of the MA model.

As described in the highway scenario, the vehicles are forced to reduce their speed at the speed bump. In the case of Krauss, the only reduction in speed profile corresponds to that event. In the MA approach, vehicles also reduce their speed a time before the bump (around the 40th second), as they are also influenced by vehicles beyond the preceding car. Another noteworthy difference is the maximum speed with the MA model, which is lower than in the case of the Krauss model.

The position profiles in Figures 15c and 15d show that vehicles using the MA model spend more time reaching the speed bump, which is consistent with the lower speed of that model. In this case, as the speed bump defines a fixed maximum speed limit, no advantages of avoiding rushing with MA are evidenced. Hence, at the end time, vehicles using the MA do not achieve the same position as vehicles featuring the Krauss model.

Figures 15e and 15f show the acceleration profiles. In the case of Krauss, vehicles start moving simultaneously, so no differences in speed are produced, and the acceleration ramp is the same for all vehicles. Therefore no oscillation is obtained. In the case of the MA model, similar to the urban case, in acceleration phases with a short inter-vehicle gap, vehicles are forced to speed down and up frequently as a longer inter-vehicle distance must be kept. Therefore, high frequent acceleration oscillations are evidenced around the 10th and the 50th seconds.

Also, similar to the urban case, the deceleration in the Krauss model is characterized by rapid oscillations in vehicles with a short inter-vehicular distance. In the case of the MA model, such oscillations are avoided thanks to more coordinated braking, which implies that even with a short inter-vehicle distance, the speed difference will not cause a significant change in deceleration, as occurred with Krauss.

Figures 15g and 15h show the state of charge of the battery for both the Krauss and the MA models. Despite of the better results the MA models shows at the end of the simulation time, a fairer comparison can be made at the time the vehicles achieve the speed bump. For instance, the Figure 15g shows that the battery of vehicles 0 and 3 hold 96.75% and 97.25% respectively, at the speed bump, whereas the vehicles hold 97.6% and 97.9% using the MA model at the same place, as shown in Figure 15h. These results show that the MA model achieves a higher energy economy than the Krauss model for the distance traveled.

Since the MA model is susceptible to movements of vehicles beyond the preceding one, more frequent braking maneuvers are expected when using this model, as evidenced in 15f if compared with 15e. It could represent more energy recovery through regenerative braking. Nonetheless, the main reason for the higher final SoC of the MA model is the shorter acceleration pulses in 15f, which results in lower energy consumption.

4.6 Chapter Summary

This chapter has presented the development of an ns-2-based platform to simulate VANETs. The chapter begins by describing the traditional methodology used by ns-2. Secondly,

Figure 15 – Results in the highway scenario: (a) Speed with Krauss model, (b) Speed with MA model, (c) Position with Krauss model, (d) Position with MA model, (e) Acceleration with Krauss model, (f) Acceleration with MA model, (g) State of charge with Krauss model, (h) State of charge with MA model.

(a) Speed with Krauss model

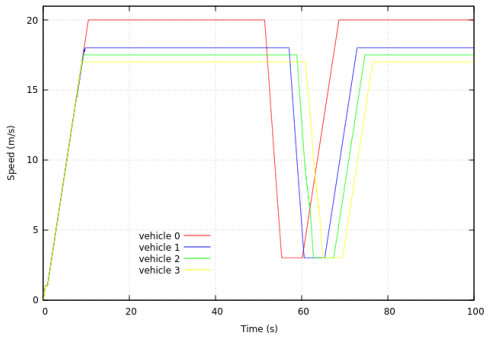

(b) Speed with MA model

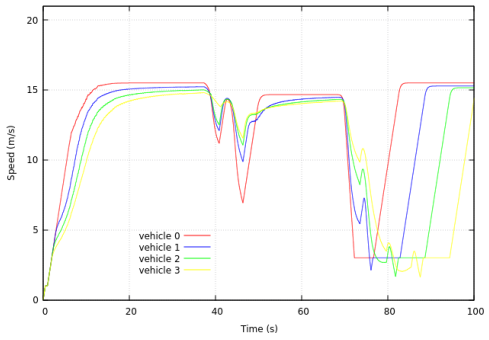

(c) Position with Krauss model

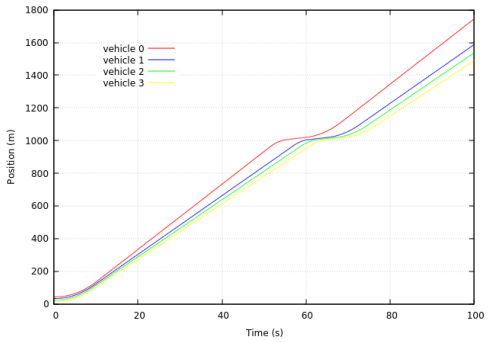

(d) Position with MA model

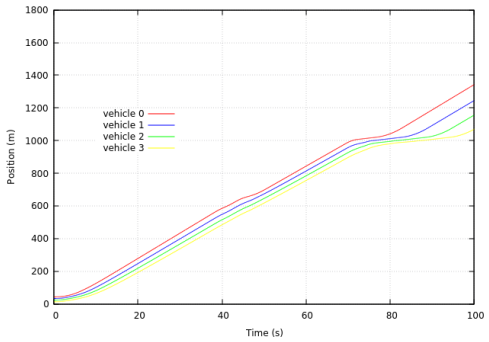

(e) Acceleration with Krauss model

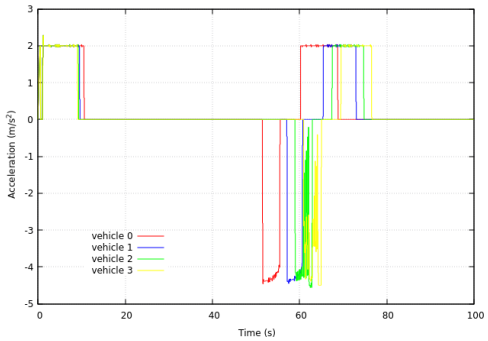

(f) Acceleration with MA model

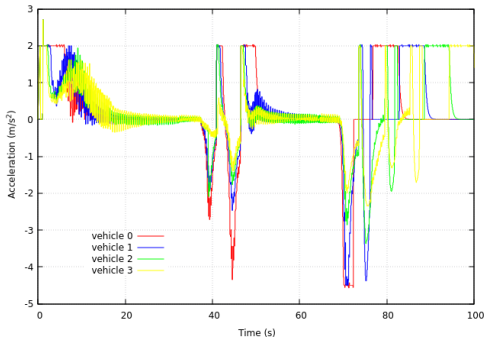

(g) State of charge with Krauss model

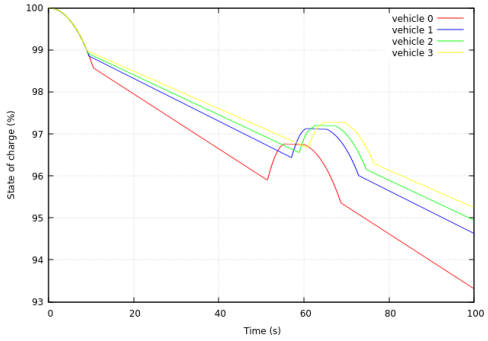

(h) State of charge with MA model

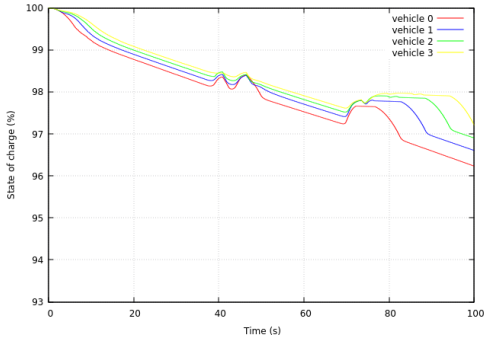

Source: Own authorship (2022).

the description of the enhanced version of ns-2 for simulation of a VANET-based CFM is presented. Finally, two car-following models, Krauss and Multi-anticipative (MA), were simulated and compared using urban and highway scenarios.

The results show that the MA model employs a lower speed than the Krauss model. Such condition, added to the information coming from every ahead vehicle, helps the MA model to waste less energy than the Krauss model. The results show that the MA model permits a higher final state of charge, around 0.1% to 0.2% in the urban scenario and around 0.6% to 0.9% in the highway case compared with the Krauss model.

The results also show that more energy savings are achieved by avoiding unnecessary accelerations than through energy recuperation. That happens because the MA model employs lower kinematic energy on stepping up the vehicle, so a lower amount of energy can be recuperated through regenerative braking. Likewise, a lower deceleration slope is necessary, as vehicles with the MA start braking earlier than with the Krauss model.

5 ASSESSMENT OF ROUTING PROTOCOLS IN VANET

The evaluation of routing protocols is an essential task in VANETs that seeks to establish the benefits and drawbacks of using a routing strategy to transmit messages in a specific scenario. In this chapter, a comprehensive evaluation of four DTN protocols: Epidemic, BS&W, PRoPHET, and Direct Delivery, as well as two typical protocols, AODV and GPSR, is performed. The primary purpose is to find the most suitable protocol for exchanging short data packets containing vehicle traffic information. Such a protocol must deliver the largest number of messages using the shortest time and produce a low impact on end-user communication regardless of the traffic density conditions. With that in mind, a large set of vehicular densities and a wide transmission range were considered for evaluation. Likewise, the role the beacon interval time plays in the network's performance is also addressed.

5.1 Description of the experiment

In order to assess the performance of DTN and traditional VANET protocols, a broad set of transmission ranges (TR) (100 to 500 m) is configured. First, we evaluate the impact of traffic density by considering the minimum and maximum TR. Then, extensive simulations are performed to obtain results for four metrics: Delivery Rate, End-To-End Delay, Overhead, and the Average number of hops. Each simulation uses the same number of vehicles and transmission range for each protocol as described in Algorithm 1. The results are averaged over ten observations (simulation runs) considering a confidence interval of 95%.

Algorithm 1 – Pseudo-code for generating the simulation results.

```
for each Protocol ∈ {Epidemic, BS&W, PRoPHET, DD, GPSR, AODV} do
    for each TR ∈ {100,200,300,400,500} do
        for each # Nodes ∈ {4,8,12,20,28,36,52,68,84,100} do
            repeat
                Run simulation in ns-2 with parameters of Table 6
            until # simulation runs ≤ 10
            Compute DR, E2E Delay, Overhead, and # Hops
            averaged over ten runs
        end for
    end for
end for
Plot the results
```

Source: Own authorship (2022).

A VANET scheme featuring the IEEE 802.11p standard over the urban scenario described in chapter 4 was created using the sumo simulator and the ns-2. In the proposed scheme, four vehicles that have established a communication contact while stopped at the traffic light are defined as sender and receiver nodes. The remaining vehicles, which arrive immediately after

Figure 16 – Communication among four vehicles of the traffic flow: (a) Four vehicles communicate at the intersection, (b) Communication links once the traffic light opens.

(a) Four vehicles communicate at the intersection **(b) Communication links once the traffic light opens**

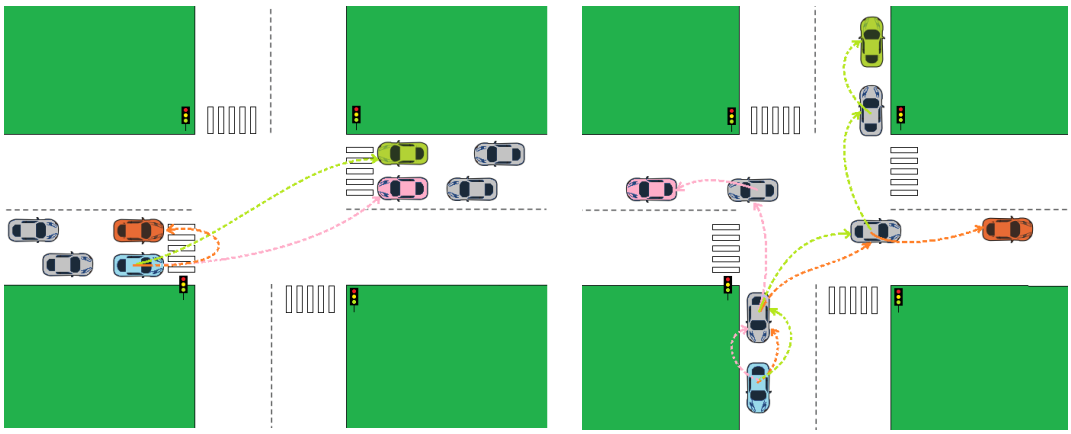

Source: Own authorship (2022).

the first ones, play the role of potential forwarding nodes. The four communicating vehicles are headers of the traffic flow on each lane, as depicted in Figure 16a.

The four vehicles involved in the communication are defined as headers of the traffic flow. On the other hand, forwarding vehicles come into the scene in different amounts, ranging from 0 to 96, for a total of 100 vehicles equally distributed on both departing roads. In the communication scheme, one of the vehicles (source vehicle) tries to inform the destination vehicles about the previous occurrence of a set of events.

The communication starts once the four vehicles are completely stopped at the red light, as shown in Figure 16a. Then, the source vehicle starts a transmission with information about ongoing events. Depending on the amount of data to transmit, the necessary communication time exceeds the stop time interval. Hence, the transmission routine continues with vehicles resuming their trips on the green light. From this moment on, vehicles initially located behind the four headers (gray-colored) are responsible for re-transmitting the messages, as depicted in Figure 16b for the initial case of four vehicles.

In this work, the European Telecommunications Standards Institute (ETSI) recommendation is adopted for the message generation period. The institute defines lower and upper bounds of Tms in milliseconds as $100 \leq Tms \leq 1000$ for Cooperative Awareness Messages (CAM) (ETSI, 2011). The lower bound period is usually employed in most time-critical approaches, like in Cooperative Adaptive Cruise Control (CACC) applications (AMOOZADEH *et al.*, 2015; WANG *et al.*, 2019). In addition, the warning messages are supposed to contain information about events that permits improving the traffic dynamics but are not to be used for self-driving purposes or collision avoidance. Therefore, the generation period of 1000 ms is chosen. It is a prudential time to keep vehicles aware of traffic events while avoiding excessive flooding of messages in the network.

It is worth noting that warning messages are not intended for autonomous driving but for advising drivers about incoming events. Hence, in this section, a traditional simulation using a fixed mobility pattern is performed through the SUMO simulator and the Krauss model. Likewise, the message's size has been defined as 512 bytes, a typical packet size on VANETs, and the buffer size has been set to 100 GByte, intending to avoid the saturation of the buffer-based protocols. Table. 6 summarizes the communication parameters.

Table 6 – Simulation parameters.

Parameter	Value
Simulation area	(0.6 x 0.6) km^2
Number of nodes	{4, 8, 12, 20, 28, 36, 52, 68, 84, 100}
Mobility model	Traffic lights crossing
Lane configuration	Two flows / four ways
Maximum speed of nodes	12 m/s
Car following model	Krauss
Channel type	Wireless
Communication time interval	30 s
Traffic type	Bundle / CBR-UDP
Propagation model	Nakagami-m (m=2)
MAC/PHY	IEEE 802.11p
Radio range	{100, 200, 300, 400, 500} meters
Message size	512 bytes
Buffer size	100 GByte
Bundle lifetime	60 s
Bundle generation period	1 s
Number of initial copies	16 (Binary Spray & Wait only)
Simulation replications	10
Confidence interval	95 %

Source: Own authorship (2022).

5.2 Performance Metrics

Four metrics are used to evaluate and compare the routing protocols: i) delivery ratio, ii) average end-to-end delay, iii) overhead, and iv) average number of hops.

Packet Delivery Ratio (PDR) or simply Delivery Rate (DR) is the ratio between the number of successfully delivered messages and the number of sent messages. Better routing protocol performance is obtained for high DR values (VERMA; SAVITA; KUMAR, 2021).

$$DR = \frac{\sum N_{dm}}{\sum N_{sm}}, \tag{30}$$

where N_{dm} corresponds to the total delivered messages and N_{sm} the total sent messages.

End-To-End Delay is the average time interval between sending and receiving a message from source to destination (SETIABUDI *et al.*, 2016) as expressed in (31)

$$E2E\ Delay = \sum_{i}(T_{a,i} - T_{d,i})/N_{rm} \tag{31}$$

with the arrival time $T_{a,i}$ and departure time $T_{d,i}$ of message i for a total number of N_{rm} received messages.

Overhead is the ratio between the number of messages necessary to send user data in the network (VERMA; SAVITA; KUMAR, 2021) and the number of messages with user data. The overhead can be expressed as in (32)

$$Overhead = N_t/N_s \tag{32}$$

where N_t is the total number of messages, and N_s is the number of messages sent with user data. For DTNs, $N_t = B_c + B_{tc} - B_r$, with B_c as the number of copies of bundles made during transfers, B_{tc} the number of transfers of bundles during routing, and B_r as the number of received bundles (Gonçalves Filho *et al.*, 2016). In the case of VANET protocols, the overhead is also known as the normalized routing load; in that case, N_t represents the number of additional routing packets needed to successfully transmit data packets (MALIK; SAHU, 2019). The overhead should be reduced for better performance.

Average number of hops is the average number of hops a message needs to perform in order to meet the final destination. It represents how many intermediary nodes are necessary to complete the path between source and destination. In the case of DTN fewer hops usually mean longer carrying intervals, implying an increase in delay (TORNELL *et al.*, 2015).

5.3 The Impact of Vehicular Density

First, the effect of vehicular density for a short transmission range of 100 m is evaluated. Such a range is lower than the most common values used to simulate vehicular networks. A transmission range as short as 100 m reveals how vehicles benefit from the traffic density to successfully deliver a message when the destination node is located out of the transmission range. In this case, the low traffic density represents a condition where vehicles have a minimum direct contact, which is the case of sparse networks, the most studied condition in the literature.

Then the same metrics but using a transmission range of 500 m are evaluated. Such a value of 500 m is among the highest in literature. It allows the evaluation of the effect of a large number of vehicles in the transmission range. In this case, the vehicular density permits observing how the routing protocols perform when multiple paths are available.

Figure 17 – Results of Delivery rate with: (a) TR=100 m, (b) TR=500 m.

(a) Delivery rate with TR=100m **(b) Delivery rate with TR=500m**

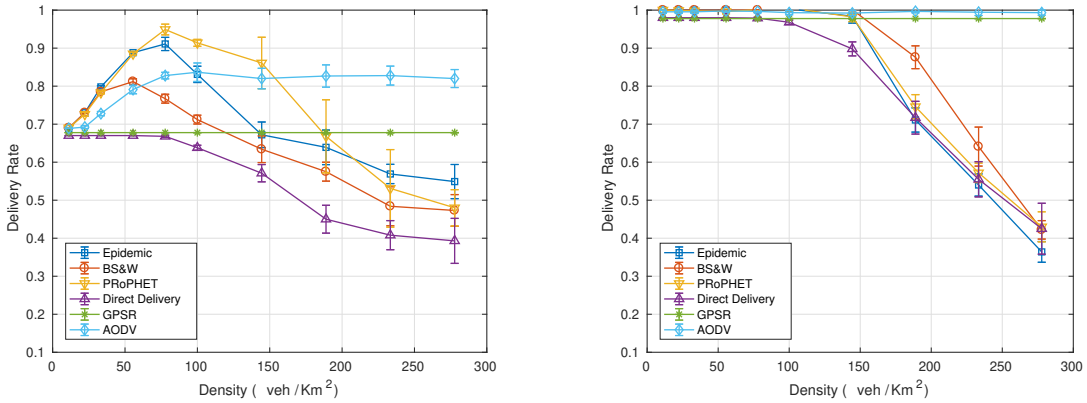

Source: Own authorship (2022).

5.3.1 Delivery Rate (DR)

Fig. 17a shows the results for Delivery Rate (DR) versus vehicular density. The results show that multi-copy DTN protocols (i.e. Epidemic, BS&W, PRoPHET) and AODV outperform Direct Delivery (DD) and GPSR at low densities. Fig. 17a also reveals that those protocols benefit the most from increasing densities until 50 vehicles/km^2.

For densities higher than 75 vehicles/km^2, DR for all DTN protocols decreases as density increases. That occurs because of the network saturation and the need to process every node in the transmission range. In the case of AODV and GPSR, DR remains almost the same due to the no-need to evaluate every node, but employing recently used routes in the case of AODV or an opportunistic route, in the case of GPSR.

The results for a high transmission range of 500 m are depicted in Figure 17b. For low densities (under 100 vehicles/km^2), all protocols achieve maximum DR, which is an evident improvement regarding the results with TR=100 m. The results for high densities indicate that DR is lower than those with TR=100 m for all DTN protocols. That occurs because more nodes are in the TR, so more saturation comes up. In contrast, for AODV and GPSR, the results are better for all densities as more directly can the messages be delivered.

5.3.2 Average End-To-End Delay

The results for End-To-End Delay with the shortest transmission range are depicted in Figure 18a. The results show that E2E-Delay for DTN protocols increases as the vehicular density increases. The Epidemic protocol has the highest delay, and Direct Delivery has the lowest one. Furthermore, the results for AODV and GPSR are just a few milliseconds, which seem neg-

Figure 18 – Results of Average End-to-End Delay with: (a) TR=100 m, (b) TR=500 m.
(a) Average End-to-End Delay with TR=100m (b) Average End-to-End Delay with TR=500m

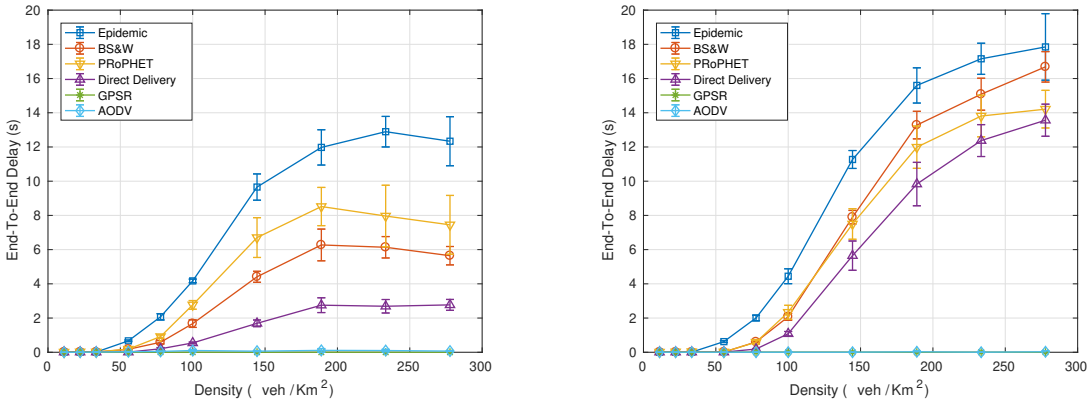

Source: Own authorship (2022).

ligible if compared with DTN. However, for low-density conditions (under 50 vehicles/km^2), the results for DTN protocols are comparable with those of AODV and GPSR.

The results for the highest transmission rate, plotted in Figure 18b, show that for DTN protocols, the E2E Delay increases as long as the density does too. For higher density (over 100 vehicles/km^2), the End-To-End (E2E) Delay of all DTN approaches becomes higher than in the case of TR=100 m. On the other hand, contrary to DTN protocols, in AODV and GPSR, the E2E Delay becomes lower for a higher transmission range for any density. Hence, in the case of DTN, a larger TR implies more neighbor nodes to share information, whereas, in the case of traditional approaches, the result is a higher chance of direct delivering the message to the destination node.

5.3.3 Overhead

Figure 19a shows the results for overhead using the minimum TR. The response of DTN protocols with no spread control (e.g. Epidemic and PRoPHET) shows an increase of overhead as the density grows. In the case of Epidemic, the high number of copies causes a buffer overflow and leads the network to achieve a local maximum at a density of 55 vehicles/km^2. Thereupon, any further increase in density implies an increase in delay and reduction of DR, which reduces overhead. However, a high density and short TR entail exchanging the messages with more neighbors beyond the TR coverage, which increases the overhead again.

Figure 19b shows the results of the overhead for TR=500 m. As in the case of TR=100 m, for all protocols except DD and at low densities, the overhead tends to increase. In the case of DTN, the overhead reaches a peak value with 55 vehicles/km^2 and 75 vehicles/km^2 for epidemic and BS&W, respectively. Those points coincide with the first peak values obtained with

Figure 19 – Results of Overhead with: (a) TR=100 m, (b) TR=500 m.

(a) Overhead with TR=100m **(b) Overhead with TR=500m**

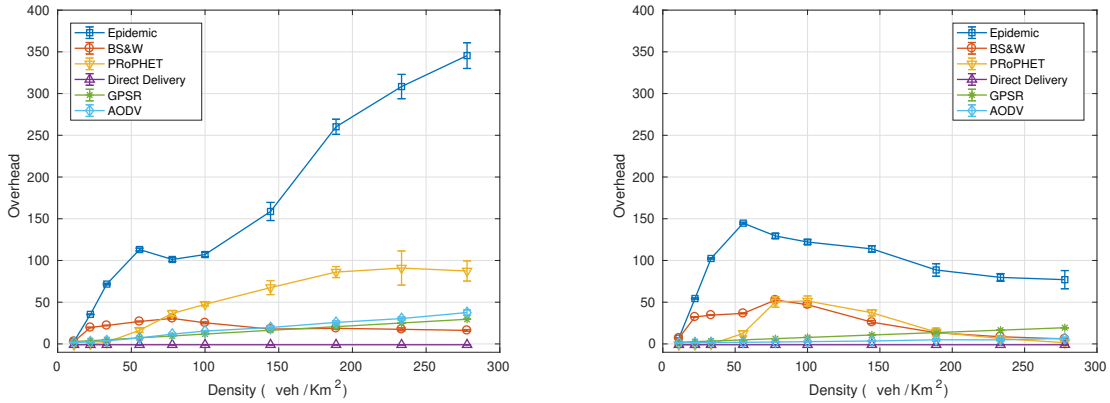

Source: Own authorship (2022).

TR=100 m. In the case of PRoPHET, the maximum overhead occurs earlier (75 vehicle/km^2) than that for TR=100 m.

Unlike GPSR and AODV, whose overhead increases with density for both TR values, the non-controlled multi-copy DTN protocols (i.e. Epidemic, and PRoPHET) show different responses for each value of TR. The overhead of these two DTN protocols for TR=100 m increases as density is very high, whereas the overhead decreases for TR=500 m in the same condition. In the case of TR=100 m, when a vehicle does not find the message's destination within the transmission range, it must transmit copies to every neighbor. This process is replicated to each neighbor, increasing the overhead. In the case of TR=500 m, there is no need to share messages with a large number of vehicles due to the presence of more neighbors within the transmission range.

5.3.4 Average number of hops

Figure 20a shows the results of the average number of hops for the lowest TR. As expected, the epidemic results are higher than in other protocols, and as with other DTN protocols, the number of hops grows as the density increases. Nonetheless, this metric tends to reduce at very high densities. In these conditions, the great difficulty of delivering a message, as seen in DR results, makes the average count of hops drop in the case of DTN.

The results in Figure 20a also permits concluding that multi-copy DTN protocols employ more hops than the traditional VANET options. Surprisingly, the GPSR performs quite similarly to DD, delivering the messages using just one hop transmission. It suggests that the greedy search strategy is not fast enough to find optional paths when vehicles turn away from each other. It is worth noting that delivering a message from one node to another is regarded as a one-hop transmission in the context of this work.

Figure 20 – Average number of hops with: (a) TR=100 m, (b) TR=500 m.

(a) Average number of hops with TR=100m **(b) Average number of hops with TR=500m**

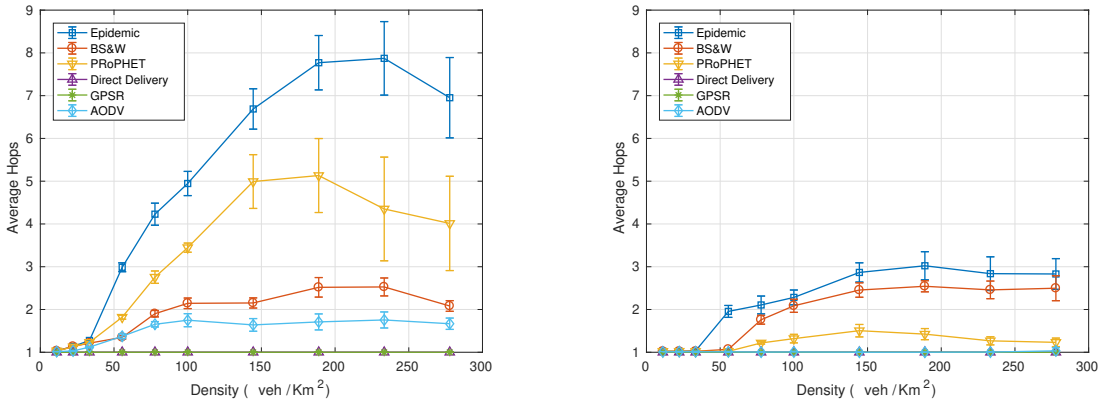

Source: Own authorship (2022).

On the other hand, the results in Figure 20b show the average number of hops for TR=500 m. Compared with Figure 20a, a significant reduction of this metric for Epidemic, PRoPHET, and AODV is observed. On the contrary, the BS&W and the GPSR tend to keep similar behavior to that of TR=100 m, with results ranging from 2 to 3 after the 100(vehicle/km^2) in the BS&W case, and around 1.0 in GPSR for any density. It means protocols with no copy limitations can deliver messages to farther neighbors within their transmission range, thus achieving the destination node with fewer hops.

5.4 The impact of beacon interval time

Once concluded that DTN is not a feasible choice for transmission of warning messages and that traditional VANET protocols deal better with high vehicular density for any transmission range, the next step is to evaluate how these last protocols perform with different BIT. With that in mind, a more detailed simulation for both AODV and GPSR, focusing on the beacon time interval effect, is performed in this section.

The simulation scenario corresponds to the urban case with the same set of vehicles and densities used in the previous section. In this case, the radio range has been set to 300m and the transmission rate to 3 Mbps. The first one corresponds to a typical range for simulation of VANETs, whereas the second one is slightly higher than the most usually employed values but significantly lower than the maximum theoretical rate of 27 Mbps (BOUSSOUFA-LAHLAH; SEMCHEDINE; BOUALLOUCHE-MEDJKOUNE, 2018; MALIK; SAHU, 2019).

As mentioned before, the routing protocol can be aware of mobility changes in more quick and accurate localization of hops by using *Hello* packets (or beacons). However, transmitting a large number of *Hello* packets may damage the network performance. For evaluation of such

Figure 21 – Impacts of the Beacon interval time: (a) Packet delivery ratio, (b) Average End-To-End Delay.

(a) Packet delivery ratio with AODV and GPSR

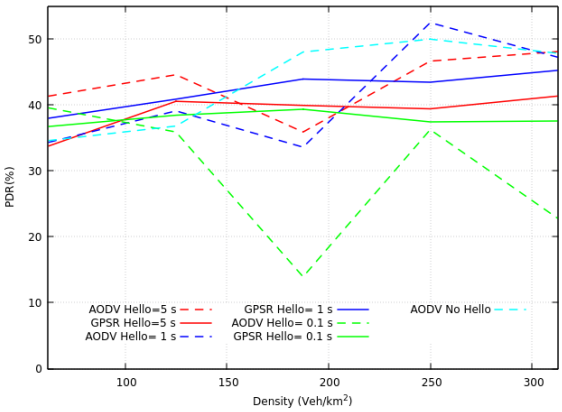

(b) Average End-To-End Delay with AODV and GPSR

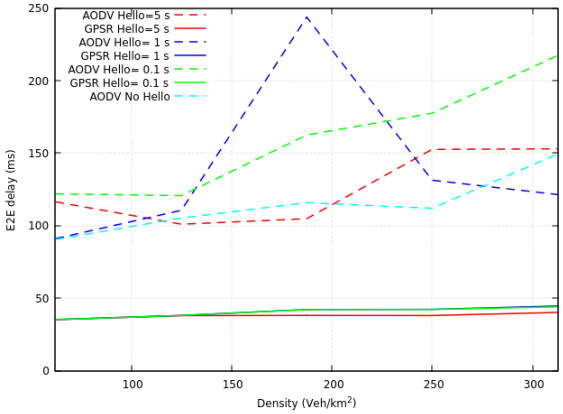

Source: Own authorship (2022).

impact, two of the most meaningful metrics for VANETs, the packet delivery ratio and the End-To-End Delay, are evaluated in this section.

The results of packet delivery ratio (PDR) versus vehicular traffic density for different *Hello* time intervals are shown in Figure 21a. Unlike AODV, where RREQ can perform the *Hello* function, the GPSR depends on *Hello* messages to know the neighbors' position. Hence no curve for *No Hello* was considered in GPSR. The results show that GPSR is more stable than AODV and seems to converge to a constant value as the *Hello* time interval decreases.

The results of End-to-End Delay (E2E Delay) versus traffic density for different *Hello* time intervals are shown in Figure 21b. The results show that the time reduction of *Hello* interval causes more impacts in AODV than in GPSR. Furthermore, for low densities, no increments of E2E Delay are obtained with GPSR. As evidenced in PDR, stability remains a characteristic feature of GPSR in the E2E Delay.

Also from Figure 21b a particular out of fit point for AODV at 187.5 (vehicle/km^2) for the case of *Hello* interval of 1 comes up. It is a singular case where the protocol can not keep a stable path between the origin and destination nodes. There exist two possible reasons: First, the ruling out of a large number of packets, as evidenced in Figure 21a for the same density, and second, the persistence on transmitting the packets, despite the considerable time it may demand. Figure 21b also permits us to see that GPSR performs better in such conditions.

5.5 Chapter Summary

This chapter presents an evaluation of Delay Tolerant Networks (DTN) and traditional VANET routing protocols with a particular focus on high-density conditions. The chapter begins with the experiment description and details of the methodology and the communication test. The

performance metrics are also mathematically described, and graphical results are comprehensively presented.

The main focus of the assessment is given to the role the vehicular density and beacon interval time (BIT) play on the network's performance. The results show that DTN is not a reliable choice for transmission of small-sized and frequent traffic information, the so-called beacons. From the traditional options addressed, the GPSR has shown to suffer the lowest impact from a short BIT, mainly because of the shorter E2E Delay the protocol has shown. Therefore, the GPSR becomes the most suitable protocol to be used for this work.

6 AN ADAPTIVE BEACON STRATEGY FOR A VANET-BASED CFM

The risk of network flooding is the main issue of using beacons to transmit kinematic information through VANET. A feasible VANET-based CFM implementation demands a high beacon transmission rate. Nonetheless, using so many beacons can drastically deteriorate the network performance.

This chapter describes a strategy to control the beacon time interval depending on traffic conditions. Despite the fact that the strategy can be used by any beacon-based protocol, in this work the GPSR protocol is employed, so the strategy is called Traffic Aware Beacon Interval for GPSR (TABI-GPSR). Similar to other works (LI; WANG; WANG, 2016), we consider both the upper and lower bounds T_{max} and T_{min}. Hence we employ them to define the bit interval time of the i_{th} vehicle (BIT_i), as indicated in equation (33),

$$BIT_i = T_{max} - (T_{max} - T_{min}) \cdot \alpha_i \tag{33}$$

where $0 \leq \alpha_i \leq 1$ represents the beacon rate coefficient, and the i_{th} vehicle is supposed to be placed at the center of a neighborhood Γ which is bounded to a radial range of 50 meters (approximately the half of typical street block).

The coefficient α_i changes according to the traffic conditions vehicle i is subject to. Vehicles with low mobility in highly dense areas do not need to maintain a short beacon interval. This coefficient depends on three functions: $f(\Delta v_i)$, $g(n)$, and $h(\Delta\theta_i)$, as stated in Equation 34

$$\alpha_i = K_1 \cdot f(\Delta v_i) + K_2 \cdot f(n) + K_3 \cdot f(\Delta\theta_i) \tag{34}$$

where K_1, K_2, and K_3 are weight constants also ranging from 0 to 1.

Each of these functions represents the effect of a different traffic condition experienced by vehicle i. For instance, the first function reflects the homogeneity of the speed among near-located neighbors, which can be expressed in terms of the mean difference of speed as stated in (35),

$$f(\Delta v_i) = 1 - e^{-\Delta v_i} \tag{35}$$

where Δv_i is computed according to equation (36),

$$\Delta v_i = \frac{1}{n}\sum_{j=1}^{n} v_i - v_j \qquad \forall j \in \Gamma \tag{36}$$

and n represents the number of vehicles in the neighborhood (Γ).

According to (35), a high difference between the speeds of vehicle i and its neighbors contributes to increasing α_i and decreasing BIT_i. In other words, vehicles with significant speed differences are prone to face rapid changes and may require a shorter beacon interval.

The second function $g(n)$ represents the effect of n neighbor vehicles. Such an effect is considered because vehicles in a highly dense area can quickly flood the network with excessive beacons. The exponential model (37) was previously employed to represent vehicular density in other beacon control formulations (LI; WANG; WANG, 2016). However, a square root factor was included in (37) for extending $g(n)$ to high densities.

$$f(n) = e^{1-\sqrt{n}} \tag{37}$$

The third function considers the difference of the angle $\Delta\theta_i$ among the neighbors of the i_{th} vehicle as defined in (38), where $\Delta\theta_i$ corresponds to the mean difference of the angle between two neighbors according to (39). Such an angle difference is exemplified in Figure 22 for the case of two neighbors.

Figure 22 – Angle between two neighbors of vehicle i.

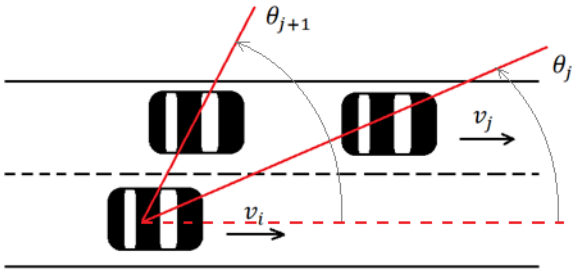

Source: Own authorship (2022).

This function reflects the position of the i_{th} vehicle in a vehicular stream. It considers that vehicles traveling at the front or rear end of a stream ($\Delta\theta_i = 0$) must search for new neighbors, so a higher beacon rate is necessary. On the other hand, vehicles at the stream's center can reduce the beacon frequency as little changes in the neighbors' position are expected.

$$f(\Delta\theta_i) = (1 - sin(\Delta\theta_i)) \tag{38}$$

The average angle is computed by (39).

$$\Delta\theta_i = \frac{1}{n}\sum_{j=1}^{n} \theta_{j+1} - \theta_j \qquad \forall j \in \Gamma \tag{39}$$

The three parameters K_1, K_2, and K_3 of equation (34) can be determined through simulation to find the most suitable operational point. In this work, such a condition is characterized by reduced communication overhead and minor kinematic disturbance, which are measured by two communication metrics (packet delivery ratio and the end-to-end delay) and one kinematic metric (the acceleration deviation). This last metric is defined as the standard deviation of the

acceleration. It is computed according to equation (40).

$$A_d = \sqrt{\frac{\sum_{t=1}^{N}(A_t - \overline{A})^2}{N}} \tag{40}$$

where A_t is the instantaneous acceleration at the time step t, $\overline{A}$ is the mean acceleration computed from all the results, and N is the total number of time steps.

The experiment encompassed extensive simulations using the urban scenario over the enhanced version of ns-2 with all combinations of K_1, K_2, and $K_3 \in \{0, 0.1, 0.2, \ldots, 1.0\}$. As each of the three functions is also bounded to the interval [0,1], the three weight constants must satisfy the condition:

$$K_1 + K_2 + K_3 \leq 1.0 \tag{41}$$

The results are depicted in the Figure 23.

Figure 23 – Space of solutions for all feasible combinations of K_1, K_2 and K_3.

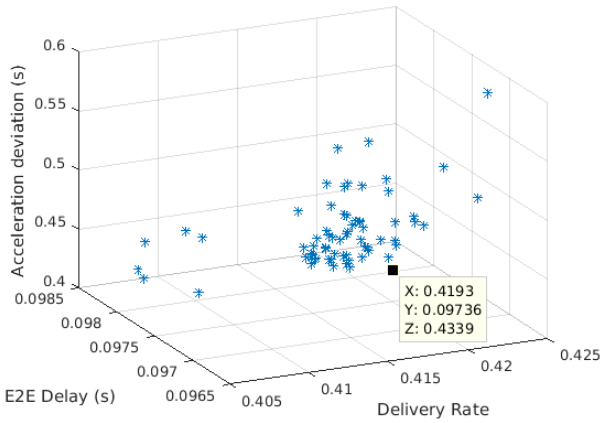

Source: Own authorship (2022).

The results show that many combinations of K_1, K_2 and K_3 perform well. However, the best result corresponds to Delivery Rate of 41.93%, an E2E Delay of 97.36 ms, and acceleration deviation of 0.4339 m/s^2 as shown in Fig. 23. This condition is achieved with $K_1 = 0.6$, $K_2 = 0.3$ and $K_3 = 0.1$ that are chosen for the next experiments.

6.1 Evaluation through a standard VANET simulation

A simulation test over an urban 450x450m, three road-by-side grid using the Manhattan mobility model, the Krauss CFM, and the parameters: $K_1 = 0.6$, $K_2 = 0.3$ and $K_3 = 0.1$ is performed to assess the global behavior of the adaptive BIT scheme. It is worth noting that the TABI-GPSR can also be used just for online adaptation of the BIT without mobility purposes. This section shows how the TABI-GPSR performs in a standard simulation of VANETs.

Figure 24 shows the evolution of the beacon interval time (BIT) using the TABI-GPSR strategy when compared with another traffic-aware beacon strategy, the GPSR-B&O (LI; WANG; WANG, 2016), where authors also employ traffic conditions for adaptation of the beacon interval. The simulation is performed with 5 and 40 vehicles, and, as no mobility control is involved, the largest BIT boundary has been set to 2 seconds.

Figure 24 – Evolution of the beacon interval using the proposed strategy.

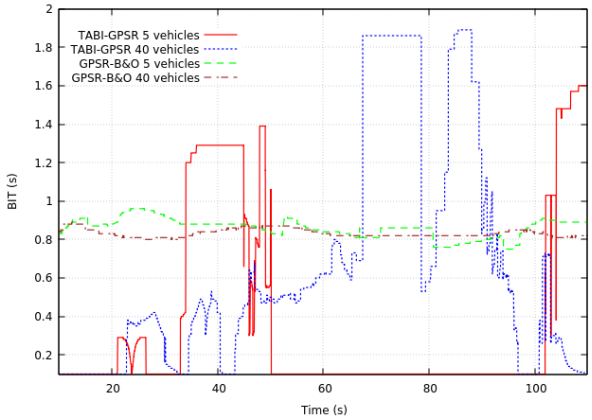

Source: Own authorship (2022).

Likewise, Figure 24 shows that vehicles using the TABI-GPSR change the beacon intervals across time. The broadest beacon interval time is reached for 40 vehicles. On the other hand, the GPSR-B&O scheme maintains an almost constant BIT with minor variations between 5 and 40 vehicles.

The average beacon processing delay, which corresponds to the mean time the processor takes to prepare the beacon for transmission and average beacon transmission delay, which corresponds to the mean time between the emission and the reception of a beacon, were evaluated and compared. The results of Figure 25 show that both beacon schemes add a delay of some microseconds. Nonetheless, the TABI-GPSR maintains a roughly constant delay, while the GPSR-B&O grows as the density of vehicles increases.

The results in Figure 25b reveal that the transmission delay for any beacon approach rapidly increases in high-traffic density situations. Specifically, the transmission delay for BIT=100ms is two milliseconds higher than for BIT=2s with the maximum number of vehicles. It reaffirms the importance of controlling the beacon interval in high-density environments, as performed by TABI-GPSR, which outperforms the GPSR-B&O for both processing and transmission delays.

Figure 25b also shows no relevant differences between short and long BIT values for low-density environments. In addition, a decreasing tendency is evidenced from 5 to 10 vehicles. It occurs because adding vehicles in low-density scenarios naturally helps the protocol achieve more successful and faster delivery of messages, as demonstrated in chapter 5.

Figure 25 – Average Delay of beacon schemes: (a) Processing Delay, (b) Transmission Delay.

(a) Average beacon processing delay. **(b) Average beacon transmission delay.**

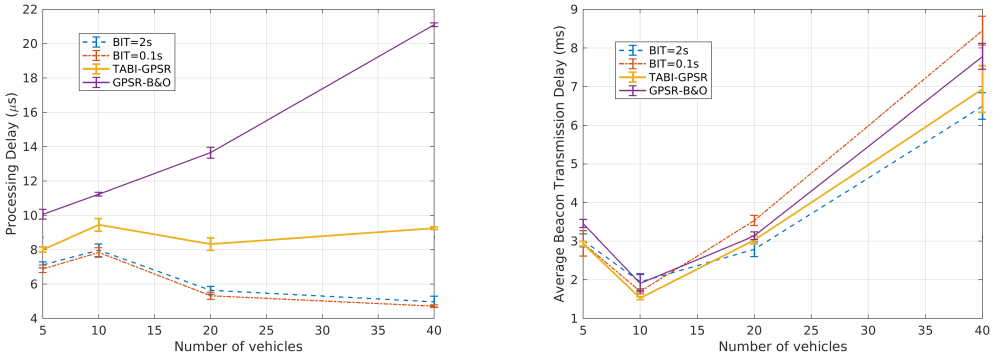

Source: Own authorship (2022).

6.2 Evaluation of network and mobility performance

The effectiveness of our strategy is also evaluated using both scenarios (Urban and Highway) for vehicles using the Multi-Anticipative car-following model (MA CFM) and the TABI-GPSR scheme. For each scenario, both the network performance and the kinematic response of vehicles are evaluated. For the first one, four different sets of vehicles (10, 15, 20, and 30) are employed, whereas, in the second one, the worst density case is considered.

6.2.1 Network performance

Although the same number of vehicles is considered in both scenarios, the global density is slightly different in both cases. In the urban scenario, vehicles at the intersection can pass through and take one of two orthogonal routes. In the highway scenario, vehicles are confined to just one route. For a fair comparison of the results, the local density is employed in this part.

As stated by (ARTIMY, 2007), the local density can be expressed as the number of vehicles per kilometer by lane $(veh/km/lane)$. However, traffic streams are not uniform, as they can vary over space and time. For that reason, in this work, the local density is computed using the average value from three stages: the beginning (once vehicles enter the scenario), the halftime (once vehicles are in the middle of the travel), and the end of the simulation (just before vehicles get out the scene).

For the density computation, the maximum euclidean distance between two vehicles is assumed as the road length. Likewise, only the effectively employed lanes at each stage are considered. For example, in the urban scenario, at the beginning (1st stage), cars are distributed over two lanes and two 300-meter length roads. As the furthest vehicles are placed at the end of each road, the Euclidean distance (E-dist) is 0.6 km and the minimum local density can be computed as $Dens_{min} = 10/0.6/2 = 8.36\ vehicle/km/lane$.

At halftime (2nd stage), vehicles are grouped at the traffic intersection, so the maximum euclidean distance is reduced to 40 meters. In the case of the highway, the same reduction occurs at the speed bump, so the maximum distance is reduced to 0.26 meters. In the third stage, vehicles in the urban scenario are distributed through the four roads using just a lane on each, so the euclidean distance is twice the used in the first stage. However, both distance and number of lanes doubled; therefore, the local density remains the same of the first stage.

The resultant average density in $vehicle/km/lane$ is then computed using the geometric mean from the partial results of each stage. Frame 2 summarizes these and other results. In this section, the maximum number of vehicles has been reduced to 30 because the simulation area is smaller than the Manhattan model's case. Therefore, the effective density is much higher, and the simulation consumes more computational resources than before.

Frame 2 – Average local densities.

# Veh	Stage	Urban					Highway				
		Roads	Lanes	E-dist (km)	Density (veh/km/lane)	Average density	Roads	Lanes	E-dist (km)	Density (veh/km/lane)	Average density
10	1	2	2	0.6	8.36	19.93	1	3	0.3	11	9.19
	2	2	2	0.04	113.37		1	3	0.26	12.57	
	3	4	1	1.19	8.36		1	3	0.59	5.62	
15	1	2	2	0.6	12.5	30.17	1	3	0.33	15.15	12.55
	2	2	2	0.043	174.41		1	3	0.29	17.24	
	3	4	1	1.19	12.6		1	3	0.66	7.57	
20	1	2	2	0.6	16.72	39.87	1	3	0.35	18.67	15.55
	2	2	2	0.044	226.74		1	3	0.31	21.03	
	3	4	1	1.19	16.72		1	3	0.69	9.59	
30	1	2	2	0.6	25	50.78	1	3	0.4	24.44	20.5
	2	2	2	0.072	208.15		1	3	0.37	26.88	
	3	4	1	1.19	25.08		1	3	0.76	13.07	

Source: Own authorship (2022).

The existence of a high number of neighbors and the sudden saturation of the channel because of excessive beacons may imply the use of multiple paths for delivering a stream of packages, which in turn can entail a high oscillatory behavior of the End-to-End delay. Hence, in this part, besides the Packet Delivery Ratio, E2E Delay, and Overhead, we study the Jitter, which is defined as the mean variation of the inter-arrival time of packets, as expressed in (42).

$$Jitter = \frac{\sum_{i=1}^{N-1}(D_{i+1} - D_i)}{N} \tag{42}$$

where D_i is the difference between the receiving and sending times of a packet i and N is the total number of received packets. The Jitter is a statistical disturbance of the Delivery Delay of packets in a network. This metric must be kept low for a better performance of the network (UPADHYAYA; SHAH *et al.*, 2019).

Figure 26 – Communication Metrics using the MA model in the urban scenario: (a) PDR, (b) E2E Delay, (c) Overhead, (d) Jitter.

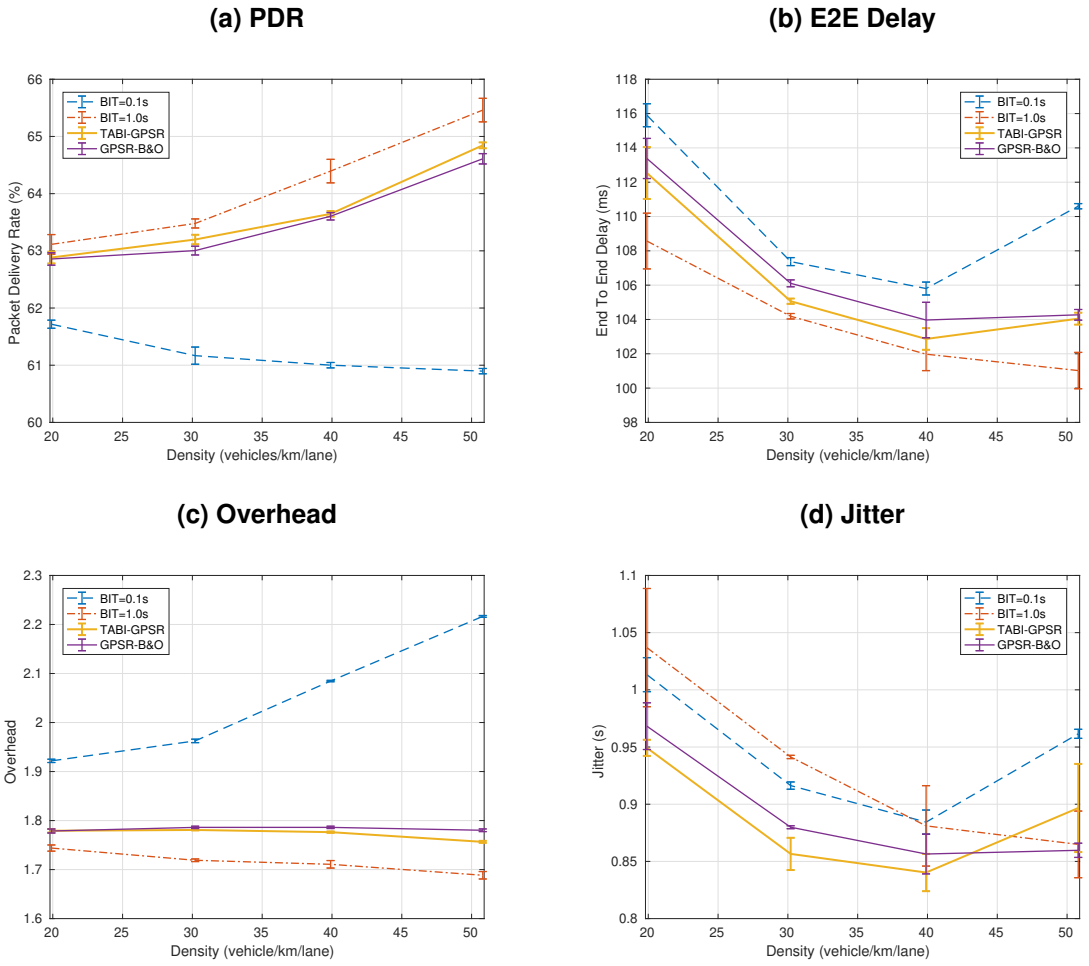

Source: Own authorship (2022).

The results of Packet Delivery Ratio, E2E Delay, Overhead, and Jitter are shown in Figure 26. According to the previously defined density equivalence, the original x-axis of 10, 15, 20, and 30 vehicles is replaced by the respectively average local density of Frame 2. The results of $BIT = 100ms$ and $BIT = 1s$ are also included for comparison purposes. Likewise, the performance of another approach for controlling the beacon rate, the GPSR-B&O, is also shown.

The delivery rate results in Figure 26a illustrate the impact of the vehicular density on the beacon time interval. In the case of a short BIT, as short as 100 ms, the DR decreases as the vehicular density increases. In the case of BIT=1s, the DR increases as the density grows. That result means that a short BIT reduces the protocol's capacity in delivering a packet, whereas a long BIT contributes to more delivery.

As in the case of the most extended BIT, The results of TABI-GPSR contribute to increasing the delivery rate of the GPSR as the density grows. Likewise, the TABI-GPSR matches the results of GPSR-B&O in the lowest density and outperforms it for the highest.

On the other hand, Figure 26b demonstrates that the End to End Delay is the highest for the shortest BIT and the lowest for the higher BIT. As for the effects of the density, Figure 26b shows that the increase of vehicles initially contributes to reducing the delay in a low-density environment. However, as the density increases, a short BIT increases the delay. The results show that TABI-GPSR keeps the delay between the two boundaries while outperforming the GPSR-B&O approach.

Figure 26c shows the results of the overhead. As in previous metrics, the case of BIT=100 ms shows the worst performance with the highest overhead of all options, whereas the BIT=1 s yields the better one. The results of TABI-GPSR are closer to the best case and outperform the GPSR-B&O approach for the highest density.

Similar to the case of the E2E Delay, the Jitter results in Figure 26d show an increasing trend in high densities for the shortest BIT and a reduction for the largest one. The results of TABI-GPSR and GPSR-B&O also perform well, as they remain better than the boundary conditions. Moreover, both beacon approaches outperform the results of BIT=1 s for low density.

In the case of highway scenario, the Figure 27a shows the results of the packet delivery ratio (PDR). Unlike urban results, where increasing the density improves the PDR, except the case of BIT=100ms, in the highway scenario, the PDR steps down for every beacon case. Nonetheless, in this scenario, the GPSR-B&O outperforms the TABI-GPSR for every density.

Figure 27b shows an incremental response of the E2E Delay regarding all beacon cases. Similar to the PDR, these results suggest that the higher the density, the greater difficulty a packet has in reaching its destination. As expected, the higher delay is obtained with the shortest BIT. Likewise, as occurred with PDR, the GPSR-B&O outperforms the TABI-GPSR. The E2E Delay results also differ from the urban case, where this metric reduces as the vehicle density increases for most cases, except for BIT=100ms.

Similar to the E2E Delay, the overhead results in Figure 27c show a growing trend as the density increases. Like previous metrics, these results show the challenge the flooding imposes on delivering messages, particularly for BIT=100ms. In addition, and similar to the urban case, the TABI-GPSR keeps the overhead closer to the minimum beacon boundary.

The results in Figure 27d show that more Jitter is attached to packets transmitted in high congested networks, especially for short BIT cases. As in previous results, the TABI-GPSR maintains a good performance, remaining between both boundaries despite not outperforming the GPSR-B&O results.

A global comparison between the urban and highway results can also be made. As evidenced in Figures 26 and 27, consistent differences on each graph can be observed. In the highway scenario, the PDR is higher than in the urban case, whereas the E2E Delay, Overhead, and Jitter are higher in urban than in the highway scenario. These results are consistent with the findings of chapter 5, where a significant reduction in the general performance is evidenced when vehicular density is largely increased.

Figure 27 – Communication Metrics using the MA model over the highway scenario: (a) PDR, (b) E2E Delay, (c) Overhead, (d) Jitter.

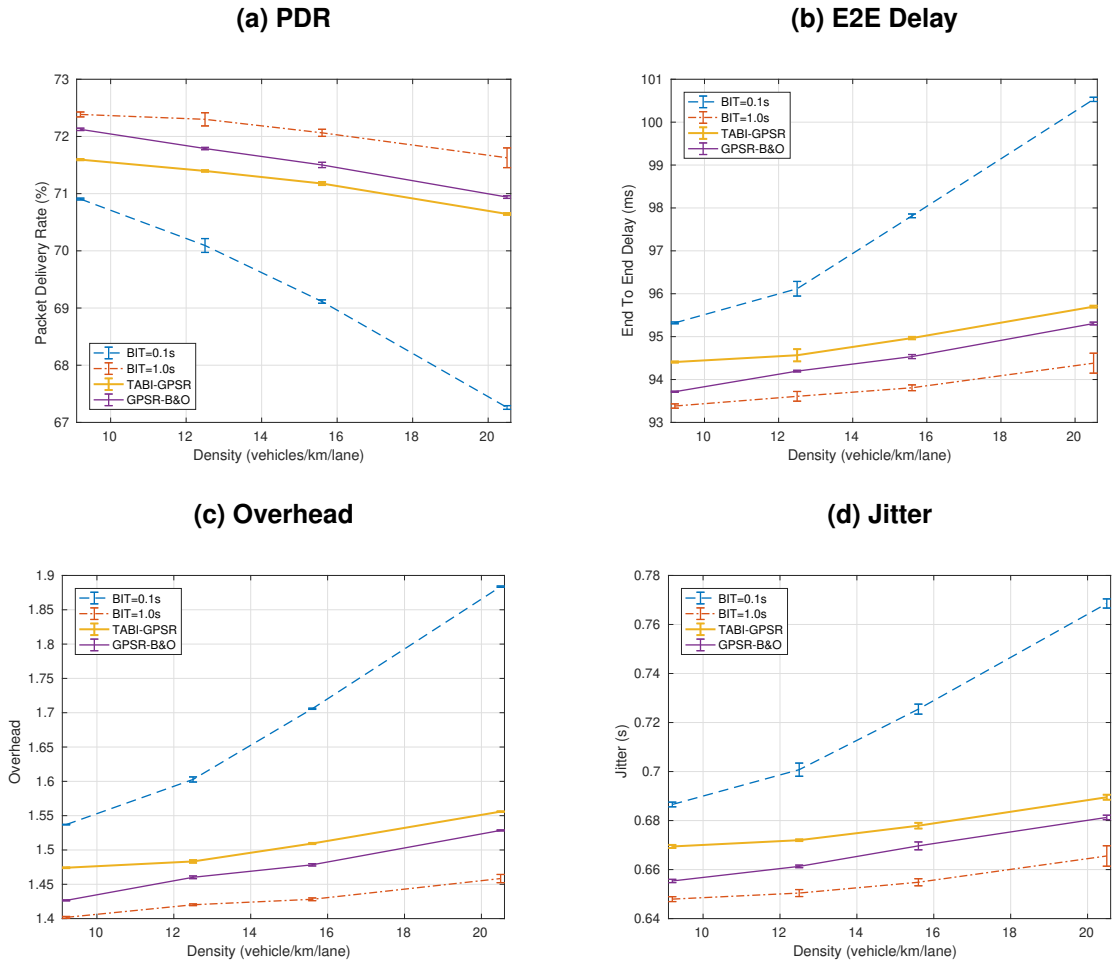

Source: Own authorship (2022).

As for specific behaviors of each metric, the reduction of PDR in the highway scenario, for instance, occurs because the vehicle's distribution and the total coincidence of the movement direction make no need to add more vehicles to improve the communication. The actual effect of such vehicles contributes to the network's flooding, as studied in chapter 5. In the case of the Urban case, the additional vehicles help to compensate for the increasing inter-vehicle distance produced by vehicles moving far away from each other after the traffic light.

The same argument works to understand the reduction of each metric: E2E Delay, Overhead, and Jitter in the case of the urban scenario, whereas, in the case of the highway scenario, the same metrics present a growing response. It is worth noting that, in general, better communication performance is obtained with a constant BIT of one second. However, such a rate is not reliable for use in driver assistance systems. An adaptive approach such as the TABI-GPSR may achieve a similar performance while enabling vehicles to be safely driven, as shown in the following section.

6.2.2 Mobility performance

For assessment of the mobility performance, simulations in this part employ only the highest number of vehicles for each scenario. As showing the dynamics of all the vehicles may difficult the graphical comparison, only the results of vehicles over one of the lanes are considered. This section presents the performance of the most internal lane's vehicular stream versus the traveled time for both scenarios.

Figure.28 shows a comparison of the mobility metrics (i.e. Speed, position, acceleration, and State of charge) for three different options of beacon interval time (100 ms, 1 s, and TABI-GPSR) using the urban scenario. As indicated by the speed and position profiles of the first vehicle (Green plot), the vehicle speed up once the simulation starts and achieves a maximum speed of over 14 m/s. The vehicle starts to brake just after surpassing 250 meters to stop at the traffic light placed at 300 meters. Then, it remains stopped until the 45th second, when the traffic light opens, and the vehicle resumes the trip.

The results in Figure 28a show the smoothness of speed profile with BIT=100 ms if compared with BIT=1 s in Figure 28b. Such a behavior reflects in a higher disturb in acceleration profile of Figure 28h if compared with Figure 28g. Such behavior occurs because vehicles working with outdated neighbor's information tend to brake as they reason that preceding vehicles have stopped moving.

Besides the disturbance in acceleration, Figure 28e reveals that vehicles using a BIT=1 s may experience an increase of the inter-vehicle gap if compared with BIT=100 ms. For instance, vehicles with a BIT=1.0 s at the 20th second are fully spread through the road space from 100 m to 200 m, whereas vehicles using BIT=100ms are grouped in a shorter space. Likewise, the last vehicle reaches a final position of 300 m with BIT=100 ms, whereas the same vehicle ends up behind 300 m when using a BIT=1 s.

As for energy results, Figures.28j and 28k suggests that the final state of charge with both boundary conditions is not different. However, a slightly lower SoC is observed in the case of BIT=1 s once vehicles stop at the traffic light. The graph 28k shows that the frequent speed up and down makes the vehicles waste more energy as the minimum SoC of vehicles before the traffic light is lower in the case of BIT=1 s than in the case of BIT=100 ms.

The speed profile resultant from using the TABI-GPSR strategy is depicted in Figure 28c. This graph shows a significant reduction in the disturbance of the speed profile if compared with the BIT=1s case. Likewise, the position profile shown in Figure 28f demonstrates that TABI-GPSR reduces the inter-vehicle gap of the BIT=1s case, as the distance between the first and the latest vehicles is shorter at the 20th second and vehicles show a more closely tracking of the preceding vehicles at the end of the travel.

The results of the highway tests are depicted in Figures 29 and 27. Figure 29 shows a comparison of the mobility metrics for ten of the vehicles. As evidenced, vehicles on the highway can travel at a constant speed for a longer time compared to the urban case. In addition, vehicles

Figure 28 – Mobility metrics using MA CFM over an urban scenario with high density: (a), (b) and (c) Speed, (d), (e) and (f) Position, (g), (h) and (i) Acceleration, and (j), (k), (l) State of charge.

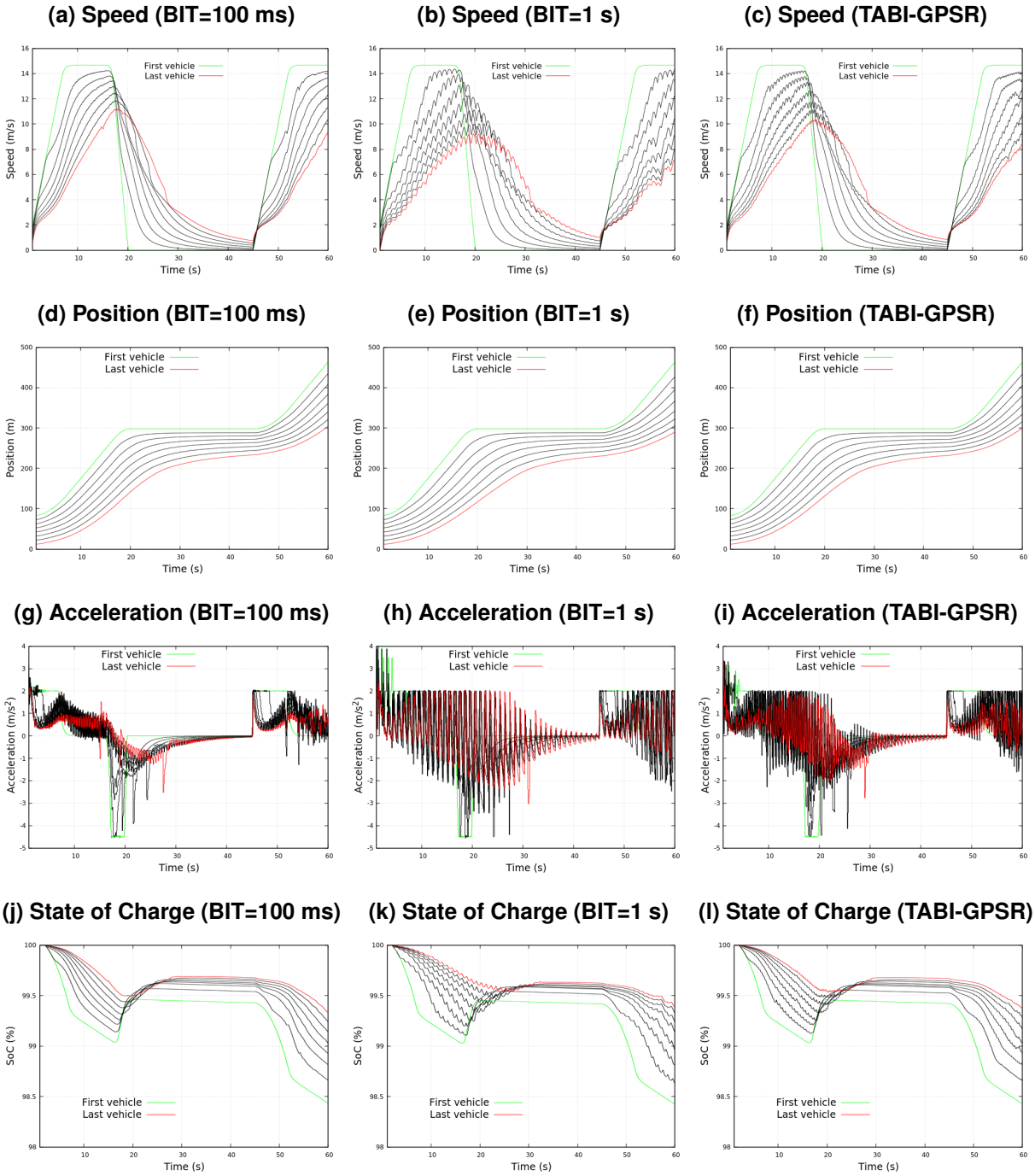

Source: Own authorship (2022).

Figure 29 – Mobility metrics using MA CFM over a highway scenario with high density: (a), (b) and (c) Speed, (d), (e) and (f) Position, (g), (h) and (i) Acceleration, and (j), (k), (l) State of charge.

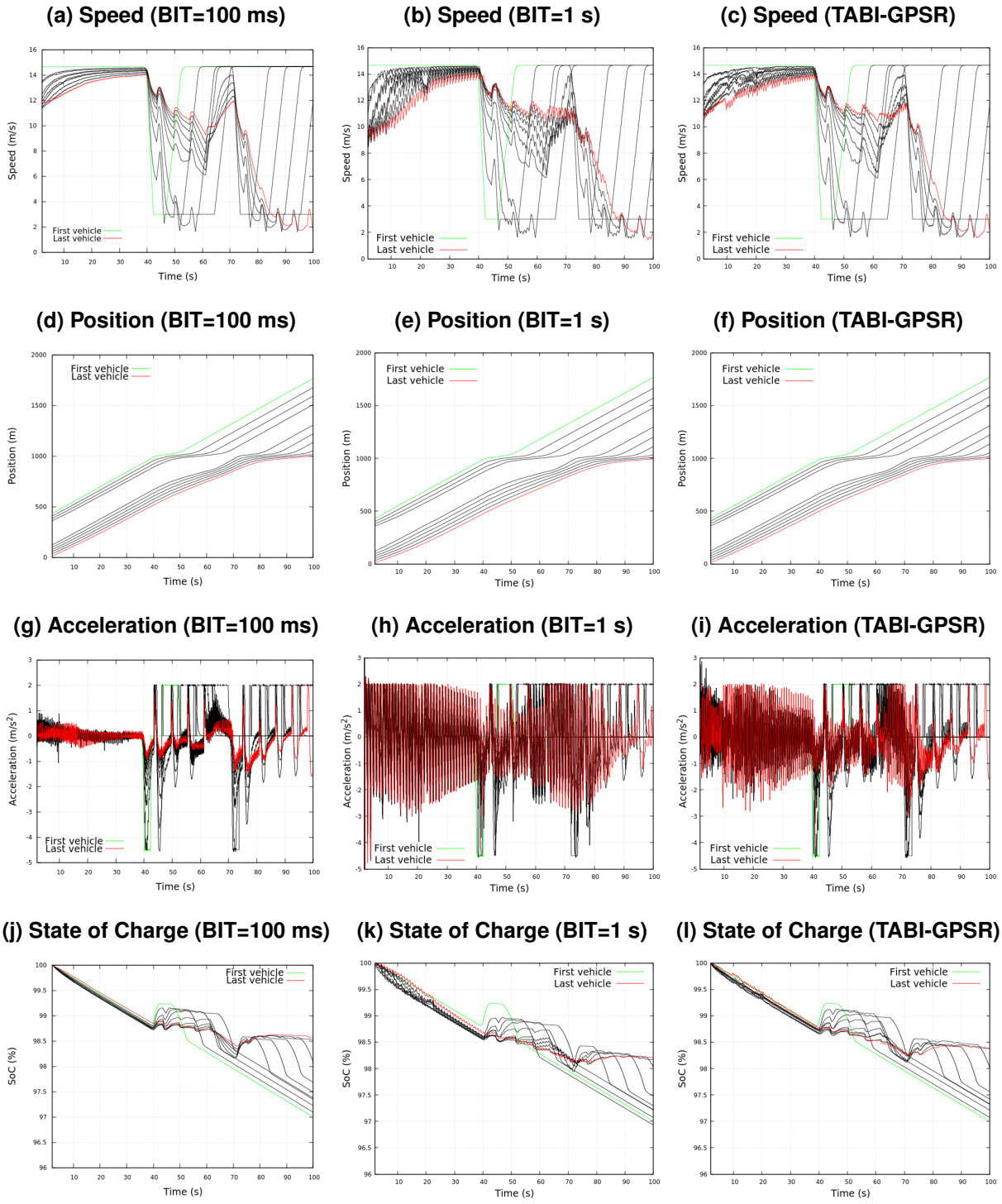

Source: Own authorship (2022).

are not expected to stop completely for longer periods, so a higher homogeneity of performance is expected.

As the speed profiles in Figure 29 suggest, vehicles in the highway scenario are expected to appear in the scene at a certain speed, higher than in the case of the urban case. Then, the

vehicles must reduce their speed to 3 m/s maximum while driving through the speed bump at half of the trip.

As shown in Figures 29a and 29d the first vehicle (green plot) meets the minimum speed at 1000 m. Once it has surpassed the speed bump, it speeds up to its maximum capacity, and the position plot linearly grows again.

From Figure 29a, it can be seen that each vehicle has a high sensitivity to changes in the speed of the proceedings. In the case of the rear group, the vehicles are influenced to reduce their speed simultaneously with the head group. However, as the first vehicles overcome the speed bump, the vehicles in the rear group need to speed up again to meet the speed bump's position.

Similar to the urban case, using a BIT=1s in the highway scenario makes the speed profile in Figure 29b have a high distortion, which is certainly reflected in the acceleration profile of Figure 29h. Likewise, as in the urban case, such a distortion causes a response delay that makes the inter-vehicle gap more prominent than in the case of BIT=100 ms, as evidenced in Figure 29e.

In the case of the TABI-GPSR, the results in Figure 29c show low distortion while keeping an inter-vehicle gap similar to the BIT=100 ms case, as evidenced in Figure 29f. In addition, as the TABI-GPSR tends toward a short BIT for high variations of speed, the speed profile through the braking phase is more similar to that of 100 ms. This feature makes the vehicles keep more aware of potential risks when necessary.

The battery results in Figures.29j and 29k unveil that vehicles with a higher dependence on preceding neighbor's information, like the rear group, are the most prone to lose energy when using a BIT of one second, as the frequent speed up and down make the vehicle waste more energy than that recovered through regenerative braking. On the other hand, Figure 29l shows that the energy profile of TABI-GPSR is more similar to the case of BIT=100 ms than the case of BIT=1s.

6.3 Chapter Summary

This chapter presents the formulation and performance of an adaptive beacon strategy applied to the GPSR protocol, the so-called TABI-GPSR. The strategy relies on harnessing traffic information gathered from the VANET, like the vehicular density, the mean spatial distribution, and the speed of neighbors. Unlike other traffic-aware approaches, such as the GPSR-B&O, the proposed strategy employs all the available BIT range and achieves better results in the urban scenario.

The strategy's performance is evaluated through intensive simulations using mobility metrics and communication statistics. The results show the benefits on comfort and energy the TABI-GPSR yields if compared with the case of BIT=1 s. Likewise, the results show the impacts a short

BIT represents on network performance and how the TABI-GPSR contributes to alleviating such issues by continuously adapting the beacon rate.

7 CONCLUSION

This thesis has presented a comprehensive study on the practical impacts that controlling the mobility of an electric vehicle through beacons would have on network performance. Likewise, a novel adaptive strategy for controlling the network beacon burden over the GPSR protocol has been introduced and evaluated.

The results of this work show that if the ETSI recommended beacon time interval of 100 ms is employed for automatic driving of an electric and connected vehicle, a drastic reduction of the network performance is obtained. Such affirmation is particularly valid for high-dense networks in urban and highway scenarios. Therefore, vehicular assistance systems, particularly time-critical ones, can not rely on high-frequency beacon messages without affecting network performance.

As an alternative to overcome the negative impacts of using a high-frequent beacon transmission, a novel adaptive beacon scheme has been proposed, the so-called TABI-GPSR. It is a mathematical model which uses three components, the number of neighbors, the homogeneity of the speed among near-located neighbors, and the spatial distribution of neighbors represented by the relative angle. As envisioned by this work, the TABI-GPSR permits a satisfactory operation of a multi-anticipative car-following model while reducing the impacts of excessive beacons on the network performance.

The proposed approach has also been compared with another beacon control approach, the GPSR-B&O. The results demonstrate that TABI-GPSR performs better in urban scenarios with a high vehicular density. The main reason is that TABI-GPSR uses a better formulation for dimensioning the number of neighbors and permits detecting situations where the beacon time interval can be largely augmented, as in the case of vehicular congestion. It enables the TABI-GPSR to employ the whole available beacon time interval, depending on highly variant traffic conditions.

The multi-anticipative model (MA) has been employed in this work in response to another guiding hypothesis, that an electric vehicle can perform a more effective energy recuperation than any other. The results in chapter 4 show that vehicles using the MA model achieve a higher final state of charge (SoC) than vehicles using the Krauss model. However, the energy savings are more expressive in a highway scenario than in an urban one.

Despite the MA model showing better energy results, the SoC profile reveals that avoiding an unnecessary effort at the acceleration phase has a higher impact on final energy results than performing a more extended regenerative braking phase. In the case of a traditional choice, such as the Krauss model, a sudden and heavy braking effort may theoretically contribute to more significant energy recuperation. However, in the real world, such a recuperation may be limited by battery capacity and other physical challenges. Therefore, avoiding unnecessary energy waste through an anticipative method, as employed in this work, can be a better choice for more efficient mobility with electric vehicles.

The difficulty in reproducing the most recently proposed VANET-based CFMs in current simulation tools, for instance, the MA model, has made it necessary to build an adaptation of the ns-2 software. The developed tool is another valuable outcome of this work. The effectiveness of the software has been verified using the Krauss model, as it is also available in the SUMO simulator. Thanks to the modular structure of the software, the use of a large variety of beacon-based routing protocols in VANETs becomes possible.

For delivering the traffic information among vehicles, a large set of protocols were studied in this work, including delay-tolerant like Epidemic, PRoPHET, BS&W, and Direct Delivery, as well as traditional options like AODV and GPSR. The results show that DTN protocols exhibit great difficulty performing in high-density and high transmission range scenarios. In such conditions, the number of hops and overhead is enhanced, whereas the delivery rate and average end-to-end delay worsen. It means that a higher number of neighbors in the transmission range demands a high amount of resources, which makes the DTN protocols fail. The low delivery rate and high end-to-end delay make the DTN unreliable for transmitting warning messages in high-dense scenarios.

On the other hand, the traditional routing protocols (AODV and GPSR) have shown a better performance than DTN for high density within any transmission range. In that case, a high number of vehicles, resulting from a higher density, guarantees the existence of a path between source and destination nodes, which is a suitable scenario for traditional VANET protocols. Moreover, the route storage capacity of AODV leads to a higher delivery rate than in GPSR, particularly in urban scenarios, where vehicles are expected to get closer and move away from each other frequently. However, the reduced End-to-End Delay of GPSR makes it more indicated than AODV to the application proposed in this thesis.

Many other routing protocols could be assessed in this work – mainly those specifically envisioned for VANETs. Unfortunately, some of them are not publicly available, which represents a significant drawback. In addition, although both urban and highway scenarios model different traffic conditions, the routing protocols could be evaluated in a mixed and large-scale scenario. In this case, the benefits of the MA model could be evaluated for energy consumption as well. Actually, many assumptions should be made for implementing multi-preceding-based models such as the information necessary from the preceding vehicles. This particular feature imposes significant limitations to overcome.

7.1 Future work

Future work aims to apply our strategy to other position-based protocols in VANETs as GPCR and VADD, for instance. Unfortunately, these and other routing protocols are not publicly available. Nonetheless, the modular structure of the simulation used in this thesis can include other routing protocols if they are available.

Besides the evaluation of other routing protocols, future work will address the impact of using other physical-layer features, for instance, variations of the propagation model, transmission power adaptation, integration of infrastructure resources (V2I), predictive techniques for tracking vehicles over VANETs, or even incorporating other communication techniques like Vehicular Light Communication networks (VLC) or Free-space Optical communication (FSO).

The adapted VANET simulation tool also allows the optimization of the studied CFM for dynamically achieving maximum efficiency depending on traffic conditions. That includes the integration of low-computational-cost algorithms for the application of heuristic techniques. Other VANET-based CFMs can also be studied and even the proposition of a novel CFM approach is a feasible task.

BIBLIOGRAPHY

ABDALLA, A. M.; SALAMAH, S. H. Performance comparison between delay-tolerant and non-delay-tolerant position-based routing protocols in VANETs. **International Journal of Communications, Network and System Sciences**, Scientific Research Publishing, v. 15, n. 1, p. 1–14, jan 2022. Disponível em: https://doi.org/10.4236/ijcns.2022.151001.

ABUASHOUR, A.; KADOCH, M. Control overhead reduction in cluster-based vanet routing protocol. *In*: **Ad hoc networks**. [*S.l.*]: Springer, 2018. p. 106–115.

AL-RABAYAH, M.; MALANEY, R. A new hybrid location-based ad hoc routing protocol. *In*: IEEE. **2010 IEEE Global Telecommunications Conference GLOBECOM 2010**. Miami, FL, USA, 2010. p. 1–6.

ALLOUCHE, Y.; SEGAL, M. Cluster-based beaconing process for VANET. **Vehicular Communications**, Elsevier BV, v. 2, n. 2, p. 80–94, apr 2015.

ALSAQOUR, R. *et al.* Dynamic packet beaconing for GPSR mobile ad hoc position-based routing protocol using fuzzy logic. **Journal of Network and Computer Applications**, Elsevier, v. 47, p. 32–46, 2015. Disponível em: https://doi.org/10.1016/j.jnca.2014.08.008.

ALZAMZAMI, O.; MAHGOUB, I. Geographic routing enhancement for urban vanets using link dynamic behavior: A cross layer approach. **Vehicular Communications**, v. 31, p. 100354, 2021. ISSN 2214-2096. Disponível em: https://www.sciencedirect.com/science/article/pii/S2214209621000231.

AMAYA, A. T. *et al.* Performance assessment of DTN and VANET protocols for transmitting periodic warning messages in high vehicular density networks. **Journal of Communication and Information Systems**, v. 37, n. 1, p. 91–103, 2022. Disponível em: https://doi.org/10.14209/jcis.2022.10.

AMAYA, A. T. *et al.* Traffic-aware beacon interval for position-based protocols in VANETs. *In*: IEEE. **2022 IEEE Latin-American Conference on Communications (LATINCOM)**. Rio de Janeiro, Brazil, 2022. (to be published).

AMAYA, Á. T.; POHL, A.; LÜDERS, R. Performance evaluation of GPSR and AODV routing protocols for high vehicular density vanets. *In*: SBRT. **SBrT 2021, XXXIX Simposio Brasileiro de Telecomunicaçoes e Processamento de Sinais**. Fortaleza, CE., Brazil, 2021.

AMOOZADEH, M. *et al.* Platoon management with cooperative adaptive cruise control enabled by VANET. **Vehicular communications**, Elsevier, v. 2, n. 2, p. 110–123, Apr. 2015. Disponível em: https://doi.org/10.1016/j.vehcom.2015.03.004.

ARTIMY, M. Local density estimation and dynamic transmission-range assignment in vehicular ad hoc networks. **IEEE Transactions on Intelligent Transportation Systems**, Institute of Electrical and Electronics Engineers (IEEE), v. 8, n. 3, p. 400–412, sep 2007.

ASAITHAMBI, G. *et al.* Study of traffic flow characteristics using different vehicle-following models under mixed traffic conditions. **Transportation letters**, Taylor & Francis, v. 10, n. 2, p. 92–103, 2018. Disponível em: https://doi.org/10.1080/19427867.2016.1190887.

AZNAR-POVEDA, J. *et al.* Approximate reinforcement learning to control beaconing congestion in distributed networks. **Scientific Reports**, Nature Publishing Group, v. 12, n. 1, p. 1–11, jan 2022. Disponível em: https://doi.org/10.1038/s41598-021-04123-9.

BABU, S.; P, A. R. K. A comprehensive survey on simulators, emulators, and testbeds for vanets. **International Journal of Communication Systems**, Wiley Online Library, v. 35, n. 8, p. e5123, 2022. Disponível em: https://doi.org/10.1002/dac.5123.

BAKIBILLAH, A. S. M. *et al.* Predictive car-following scheme for improving traffic flows on urban road networks. **Control Theory and Technology**, Springer Science and Business Media LLC, v. 17, n. 4, p. 325–334, nov 2019.

BALA, R.; KRISHNA, C. R. Scenario based performance analysis of AODV and GPSR routing protocols in a VANET. *In*: IEEE. **2015 IEEE International Conference on Computational Intelligence & Communication Technology**. Ghaziabad, India, 2015. p. 432–437.

BAO, X. *et al.* Efficient clustering V2V routing based on PSO in VANETs. **Measurement**, v. 152, p. 107306, feb 2020. ISSN 0263-2241. Disponível em: https://www.sciencedirect.com/science/article/pii/S0263224119311704.

BENAMAR, N. *et al.* Routing protocols in Vehicular Delay Tolerant Networks: A comprehensive survey. **Computer Communications**, v. 48, p. 141–158, Jul. 2014. ISSN 01403664.

BENGAG, A.; BENGAG, A.; ELBOUKHARI, M. Routing protocols for VANETs: a taxonomy, evaluation and analysis. **Advances in Science, Technology and Engineering Systems Journal**, v. 5, n. 1, p. 77–85, Jan. 2020. Disponível em: https://dx.doi.org/10.25046/aj050110.

BILSTRUP, K. *et al.* Evaluation of the IEEE 802.11 p MAC method for vehicle-to-vehicle communication. *In*: IEEE. **2008 IEEE 68th Vehicular Technology Conference**. Calgary, AB, Canada, 2008. p. 1–5.

BOUSSOUFA-LAHLAH, S.; SEMCHEDINE, F.; BOUALLOUCHE-MEDJKOUNE, L. Geographic routing protocols for vehicular ad hoc networks (VANETs): A survey. **Vehicular Communications**, Elsevier, v. 11, p. 20–31, 2018. Disponível em: https://doi.org/10.1016/j.vehcom.2018.01.006.

CAO, X.; WANG, J.; CHEN, C. A Modified Car-following Model Considering Traffic Density and Acceleration of Leading Vehicle. **Applied Sciences**, MDPI AG, v. 10, n. 4, p. 1268, feb 2020.

CARLA. 2022. Disponível em: http://carla.org/.

CHITRA, M.; SIVASATHYA, S.; MUTHAMIZH, B. Performance analysis of topology based routing protocols in VANET. **International Journal of Computer Science and Mobile Computing**, v. 3, n. 3, p. 966–975, 2014.

CODY, J. *et al.* Regenerative braking in an electric vehicle. *In*: **Problems of operating machines and electric drives**. Rytro, Poland: [*s.n.*], 2009. Disponível em: https://www.researchgate.net/publication/229008205.

ETSI, T. Intelligent transport systems (its); vehicular communications; basic set of applications; part 2: Specification of cooperative awareness basic service. **Draft ETSI TS**, v. 20, n. 2011, p. 448–51, 2011.

FORSTER, M. *et al.* A cooperative advanced driver assistance system to mitigate vehicular traffic shock waves. *In*: IEEE. **IEEE INFOCOM 2014-IEEE Conference on Computer Communications**. Toronto, ON, Canada, 2014. p. 1968–1976.

Gonçalves Filho, J. *et al.* A systematic technical survey of DTN and VDTN routing protocols. **Computer Standards and Interfaces**, Elsevier B.V., v. 48, p. 139–159, 2016. ISSN 09205489. Disponível em: http://dx.doi.org/10.1016/j.csi.2016.06.004.

GUNTER, Y.; WIEGEL, B.; GROSSMANN, H. P. Cluster-based medium access scheme for VANETs. *In*: IEEE. **2007 IEEE Intelligent Transportation Systems Conference**. Bellevue, WA, USA, 2007. p. 343–348.

HAMZA-CHERIF, A. *et al.* Performance evaluation and comparative study of main VDTN routing protocols under small- and large-scale scenarios. **Ad Hoc Networks**, Elsevier B.V., v. 81, p. 122–142, Dec. 2018. ISSN 15708705. Disponível em: https://doi.org/10.1016/j.adhoc.2018.07.008.

HARRI, J.; FILALI, F.; BONNET, C. Mobility models for vehicular ad hoc networks: a survey and taxonomy. **IEEE Communications Surveys & Tutorials**, IEEE, v. 11, n. 4, p. 19–41, 2009.

HOUSSAINI, Z. S. *et al.* Trade-off between accuracy, cost, and QoS using a beacon-on-demand strategy and Kalman filtering over a VANET. **Digital Communications and Networks**, Elsevier, v. 4, n. 1, p. 13–26, Sep. 2018. Disponível em: https://doi.org/10.1016/j.dcan.2017.09.001.

HU, L.; DING, Z.; SHI, H. An improved GPSR routing strategy in VANET. *In*: IEEE. **2012 8th International Conference on Wireless Communications, Networking and Mobile Computing**. Shanghai, China, 2012. p. 1–4.

HUANG, D.; SHERE, S.; AHN, S. Dynamic highway congestion detection and prediction based on shock waves. *In*: **Proceedings of the seventh ACM international workshop on VehiculAr InterNETworking**. Chicago, Illinois, USA: Association for Computing Machinery, 2010. p. 11–20. ISBN 9781450301459. Disponível em: https://doi.org/10.1145/1860058.1860061.

JIA, D.; NGODUY, D. Enhanced cooperative car-following traffic model with the combination of V2V and V2I communication. **Transportation Research Part B: Methodological**, Elsevier BV, v. 90, p. 172–191, aug 2016.

JIA, D.; NGODUY, D.; VU, H. L. A multiclass microscopic model for heterogeneous platoon with vehicle-to-vehicle communication. **Transportmetrica B: Transport Dynamics**, Informa UK Limited, v. 7, n. 1, p. 311–335, feb 2018.

JIANG, R.; WU, Q.; ZHU, Z. Full velocity difference model for a car-following theory. **Physical Review E**, APS, v. 64, n. 1, p. 017101, 2001. Disponível em: https://doi.org/10.1103/PhysRevE.64.017101.

JIAO, S. *et al.* An extended car-following model considering the drivers' characteristics under a V2V communication environment. **Sustainability**, MDPI AG, v. 12, n. 4, p. 1552, feb 2020.

JIMÉNEZ, F. *et al.* Advanced driver assistance system for road environments to improve safety and efficiency. **Transportation Research Procedia**, Elsevier BV, v. 14, p. 2245–2254, 2016.

JORDANOSKA, V.; GJURKOV, I.; DANEV, D. COMPARATIVE ANALYSIS OF CAR FOLLOWING MODELS BASED ON DRIVING STRATEGIES USING SIMULATION APPROACH. **Mobility and Vehicle Mechanics**, Faculty of Engineering, University of Kragujevac, v. 44, n. 2, p. 1–11, oct 2018.

JUSSIANI, W. A. *et al.* **Desempenho e conectividade de redes híbridas em sistemas de transporte inteligente cooperativo**. 2019. Dissertação (Mestrado) — Universidade Tecnológica Federal do Paraná, 2019.

KAKARLA, J. *et al.* **A Survey on Routing Protocols and its Issues in VANET**. 2011. International Journal of Computer Applications (0975 – 8887).

KARP, B.; KUNG, H.-T. GPSR: Greedy perimeter stateless routing for wireless networks. *In*: **Proceedings of the 6th annual international conference on Mobile computing and networking**. [*s.n.*], 2000. p. 243–254. Disponível em: https://doi.org/10.1145/345910.345953.

KENNEY, J. B. Dedicated short-range communications (DSRC) standards in the united states. **Proceedings of the IEEE**, IEEE, v. 99, n. 7, p. 1162–1182, 2011.

KNORR, F. *et al.* Reducing traffic jams via VANETs. **IEEE Transactions on Vehicular Technology**, Institute of Electrical and Electronics Engineers (IEEE), v. 61, n. 8, p. 3490–3498, oct 2012.

KUANG, H. *et al.* An extended car-following model considering multi-anticipative average velocity effect under V2V environment. **Physica A: Statistical Mechanics and Its Applications**, Elsevier, v. 527, p. 121268, 2019. Disponível em: https://doi.org/10.1016/j.physa.2019.121268.

LAN, K.-C. MOVE: a practical simulator for mobility model in VANET. *In*: **Telematics communication technologies and vehicular networks: wireless architectures and applications**. [*S.l.*]: IGI Global, 2010. p. 355–368.

LAQUAI, F. *et al.* A multi lane car following model for cooperative adas. *In*: IEEE. **16th International IEEE Conference on Intelligent Transportation Systems (ITSC 2013)**. The Hague, Netherlands, 2013. p. 1579–1586.

LI, J.; WANG, P.; WANG, C. Comprehensive GPSR routing in VANET communications with adaptive beacon interval. *In*: IEEE. **2016 IEEE International Conference on Internet of Things (iThings) and IEEE Green Computing and Communications (GreenCom) and IEEE Cyber, Physical and Social Computing (CPSCom) and IEEE Smart Data (SmartData)**. Chengdu, China, 2016. p. 1–6. Disponível em: https://doi.org/10.1109/iThings-GreenCom-CPSCom-SmartData.2016.28.

LI, T. *et al.* A car-following model to assess the impact of V2V messages on traffic dynamics. **Transportmetrica B: Transport Dynamics**, Informa UK Limited, v. 8, n. 1, p. 150–165, jan 2020.

LINDGREN, A.; DORIA, A.; SCHELÉN, O. Probabilistic routing in intermittently connected networks. **ACM SIGMOBILE mobile computing and communications review**, ACM New York, NY, USA, v. 7, n. 3, p. 19–20, 2003. Disponível em: https://doi.org/10.1145/961268.961272.

LOPEZ, P. A. *et al.* Microscopic traffic simulation using SUMO. *In*: **21st IEEE Intelligent Transportation Systems Conf. (ITSC)**. Maui, HI, USA: IEEE, 2018. p. 2575–2582.

LOPEZ, P. A. *et al.* Microscopic traffic simulation using SUMO. *In*: **The 21st IEEE International Conference on Intelligent Transportation Systems**. IEEE, 2018. Disponível em: https://elib.dlr.de/124092/.

LU, H.; POELLABAUER, C. Balancing broadcast reliability and transmission range in VANETs. *In*: IEEE. **2010 IEEE Vehicular Networking Conference**. Jersey City, NJ, USA, 2010. p. 247–254.

MALIK, S.; SAHU, P. K. A comparative study on routing protocols for VANETs. **Heliyon**, Elsevier, v. 5, n. 8, p. e02340, 2019. Disponível em: https://doi.org/10.1016/j.heliyon.2019.e02340.

MARTINEZ, F. J. *et al.* A survey and comparative study of simulators for vehicular ad hoc networks (VANETs). **Wireless Communications and Mobile Computing**, Wiley, v. 11, n. 7, p. 813–828, oct 2009.

MASLEKAR, N. *et al.* CATS: An adaptive traffic signal system based on car-to-car communication. **Journal of Network and Computer Applications**, Elsevier BV, v. 36, n. 5, p. 1308–1315, sep 2013.

MINTSIS, K. P. E.; MITSAKIS, E. Assessment of ACC and CACC systems using SUMO. **EPiC Series in Engineering**, v. 2, p. 82–93, 2018.

MOHAPATRA, S.; KANUNGO, P. Performance analysis of AODV, DSR, OLSR and DSDV routing protocols using NS2 simulator. **Procedia Engineering**, Elsevier, v. 30, p. 69–76, 2012. Disponível em: https://doi.org/10.1016/j.proeng.2012.01.835.

NADERI, M.; ZARGARI, F.; GHANBARI, M. Adaptive beacon broadcast in opportunistic routing for VANETs. **Ad Hoc Networks**, Elsevier, v. 86, p. 119–130, apr 2019. Disponível em: https://doi.org/10.1016/j.adhoc.2018.11.011.

NOORI, H.; OLYAEI, B. B. A novel study on beaconing for vanet-based vehicle to vehicle communication: Probability of beacon delivery in realistic large-scale urban area using 802.11 p. *In*: IEEE. **2013 International Conference on Smart Communications in Network Technologies (SaCoNeT)**. Paris, France, 2013. v. 1, p. 1–6.

OMNET++. 2022. Disponível em: https://omnetpp.org/documentation/.

PEREZ, D. P. Performance evaluation of realistic scenarios for vehicular ad hoc networks with citymob and NCTUns simulators. Universitat Politècnica de Catalunya, 2011. Disponível em: http://hdl.handle.net/2099.1/12310.

PIORKOWSKI, M. *et al.* TraNS: realistic joint traffic and network simulator for VANETs. **ACM SIGMOBILE mobile computing and communications review**, ACM New York, NY, USA, v. 12, n. 1, p. 31–33, 2008. Disponível em: https://doi.org/10.1145/1374512.1374522.

PROFENTZAS, C. Studying routing issues in vanets by using ns-3. **Alexander Technological Educational Institute of Thessaloniki in November**, 2012.

QURESHI, K. N.; ABDULLAH, A. H.; LLORET, J. Road perception based geographical routing protocol for vehicular ad hoc networks. **International Journal of Distributed Sensor Networks**, SAGE Publications, v. 12, n. 2, p. 2617480, jan 2016.

QURESHI, K. N.; BASHIR, F.; ABDULLAH, A. H. Real time traffic density aware road based forwarding method for vehicular ad hoc networks. *In*: IEEE. **2017 10th IFIP Wireless and Mobile Networking Conference (WMNC)**. Valencia, Spain, 2017. p. 1–6.

RABSATT, R. V.; GERLA, M. Multi-lane cooperative shock wave mitigation. *In*: IEEE. **2017 16th Annual Mediterranean Ad Hoc Networking Workshop (Med-Hoc-Net)**. Budva, Montenegro, 2017. p. 1–7.

RAHIMI, S.; JAMALI, M. A. J. A hybrid geographic-DTN routing protocol based on fuzzy logic in vehicular ad hoc networks. **Peer-to-Peer Networking and Applications**, Springer, v. 12, n. 1, p. 88–101, Jan. 2019.

RAHMAN, M. *et al.* Evaluation of Driver Car-Following Behavior Models for Cooperative Adaptive Cruise Control Systems. **Transportation Research Record: Journal of the Transportation Research Board**, SAGE Publications, v. 2622, n. 1, p. 84–95, jan 2017.

RAJPUT, M. *et al.* Comparison of ad-hoc reactive routing protocols using OPNET modeler. *In*: **2010 International Conference on Computer Information Systems and Industrial Management Applications (CISIM)**. Krakow, Poland: IEEE, 2010.

RAMAMOORTHY, R.; THANGAVELU, M. An enhanced hybrid ant colony optimization routing protocol for vehicular ad-hoc networks. **Journal of Ambient Intelligence and Humanized Computing**, Springer, p. 1–32, Apr. 2021. Disponível em: https://doi.org/10.1007/s12652-021-03176-y.

REGHELIN, R.; ARRUDA, L. V. Optimizing coordinated motion planning for multiple car-like robots on a segment of highway. **Robotica**, Cambridge University Press, v. 34, n. 10, p. 2274–2290, 2016. Disponível em: https://doi.org/10.1017/S0263574714002896.

REZGUI, J.; DALLY-BÉLANGER, P.; RIVEST, P. Detection and analysis algorithms of punctual road events from vehicular data in the search for the optimal route an overview of the AMNAM platform. *In*: IEEE. **2018 14th International Wireless Communications & Mobile Computing Conference (IWCMC)**. Limassol, Cyprus, 2018. p. 328–333.

SETIABUDI, A. *et al.* Performance comparison of GPSR and ZRP routing protocols in VANET environment. *In*: IEEE. **2016 IEEE region 10 symposium (TENSYMP)**. Bali, Indonesia, 2016. p. 42–47.

SILVA, A. *et al.* A reduced beacon routing protocol for inter-vehicle communications. *In*: SBRT. **SBrT 2019, XXXVII Simposio Brasileiro de Telecomunicações e Processamento de Sinais**. Petrópolis, R.J., Brazil, 2019.

SPYROPOULOS, T.; PSOUNIS, K.; RAGHAVENDRA, C. S. Single-copy routing in intermittently connected mobile networks. *In*: IEEE. **2004 First Annual IEEE Communications Society Conference on Sensor and Ad Hoc Communications and Networks, 2004. IEEE SECON 2004.** Santa Clara, CA, USA, 2004. p. 235–244.

SPYROPOULOS, T.; PSOUNIS, K.; RAGHAVENDRA, C. S. Spray and wait: an efficient routing scheme for intermittently connected mobile networks. *In*: **Proceedings of the 2005 ACM SIGCOMM workshop on Delay-tolerant networking**. [*S.l.*: *s.n.*], 2005. p. 252–259.

TANAKA, D.; ASHIDA, T.; MINAMI, S. An analytical method of EV velocity profile determination from the power consumption of electric vehicles. *In*: IEEE. **2008 IEEE Vehicle Power and Propulsion Conference**. Harbin, China, 2008. p. 1–3.

TASSOULT, N. *et al.* A survey on vehicular ad-hoc networks routing protocols: Classification and challenges. **Journal of Digital Information Management**, v. 17, n. 4, p. 227, 2019.

TONGUZ, O. *et al.* Broadcasting in VANET. *In*: **2007 Mobile Networking for Vehicular Environments**. Anchorage, AK, USA: IEEE, 2007.

Tonguz, O. K.; Wisitpongphan, N.; Bai, F. DV-CAST: A distributed vehicular broadcast protocol for vehicular ad hoc networks. **IEEE Wireless Communications**, v. 17, n. 2, p. 47–57, 2010.

TORNELL, S. M. *et al.* DTN protocols for vehicular networks: An application oriented overview. **IEEE Communications Surveys and Tutorials**, IEEE, v. 17, n. 2, p. 868–887, Jan. 2015. ISSN 1553877X.

UMER, T. *et al.* Implementation of microscopic parameters for density estimation of heterogeneous traffic flow for VANET. *In*: IEEE. **2010 7th International Symposium on Communication Systems, Networks & Digital Signal Processing (CSNDSP 2010)**. Newcastle upon Tyne, 2010. p. 66–70.

UPADHYAYA, N.; SHAH, D. J. *et al.* AODV routing protocol implementation in VANET. **International Journal of Advanced Research in Engineering and Technology**, v. 10, n. 2, p. 585–595, 2019. Disponível em: https://ssrn.com/abstract=3536290.

VAHDAT, A.; BECKER, D. *et al.* **Epidemic routing for partially connected ad hoc networks**. [*S.l.*], 2000.

VAHIDI, A.; SCIARRETTA, A. Energy saving potentials of connected and automated vehicles. **Transportation Research Part C: Emerging Technologies**, Elsevier, v. 95, p. 822–843, 2018. Disponível em: https://doi.org/10.1016/j.trc.2018.09.001.

VERMA, A.; SAVITA; KUMAR, S. Routing Protocols in Delay Tolerant Networks: Comparative and Empirical Analysis. **Wireless Personal Communications**, Springer US, v. 118, n. 1, p. 551–574, Jan. 2021. ISSN 1572834X. Disponível em: https://doi.org/10.1007/s11277-020-08032-4.

WANG, C. *et al.* Cooperative adaptive cruise control for connected autonomous vehicles by factoring communication-related constraints. **Transportation Research Procedia**, Elsevier, v. 38, p. 242–262, Jul. 2019. Disponível em: https://doi.org/10.1016/j.trpro.2019.05.014.

WANG, H.-P.; CUI, L. An enhanced AODV for mobile ad hoc network. *In*: IEEE. **2008 International Conference on Machine Learning and Cybernetics**. Kunming, China, 2008. v. 2, p. 1135–1140.

WEBER, J. S.; NEVES, M.; FERRETO, T. Vanet simulators: an updated review. **Journal of the Brazilian Computer Society**, SpringerOpen, v. 27, n. 1, p. 1–31, 2021. Disponível em: https://doi.org/10.1186/s13173-021-00113-x.

WON, M.; PARK, T.; SON, S. H. Toward mitigating phantom jam using vehicle-to-vehicle communication. **IEEE Transactions on Intelligent Transportation Systems**, Institute of Electrical and Electronics Engineers (IEEE), v. 18, n. 5, p. 1313–1324, may 2017.

WU, X. *et al.* Electric vehicles' energy consumption measurement and estimation. **Transportation Research Part D: Transport and Environment**, Elsevier BV, v. 34, p. 52–67, jan 2015.

XU, G. *et al.* Fully electrified regenerative braking control for deep energy recovery and maintaining safety of electric vehicles. **IEEE Transactions on Vehicular Technology**, Institute of Electrical and Electronics Engineers (IEEE), v. 65, n. 3, p. 1186–1198, mar 2016.

YU, H.; YOO, J.; AHN, S. A VANET routing based on the real-time road vehicle density in the city environment. *In*: **2013 Fifth International Conference on Ubiquitous and Future Networks (ICUFN)**. Da Nang: IEEE, 2013.

ZHAO, J.; CAO, G. VADD: Vehicle-assisted data delivery in vehicular ad hoc networks. **IEEE transactions on vehicular technology**, IEEE, v. 57, n. 3, p. 1910–1922, May. 2008.

ZIDANI, F.; SEMCHEDINE, F.; AYAIDA, M. Estimation of neighbors position privacy scheme with an adaptive beaconing approach for location privacy in VANETs. **Computers & Electrical Engineering**, Elsevier, v. 71, p. 359–371, oct 2018. Disponível em: https://doi.org/10.1016/j.compeleceng.2018.07.040.